



Theses and Dissertations

2024-04-12

Application of High-Deflection Strain Gauges to Characterize Spinal-Motion Phenotypes Among Patients with CLBP

Spencer Alan Baker
Brigham Young University

Follow this and additional works at: <https://scholarsarchive.byu.edu/etd>



Part of the [Engineering Commons](#)

BYU ScholarsArchive Citation

Baker, Spencer Alan, "Application of High-Deflection Strain Gauges to Characterize Spinal-Motion Phenotypes Among Patients with CLBP" (2024). *Theses and Dissertations*. 10293.
<https://scholarsarchive.byu.edu/etd/10293>

This Dissertation is brought to you for free and open access by BYU ScholarsArchive. It has been accepted for inclusion in Theses and Dissertations by an authorized administrator of BYU ScholarsArchive. For more information, please contact ellen_amatangelo@byu.edu.

Application of High-Deflection Strain Gauges to Characterize
Spinal-Motion Phenotypes Among Patients with CLBP

Spencer A. Baker

A dissertation submitted to the faculty of
Brigham Young University
in partial fulfillment of the requirements for the degree of
Doctor of Philosophy

David T. Fullwood, Chair
Anton E. Bowden
Steven K. Charles
Ulrike H. Mitchell

Department of Mechanical Engineering

Brigham Young University

Copyright © 2024 Spencer A. Baker

All Rights Reserved

ABSTRACT

Application of High-Deflection Strain Gauges to
Characterize Spinal Motion Phenotypes Among Patients with CLBP

Spencer A. Baker

Department of Mechanical Engineering, BYU

Doctor of Philosophy

Chronic low back pain (CLBP) is a nonspecific and persistent ailment that entails many physiological, psychological, social, and economic consequences for individuals and societies. Although there is a plethora of treatments available to treat CLBP, each treatment has varying efficacy for different patients, and it is currently unknown how to best link patients to their ideal treatment. However, it is known that biopsychosocial influences associated with CLBP affect the way that we move. It has been hypothesized that identifying phenotypes of spinal motion could facilitate an objective and repeatable method of determining the optimal treatment for each patient. The objective of this research was to develop an array of high deflection strain gauges to monitor spinal motion, and use that information to identify spinal-motion phenotypes.

The high deflection strain gauges used in this endeavor exhibit highly nonlinear electrical signal due to their viscoelastic material properties. Two sub-models were developed to account for these nonlinearities: the first characterizes the relationship between quasistatic strain and resistance, and the second accounts for transient electrical phenomena due to the viscoelastic response to dynamic loads. These sub-models are superimposed to predict and interpret the electrical signal under a wide range of applications. The combined model accurately predicts sensor strain with a mean absolute error (MAE) of 1.4% strain and strain rate with an MAE of 0.036 mm/s. Additionally, a multilayered architecture was developed for the strain gauges to provide mechanical support during high strain, cyclic loads. The architecture significantly mitigates sensor creep and viscoplastic deformation, thereby reducing electrical signal drift by 74%.

This research also evaluates the effects of CLBP on patient-reported outcomes. An exploratory factor analysis revealed that there are five primary components of well-being: Pain and Physical Limitations, Psychological Distress, Physical Activity, Sleep Deprivation, and Pain Catastrophizing. The presence of CLBP has adverse effects on all these components. It was also observed that different patient reported outcomes are highly correlated with each other, and the presence of CLBP is a significant moderating factor in many of these relationships.

Arrays of high-deflection strain gauges were used to collect spinal kinematic data from 274 subjects. Seven phenotypes of spinal motion were identified among study participants. Statistical analyses revealed significant differences in the patient-reported outcomes of subjects who exhibited different phenotypes. This is a promising indication that the phenotypes may also provide important information to clinicians who treat patients suffering from CLBP. Future research will be conducted to develop and identify the optimal treatments for patients according to their phenotypes, which has the potential to reduce medical costs, expedite recovery, and improve the lives of millions of patients worldwide.

Keywords: nanocomposites, high-deflection strain gauges, modeling, patient-reported outcomes, phenotyping, machine learning, chronic low back pain

ACKNOWLEDGMENTS

This work would not have been possible without the guidance and support of many mentors.

Firstly, I'm grateful to the National Institute of Health for their support. All the research endeavors described in this dissertation have been funded by the Back Pain Consortium (BACPAC) Research Program under the Helping to End Addiction Long-term Initiative NIAMS grant UH3AR076723. This grant has enabled me to dedicate my primary efforts to research throughout my doctoral studies.

I'd like to acknowledge my committee members. It's been a privilege to work with each member throughout this experience. Dr. Charles was my first research advisor. As an undergraduate in the Neuromechanics Lab, I had my first chance to present at a research conference and draft a journal manuscript. This valuable experience led me to discover a passion for research and prepared me for graduate studies. Dr. Bowden introduced me to the BACPAC project. I still remember how exciting it was to be invited to his office and hear there was a position open on the team. He's provided important guidance and facilitated several opportunities that led to conference appearances and publications. Dr. Mitchell has always been very generous with her mentorship. Her unique perspective as a practicing clinician has broadened my horizons, and her pragmatic counsel has sharpened my technical skills. My advisor, Dr. Fullwood, has been very supportive in my learning, both regarding the research project and my personal development as an engineer. He's provided essential guidance while allowing me the autonomy to gain my own experiences. This has been a unique learning opportunity that has opened the doors I've always hoped for.

I'd also like to thank my parents and siblings. My father has always been the ideal example of an engineer to me. He frequently tells me, "Picture it with your brain", knowing that if it can be envisioned, it can be done. My mother has instilled in me the value of education and hard work, starting with learning the times tables with flash cards to practicing spelling tests. She knew that I was capable of hard work and improving my mind, and she made sure I knew it too. My siblings have also played a vital role in my life, doctoral studies were no exception. They imparted freely of their time, expertise, experience, and insights throughout this experience.

Most importantly, I'd like to thank my Savior. Early in this endeavor it became apparent that my natural abilities were going to be insufficient, and success would only be possible with His help. Challenges were not immediately lifted, but little by little progress was made. Often, I would approach a problem, exhausting my best efforts on it. Finally, a thought would cross my mind, which led me to the next step, and then the next, and then the next. I learned that God honors our agency, expects our best efforts, and then magnifies our abilities. As Elder Renlund teaches, "Studying it out in one's mind—coupling faith with observation and reason—is necessary for spiritual impressions to come. We focus on a problem, study it out, and think about it. We formulate various solutions. It seems that only then can personal revelation reliably come." Christ is truly interested in our success, as well as our becoming disciples.

TABLE OF CONTENTS

TITLE PAGE	i
ABSTRACT	ii
ACKNOWLEDGMENTS	iii
TABLE OF CONTENTS	iv
LIST OF FIGURES	vii
LIST OF TABLES	xii
Chapter 1 Background	1
1.1. Introduction to Low Back Pain	1
1.1.1. Prevalence and Severity	1
1.1.2. Economic Burden	1
1.1.3. Risk Factors	2
1.1.4. Study Factors	4
1.2. Introduction to Chronic Low Back Pain	4
1.3. LBP Treatments	5
1.3.1. Current Diagnostic and Intervention Methods	5
1.3.2. Need for a Precision Medicine Technique	7
1.4. Motion-Based Phenotyping – a Promising Solution	8
1.4.1. Preliminary Evidence for Phenotyping	8
1.4.2. Challenges to Phenotyping	9
1.4.3. Plan to Effectively Identify Phenotypes	10
1.5. Understanding Metrics of Wellbeing	11
1.6. Motion-Capture Systems	11
1.6.1. Background on Strain Gauges	11
1.6.2. BYU Strain Gauges	13
1.7. Dissertation Outline	13
1.7.1. Summary of Accomplishments	13
1.7.2. Future Work	14
Chapter 2 Accounting for Viscoelasticity when Interpreting Nano-Composite High-Deflection Strain Gauges	15
2.0. Abstract	15
2.1. Introduction	15
2.2. Materials and Methods	16
2.2.1. Model Development	17
2.2.2 Model Validation	20

2.3. Results.....	21
2.3.1. Model.....	21
2.3.2. Model Validation.....	26
2.4. Discussion.....	28
Chapter 3 Multi-layered Architecture for Improved Nano-Composite Biomechanical Sensors.....	30
3.0. Abstract.....	30
3.1. Introduction.....	30
3.2. Materials and Methods.....	31
3.2.1. Nanocomposite Sensors.....	31
3.2.2. Viscous Properties.....	32
3.2.3. Electrical Signal.....	32
3.2.4. Sensor Performance.....	34
3.3. Results.....	34
3.3.1. Viscous Properties.....	34
3.3.2. Electrical Signal.....	34
3.3.3. Sensor Performance.....	37
3.4. Discussion.....	37
Chapter 4 Correlations of Patient Reported Outcomes Among Patients with Chronic Low Back Pain and Controls.....	39
4.0. Abstract.....	39
4.1. Introduction.....	40
4.2. Methods.....	42
4.2.1. Data Collection.....	42
4.2.2. Data Processing.....	43
4.2.3. Data Analysis.....	43
4.3. Results and Discussion.....	46
4.3.1. Impact of CLPB on Well-Being.....	46
4.3.2. Relationships Between Reported Outcomes.....	48
4.3.3. Distinct Components of Well-Being.....	51
4.3.4. Limitations.....	52
4.3.5. Conclusions.....	52
Chapter 5 Wearable Nanocomposite Sensor System for Motion Phenotyping Chronic Low Back Pain: A BACPAC Technology Research Site.....	54
5.0. Abstract.....	54
5.1. Introduction.....	54
5.2. System Design and Validation.....	56

5.2.1 Array Design	57
5.2.2. Array Implementation	60
5.2.3 Electronics Design	61
5.3. Subject Testing Protocol.....	61
5.4. Data Analysis	64
5.4.1. Biomechanical Analysis	64
5.4.2. Phenotype Identification and Interpretation	66
5.5. Discussion	70
Chapter 6 Phenotype Identification and Potential Clinical Application for Treating Chronic Low Back Pain	72
6.0 Abstract	72
6.1. Introduction.....	72
6.2. Methods.....	74
6.2.1. Data Collection.....	74
6.2.2. Data Analysis.....	78
6.3. Results.....	80
6.3.1. Participants	80
6.3.2. PRO Correlations.....	81
6.3.3. Phenotype Analysis	84
6.4. Discussion	88
Chapter 7 Discussions.....	90
7.1. High Deflection Strain Gauge Modeling	90
7.2. Mitigating Viscoplastic Deformation with Multilayered Architecture	90
7.3. Relationship between PROs and Moderating Effects of CLBP	90
7.4. Phenotype Identification and Analysis	91
7.5. Future Work.....	92
REFERENCES.....	93

LIST OF FIGURES

Figure 1.1 Depiction of (a) Burger's viscoelastic model and (b) the KZ model that accounts for nonlinear viscoelastic behavior. The Burger's model captures fundamental viscoelastic behavior ($E2$, $\eta2$), viscoplastic behavior ($\eta1$), and elastic behavior ($E1$). The KZ also captures these same aspects, but accounts for nonlinearities and time-dependencies in model parameters. 12

Figure 2.1 Depiction of (a) The high deflection strain gauges; (b) The strain gauge during a tensile test; and (c) A microscopic image of the sensors under a small load. During tensile tests (b), the sensor was secured between two polypropylene grips. The grips contained a copper metal interior coating to facilitate measuring the strain gauge's electrical resistance at different loads..... 17

Figure 2.2 Burger's rheological model of viscoelastic materials. The spring and damper in parallel ($E2$ and $\eta2$) capture the sensor's viscoelastic behavior, the spring in series ($E1$) models the elastic behavior, and the damper in series ($\eta2$) accounts for the viscoplastic behavior..... 19

Figure 2.3 Depiction of the strain profile that the tensile tester applied to a sensor, and which cycles constitute preconditioning, calibration, and evaluation stress-relaxations..... 20

Figure 2.4 (a) The strain profile of an incremental strain test (black line indicates the sensor performances as it is being pulled in tension, and the gray line indicates the sensor performance as it is being relaxed; dots represent the points at which empirical data was collected from the resistance test after the transient spike had dissipated for all sub-figures). (b) The electrical response from the sensors over time as the strain gauges were pulled to different incremental strains. (c) The strain-resistance relationship interpolated from the tensile tests. (d) The gauge factor (relative change in resistance with respect to strain). Spline fit curves were used to interpolate the resistance of the sensor under static conditions between the empirical points. The derivative of the spline fit curves over the spline fit depicts the relative sensitivity of the sensor at different strains..... 22

Figure 2.5 Depiction of the strain-resistance relationship during the first five stress-relaxation cycles..... 23

Figure 2.6 The sensor electrical response following (a) an incremental strain step of 0.5mm and (b) following an incremental relaxation step of 0.5mm. The solid black lines indicate the sensor resistance. The dotted red lines indicate the peak of the resistance spike during the transition between strains. 24

Figure 2.7 Stress relaxation (orange) and transient resistance response (blue) during stress relaxation following an incremental step in tension (a) and following an incremental step in relaxation (b). 25

Figure 2.8 (a) The quasi-static strain model (black line), the model prediction at the randomly selected strain points (black dots), and the actual strains (red dots) for a single sensor. Vertical distances between black and red line represent the model error. (b) Scatterplot of the randomized strains (x-axis) compared to the model prediction (y-axis) for all 10 sensors (each strain gauge is indicated by a different color). Predictions that fall on the dotted black line are exactly accurate. 26

Figure 2.9 The predicted resistance value (dotted blue line) compared to the true sensor resistance (black line) during the validation test. The top plot was conducted at a rate of 0.05 mm/s, the middle plot was the validation test conducted at a rate of 0.50 mm/s, and the bottom plot was the validation test conducted at a rate of 5.0 mm/s..... 27

Figure 2.10 (a) Scatterplot of the true strain compared to the predicted model strain for different sensors, each pulled to a random strain (between 5 and 15% strain). (b) Scatterplot of the true strain

rate of each sensor compared to the predicted strain rate, pulled at a random strain rate between 0.05 and 5.0 mm/s. Each sensor is represented by a single scatter point	28
Figure 3.1 A depiction of (a) the conventional nanocomposite sensor and (b) the multi-layered sensor in a relaxed state and (c) the multi-layered sensor under combined torsion and tensile train.....	32
Figure 3.2 Findings from previous study, in which (a) incremental strains were applied to a sensor, (b) the sensor output was captured, (c) a quasistatic model was developed ignoring transient outputs, (d) the relative signal (in terms of $\Delta R/R0$) of the sensor at different strain levels, (e-f) the relationship between resistance while the sensor is held at a constant strain [144].....	33
Figure 3.3 (a) The stress-strain diagram for single-layered nanocomposite sensor (light gray) and the multi-layered strain gauge (dark gray) and pure silicone (black) pulled at a constant rate of 3.0 mm/s. (b) Force vs strain during a cyclic test between 0 and 75% strain, depicted for a silicone sensor (black), conventional sensor (light gray), and multilayered sensor (dark gray). Notice that during the recovery, the multilayered sensor recovers more than the conventional sensor (the sensor buckles at approximately 15% strain rather than 20% strain). (c) the viscoplasticity of the different strain gauges during repeated cyclic loads, quantified as the energy absorbed and not recovered by the material.....	34
Figure 3.4 Comparison of the resistance-strain relationship (top) and the relative signal change at different strains (bottom) of the single-layered sensors (left) and the multi-layered sensors (right) during tension. The shade of each line indicates the cycle performed (darker shades represent later cycles).....	35
Figure 3.5 Depiction of the strain profile (blue) and corresponding resistance (orange). The spike magnitude is indicated by the dashed red line and the spike dissipation under constant strains is estimated as an exponential decay with a time constant of λ	36
Figure 3.6 A summary of the strain interpretation performance for the multi-layered sensor (black) and the single-layered sensor (gray). Any dot that falls on the slanted black line is correct, and the mean absolute error is the vertical distance between a dot and the slanted dashed line.....	37
Figure 4.1 Individuals who were invited to participate in study and met eligibility criteria.....	42
Figure 4.2 Decision tree indicating the process for selecting whether a relationship between the legacy and PROMIS PRO exists, and if so in what manner the presence of CLBP influences the relationship.....	45
Figure 4.3 Boxplots contrasting the PRO values between controls (blue) and cases (red). The raw data collected (prior to the transformation to achieve normal sample distributions) are depicted here.....	47
Figure 4.4 Scatterplots and the respective line of best fit (when applicable) depicting the relationship between the different PROs for subjects who experience CLBP symptoms (red) and asymptomatic subjects (blue).....	48
Figure 4.5 (a) The correlation of determination between the five factors identified -Physiological Ailment, Psychological Ailment, Sleep Deprivation, Physical Activity, and Pain Catastrophizing- with the original features PROs of interest and (b) and the correlation of determination between the PROs of interest.....	52
Figure 5.1 Overview of methodology to identify and analyze movement-based phenotypes among symptomatic and asymptomatic subjects by (1) developing and validation system design (2) collecting data from symptomatic and asymptomatic subjects during several single-planar and multi-planar spinal motions, and (3) analyzing the spinal motion data to identify and interpret different motion-based phenotypes among subjects.....	56

Figure 5.2 (a) Placement of reflective markers for motion-capture study and (b) the markers on a subject’s lower back. The skin stretch during different spinal motions was estimated by calculating using the distance between markers..... 58

Figure 5.3 Summary of the extension magnitude for (a) each single-planar motion – higher magnitudes of extension indicated by darker shades of red and higher magnitudes of compression indicated by darker shades of blue – and (b) the result array design. The reflective markers are indicated by the circles, following the placement depicted in Figure 5.2..... 58

Figure 5.4 Confusion matrix, depicting the true class of exercise being performed by a subject and the corresponding predicted class, using the skin strains captured by the optimized strain gauge array design as predictors in a machine learning classification model. Predictions along the diagonal represent accurate exercise classifications..... 59

Figure 5.5 The vertebral motion tracking system of 16 nanocomposite sensors (two are visible from underneath the cover in the lower right side) on kinesiology tape with stitched wiring..... 60

Figure 5.6 (a) Custom PCB for reading the resistance across all 16 piezoresistive sensors and (b) integration of PCB with final SPINE Sensor System. 61

Figure 5.7 The SPINE Sense System is placed to the lower back using the L5 spinal process unit as a to guide the placement (a) and is aligned vertically on the lower back (b). The kinesiology tape adherence is reinforced on the edges (depicted in yellow in the figures above) using pre-tape spray..... 62

Figure 5.8 Summary of the SPINE Sense App during the different stages of motion capture. The clinician or participant (a) opens the app, (b) enters participant demographic information, (c) is guided through the series of spinal motions to perform, and (d) uploads data to the cloud server. 63

Figure 5.9 (a) An example of a comparison between the velocity, acceleration, and jerk between 16 control subjects (blue) and 28 subjects with CLBP (red) during Flexion Left collected from the IMU placed on the C7 (p-values of 0.26, 0.08, and 0.60 for velocity, acceleration, and jerk respectively) and (b) scatterplot of asymmetry of motion during flexion -estimated by the absolute value of the difference in the sensor readings during the Flexion Left and Flexion Right motions – and the PROMIS Pain T-score for participants with CLBP (blue dots) with the corresponding best fit line (red)..... 65

Figure 5.10 A depiction of how different linkage methods perform for hypothetical data sets, obtained from [217]. Single Linkage performs well on non-globular data, but performance is diminished by noisy data. Average Linkage and Complete Linkage perform well on data that exhibits clean separations between clusters, but the quality of the results is diminished if the separations are not as distinct. Ward Linkage is optimal when clustering noisy data and will be implemented in this endeavor [218]..... 67

Figure 5.11 An example of a cluster dendrogram [219]. By using a cutoff distance score of 8, three clusters were extracted from the data, marked by orange, green, red, and purple. A cutoff distance score of >8 would have resulted in fewer clusters with more observations per cluster, and a cutoff distance score of <8 would have resulted in more clusters with fewer observations..... 68

Figure 5.12 (a) The Hypothetical dataset is composed of data normally distributed around three centers and (b) the corresponding Calinski-Harabasz Criterion for 2 through 14 clusters. The Calinski-Harabasz score is the highest when the number of clusters is three, indicating three clusters provide the clearest segmentation between groups of datapoints. 68

Figure 5.13 An example of the results of a phenotype identification analysis and its corresponding clinical interpretation from preliminary data. (a) Depicts the different phenotypes by color on the first two principal components of the motion and demographic data. Phenotype A was comprised of participants who exhibited significantly different velocities between their flexion right and flexion left motions (i.e., performing flexion towards one side was much faster than the other); Phenotype B was comprised of mostly participants with CLBP, high BMI scores, and who performed flexion right and flexion left with similar velocities; and Phenotype C was comprised of mostly asymptomatic patients with low BMI scores and a dominant side during lateral bending. (b) Depicts boxplots of the Pain Intensity scores for the participants, grouped by phenotype. A one-way ANOVA test calculated an F-statistic of 7.23 and a corresponding p-value of 0.002 comparing the Intensity scores between the phenotypes. 69

Figure 6.1 Overview of the NIH BACPAC initiative. An individual’s biopsychosocial well-being influences spinal biomechanics, which can be objectively monitored using the SPINE Sense System. The objective of this work is to analyze the data from the SPINE Sense System and other relevant factors to identify phenotypes of spinal motion, which in future work will be conveyed to clinicians, who can then identify the optimal treatment paradigm for patients according to their phenotype. This can then be implemented on a widescale to reliably apply treatments best suited to patients’ needs, improving treatment outcomes and saving medical costs worldwide. 74

Figure 6.2 Depiction of (a) the SPINE Sense System adhered to a subject’s back and (b) the SPINE Sense System collecting data during motion. 75

Figure 6.3. Depiction of the different single- and multi-planar motions included in this research with the full motion name and abbreviated motion name listed below each figure. 75

Figure 6.4 Summary of the Pearson’s correlation strength (r) between (a) demographics with PROs and (b) metrics of Psychological Wellbeing with PROs. Again, the reverse of the PROMIS Physical Function T score is depicted above to provide consistent interpretation of the visualization (higher scores are indicative of worse participant health in each area). 81

Figure 6.5 Summary of the Pearson's correlation strength (r) observed between the motion features collected in this study and the PROs of interest for patients suffering from CLBP. Shades of red indicate positive correlations and shades of blue indicate negative correlations. Note: The reverse of PROMIS Physical Function T (i.e., $100 - \text{PROMIS Physical Function T}$) is depicted above for visualization purposes (lower PRO scores for each metric depicted are indicative of better wellbeing). 82

Figure 6.6 SHAP waterfall plots, depicting the effect of different features on two specific instances: (a) the ODI of a subject and (b) the PROMIS Pain Interference T of a different subject. The default value prediction (the average of all observations) is represented at the bottom of the SHAP waterfall plots (e.g., 17.5 for ODI). The values of key features are presented on the left, and the effect on the prediction are depicted by the colors and length of the horizontal bars. The net prediction for the instance (i.e., for the subject of interest) is represented by $f(x)$ at the top of the waterfall plot. 83

Figure 6.7 SHAP plots depicting the relationship of IPAQ Met Minutes / Week (left) and the SitToStand_interval (right) for different PROs of interest. The PRO of interest is noted by the subplot title. Notice that higher IPAQ MET Minutes / Week are associated with better ODI, PROMIS Pain Interference, and PROMIS Anxiety scores, and that longer SitToStand_interval durations are associated with higher ODI, PROMIS Pain Interference T, and PROMIS Depression T scores. 84

Figure 6.8 The Silhouette Criterion score for a range of clusters from 2-12. It was observed that at a separation of seven clusters, the Silhouette Criterion score was the greatest, indicating the best segmentation of clusters was achieved when the subjects were divided into seven phenotype-clusters..... 85

Figure 6.9 Scatterplot of the study participants on the first two principal components of the data, color-coded by phenotype..... 85

Figure 6.10 Summary of the comparisons between phenotypes for each PRO of interest. Each ANOVA test revealed that there were statistically significant differences between the phenotypes. Student t tests were then conducted to evaluate which phenotypes differed. Phenotypes that showed no statistically significant differences for a particular metric were indicated by underling the two or more boxplots..... 87

LIST OF TABLES

Table 2.1 The average yield strain from sensors pulled at 5.0 mm/s, 0.5 mm/s, and 0.05 mm/s. Notice that the linear strain range of the stress-strain diagram was not significantly affected by strain rate.....	21
Table 2.2 Coefficients for equation in Eq 4 to describe the strain-resistance relationship during tension.....	23
Table 2.3 The steady-state strain-resistance model (Eq 1 was estimated using the first, second, third, and fourth cycles. The resulting mean-squared error of this model (in Ohms) was used to determine how many cycles were needed for preconditioning purposes.....	23
Table 2.4 The spike magnitude, S , (in units of Ω/Ω) was found to be dependent on strain rate. At higher strain rates, the magnitude of the resistance spikes increased. Notice that at low strains, the spike magnitudes are significantly smaller, most likely due to sensor buckling.....	24
Table 2.5 The time constant, λ , (in units of s^{-1}) was found to be rate and strain dependent. At higher strains and strain rates, the sensors exhibited a faster transient response. Notice that at low strains, the stress relaxation constants are significantly lower, possibly due to strain gauge buckling.	25
Table 2.6 Model application test results (r-squared and mean-averaged error) conducted at each different strain rates.....	27
Table 3.1 Summary of the relative variation in sensor readings as a percentage of the average sensor resistance, $100 * stdev(R\epsilon)/average(R\epsilon)$, at each strain level for the single- and multi-layered sensors for the four samples taken of each and the perfect drift-reduction.	35
Table 3.2 Summary of the resistance spikes, in percent increase in sensor resistance $100 * \Omega/\Omega$, after an increase / decrease in strain, for the single- and multi-layered strain gauges.	36
Table 3.3 A summary of the spike exponential decay coefficients (λ) and stress relaxation coefficients ($\lambda\sigma$) for the single- and multi-layered strain gauges. The stress relaxation coefficients were ignored when the initial stress was less than or equal to zero.....	37
Table 4.1 Summary of the subject demographics, in terms of the average values and standard deviation (stdev), for the study participants.	43
Table 4.2 Summary of the data collected and the normality skewness before and after transformation (\sim in the after-transformation column indicates that no transformation was applied, and the Fisher-Pearson coefficient remained constant).	46
Table 4.3 Summary of the Student T-tests to evaluate the difference in PRO among the control and case groups (group averages and standard deviations are reported in terms of the raw data, and the t-statistic and corresponding p-values are reported in terms of the normalized dataset when necessary to satisfy the assumptions of a Welch T-test).	47
Table 4.4 Summary of the model parameters and overall p-values and $ r $ values for each PRO combination correlation. Note that the interaction terms ($\beta 2$ and $\beta 3$) indicate the difference in the y-intercept and slope from the baseline values ($\beta 1$ and $\beta 2$). If no statistically significant model was found to depict the relationship, the statistically insignificant parameters from Eq 1 were reported.	49
Table 4.5 Summary of the Pearson's correlation between the original PROs of interest and the identified latent factors.....	51

Table 5.1 Summary of the subject demographics in motion-marker study (the average of each demographic and the corresponding standard deviation of the motion capture participants)	57
Table 5.2 System Usability Scale scores from clinicians and patients.	60
Table 6.1 Summar of the demographics of the two cohorts of interest - those who were CLBP asymptomatic (controls) and those who reported having experienced CLBP symptoms (cases).	80
Table 6.2 A summary of the model accuracies (in terms of Pearson's correlation squared) for modeling each PRO of interest.	83
Table 6.3 A summary of the average values for the key features for each phenotype, in terms of their unscaled values.	86
Table 6.4 Summary of the resultant F-statistics, p-values, and adjusted p-values (corrected for multiple comparisons use the Holm post-hoc test)	87

CHAPTER 1 BACKGROUND

1.1. Introduction to Low Back Pain

Pain mitigation is one of the primary purposes of nearly every medical intervention [1]. One of the most common health ailments, which has even been deemed “the nemesis of medicine” [2], is low back pain (LBP). The lower back, as defined by a National Institute of Health Research Consortium, refers to “the space between the lower posterior margin of the rib cage and the horizontal gluteal fold” [3].

1.1.1. Prevalence and Severity

A plethora of studies have investigated the prevalence of LBP in modern society. Andersson and Praemer identified LBP as the most common subcategory of musculoskeletal impairments [4, 5]. When quantifying the prevalence of LBP, it is important to specify the timeframe of interest because LBP can occur (and potentially be resolved) at varying rates. Multiple studies have estimated the point-prevalent (i.e., the population of individuals with LBP at any given time). Hoy and colleagues’ literature review reported an estimated LBP point prevalence of 11.9% [6], while Walker et al. reported ranges of LBP point prevalences between 12-33% [7]. Ricci and colleagues investigated two-week prevalence of LBP among the U.S. workforce and made an estimate of 15.1% [8]. Deyo and colleagues conducted an analysis of a National health Interview Survey and estimated the three-month prevalence of LBP in the US to be 26.4% [9]. Multiple studies of diverse populations have estimated the lifetime prevalence of LBP at 50-80% [10-12]. Some studies believe that the prevalence of LBP is on the rise [13]. One study observed a 25% increase in intervertebral disc disease, a 152% increase in back pain, and 9% increase in early retirement due to back pain over a 15 year period; with an estimated 206% increase in back disorders, 628% increase in arthrosis, and 131% increase in general musculoskeletal disorders in the space of 10-15 years [14]. However, it may be that the prevalence of LBP has remained relatively constant in recent years, and the apparent rise is due to LBP receiving more attention than it has in the past: Skovron found that the sick-listing in Sweden due to LBP increased from 1% to 8% in the space of 17 years despite the overall reports of back pain remaining consistent during that time period [15]; and Robertson observed that “the use of health services has multiplied, the diagnostics of musculoskeletal disorders have improved, and the population is possibly now perceiving pain and other symptoms in a different way than before” [14]. Regardless, there is an overwhelming consensus that LBP is already prevalent among every society, and the number of individuals suffering from LBP is expected to rise as the population ages [6, 16].

Not only is LBP prevalent, but it also has the potential to be very severe. It is known to cause functional limitations and reduced quality of life [8], and has even been identified as the leading cause of disability worldwide [16, 17]. The rate of lower-back surgeries has been on the rise in recent years (even while the rate of LBP hospitalizations has decreased) [4, 18]. It is one of the most common reasons for medical consultation. Andersson and colleagues estimated that LBP-related cases account for 5.5-7.5% of office visits in the UK, and 30 million office visits in the US [4].

1.1.2. Economic Burden

Unsurprisingly, the severity and frequency of LBP have resulted in soaring medical costs during recent decades. Nachemson described LBP as “the most expensive ailment from a socio-economic viewpoint ... in patients 30-60 years” [19]. In 1996, the direct medical costs of disability in the United States were estimated as \$260 billion, LBP being a major contributor [20]. About 8% of the insured Swedish population are listed as having LBP [4], and 2% of the US workforce is compensated for annually LBP. Parthan estimated that the total healthcare costs for treating LBP ranges between \$17.7 and 105.4 billion (in 2005 US dollars) [21]. The proportion of individuals seeking health care is also on the rise [22], further increasing the overall medical costs of LBP.

Furthermore, not all economic consequences are direct. A significant portion of the financial burden related to LBP is incurred indirectly through productivity losses. Andersson found LBP to be the single largest cause of work absence, accounting for 11-19% of sick days taken across multiple countries [4]. Tubach found that at the French national electrical and gas company, approximately 4.5% of the blue-collared workers took sick leaves of eight days or more due to LBP [23]. Other studies have also affirmed that back pain is one of the most common reasons for missing work [24]. Parthan estimated the total indirect cost due to missed work days for back pain reasons was \$22 billion in 2005 [21]. Webster and Snook estimated that the breakdown of the total medical costs associated with LBP in the United States are 16-58% direct medical costs, 33-83% indemnity payments, and 0.1-19.9% other (varying significantly between state) [25].

These costs are not distributed evenly across patients. Webster and Snook also found that most of the economic resources (95%) were being directed towards treating a minority of cases (25% of cases) [25]. Rossignol and colleagues found that 6.7% of individuals who took work-leave due to LBP were still absent after 6 months, and these individuals accounted for 76% of the total LBP compensation [26]. Frymoyer and Cats-Baril estimated that of the \$50-100 billion direct and indirect costs associated with LBP, 75% of it was a result of the temporary or permanent disability of 5% of the population [14, 27].

1.1.3. Risk Factors

While no population is exempt from LBP, there are certain demographics, lifestyle, and occupational factors that influence its prevalence and severity. A plethora of studies have been conducted to identify risk factors associated with LBP [6, 14, 28-38]. While the results vary between studies, some of the most common and significant factors are included here.

Age: It is intuitive to suppose that age is a significant factor when assessing LBP, especially considering the known effects of disc degeneration and osteoporosis with time [29]. However, there are varying opinions in the literature regarding the relationship between age and LBP. Hoy and colleagues conducted a literature review of 165 articles and found that the prevalence of LBP increased until roughly middle age (40-49 years for men and 60-69 years for women), then afterwards declined [6]. Dionne and colleagues also observed this “curvilinear” pattern in a review of related studies. However, when only considering studies that evaluated the prevalence of severe LBP, they found the relationship between age and LBP prevalence to be either linear or nonexistent [12, 29]. Svensson et al. concluded from an observational study of a population aged 38-64 that age was not associated with LBP prevalence, but that LBP was more severe in the older subset of the population [12]. Overall, it appears that LBP prevalence increases until middle age. After this time, the relationship between LBP and age depends on the context of the study’s definition of LBP and potentially additional confounding factors. While the exact relationship between age and LBP is uncertain, the literature clearly demonstrates that age is an important consideration when studying LBP.

Work Loads: A plethora of studies have investigated the relationship between LBP and workloads. Riihimaki identified several “generally accepted” (i.e., detected in multiple studies) LBP risk factors relating to workloads (e.g., heavy physical work, heavy or frequent lifting, prolonged sitting, trunk rotating, pushing/pulling, vibration etc.) [2]. Frymoyer similarly found that “the complaint of medically reported LBP was significantly related to occupational factors such as truck driving ($p < 0.001$), lifting, carrying, pulling, pushing, and twisting ($p < 0.001$ for all variables) as well as nondriving vibrational exposure ($p < 0.001$).” [30]. Multiple studies have identified blue-collar workers as being at a higher risk of musculoskeletal disorders than white-collar workers [31, 32]. Schneider and colleagues evaluated different risk factors in terms of odds ratios. Odds ratio is the probability that an outcome occurs given a particular exposure, compared to the probability in the absence of said exposure [39]. The odds ratio of developing LBP for individuals who were exposed to repetitive carrying, lifting, and holding heavy loads was 1.74 compared to those who were not subject to these conditions [33]. Several works have identified long-term exposure to vibrations – usually in the context of driving – as a risk factor for back ailments [15, 30]. Most of these workload-related injuries occur during

sudden, infrequent tasks. However, it should be noted that workloads applied in a controlled manner (i.e., loads that are tailored to the individual and are gradually increased over time, such as in weightlifting) are associated with positive effects on spinal health [2].

Sex: There are mixed opinions regarding whether sex is a factor in the prevalence of LBP. Scheider and colleagues found that the seven-day LBP prevalence was 39.9% for women but only 31.8% for men, and that women were still at a 25% higher risk of experiencing LBP after adjusting for other known risk factors [33]. In 2012, Hoy and colleagues found the point prevalence and monthly prevalence of LBP was statistically higher for women for all age groups ($p < 0.001$). The study postulated that this difference may be attributed to various biophysiological (such as osteoporosis, menstruation, pregnancy), and / or sociopsychological factors (social influences on sex differences and somatization) [6]. Frymore et al. also found that the average number of pregnancies was higher for women who experienced LBP (2.6) than those without (1.6) [30]. However, other studies find no statistically significant differences were observed in the annual or lifetime prevalence comparisons of LBP between men and women [6]. Still others studies report observing a higher LBP prevalence among men [17, 40, 41], and that women in general exhibit fewer known risk factors associated with LBP than men [33]. Riihimaki identified sex as a plausible factor in LBP, but also acknowledged that it was not generally accepted due to conflicting findings [2]. The heterogeneity in study populations and contradicting literature make it difficult to determine whether sex is a relevant LBP factor or not. While this work will not attempt to determine whether sex plays a role in the prevalence and / or severity of LBP, it will consider it as a possible direct or mediating factor.

Smoking: There is an overwhelming consensus that smoking is associated with LBP [30, 33, 37], though the direct cause-and-effect relationship is unknown. One hypothesis is that smoking is often used as a coping mechanism and was therefore a conflating factor with emotional tension [30, 33]. However, there is no indication to date that smokers experience greater psychological distress than their non-smoking counterparts [30]. Other explanations are more physiological (and causative [37]) in nature, proposing that smoking induces chronic cough and indirectly induces prolonged mechanical stresses on the back [30], and / or vasoconstriction (impaired blood supply) to intervertebral discs [30, 33].

Alcohol: While alcohol has been a widely proposed risk factor of LBP, there are insufficient findings in the literature to fully substantiate it. Riihimaki observed that while some studies have identified alcohol consumption as a risk factor for LBP, there was insufficient consensus among the literature to draw conclusions [2]. Leboeuf-Yde conducted a literature review of nine studies and concluded that “alcohol consumption does not seem to be associated with low-back pain, but well-designed specific alcohol/low-back pain-centered studies are lacking” [36]. Lv and colleagues conducted a Mendelian Randomization study and found a higher-than-average odds ratio between alcohol consumption and LBP, but the results were not statistically significant [37].

BMI: It has long been observed that “an unfavorable lifestyle also correlates positively with risk of back pain” and that “people with back pain are more likely to be overweight” [33]. Shiri and colleagues reported in a literature review that there was a higher prevalence of LBP among individuals who were overweight and obese, even when accounting for potential confounding factors. Furthermore, these patients had the strongest association of seeking medical treatment for LBP [38]. Heunch and colleagues also found that a BMI of 30 or more was associated with increased risk of LBP occurrence and recurrence [42]. There are several possibilities why this may be the case. Individuals with high BMI likely experience higher spinal loads, increasing the risk of disc degeneration and Modic changes in vertebral endplates. However, Heunch et al. also noted that that increased fat mass, not lean mass, was associated with LBP and disability, indicating that high BMI does more than increase the mechanical load on the spine [42]. There is also a plethora of evidence that physical activity, which presumably also increases spinal loading, reduces pain [14, 43]. Other possibilities are that higher BMI has physiological effects – such as increased production of cytokines in adipose tissue

that activates proinflammatory pathways, or modifications in serum lip levels that inhibit the nutrition of disc cells – that result in LBP [42]. Overall, there is overwhelming consensus that a high BMI is a risk factor of LBP, even accounting for conflating factors, suggesting that a causative relationship exists.

Socioeconomics: Socioeconomics is one of the more complex but consistently identified factors that influence long-term LBP and disability [4]. When evaluating the prevalence of LBP between different countries, Hoy and colleagues found that the prevalence of LBP was greater in countries with high-income economics [6]. However, within a given society, multiple studies have identified that higher socioeconomic classes (i.e., advanced levels of education, white-collar workers, higher job rank) have a lower prevalence of LBP [9, 33]. Work experience has also been identified as a factor in LBP in multiple studies [2].

Psychosocial Wellbeing: Many studies have investigated the relationship between social and psychological wellbeing with LBP. Schneider observed that patients with LBP have weaker social networks, and that individuals who live alone are less likely to report LBP [33]. Low social support in the workplace has been identified as a factor for developing LBP [43]. Multiple studies have hypothesized that higher levels of fear-avoidance are associated with decreases in functional performance [43, 44]. This has been supported by a randomized study, in which some patients receiving therapy for LBP were forewarned of potential pain during the treatment. Individuals who received this warning exhibited decreased performance and reported higher pain than their counterparts in the trial [45]. However, not all studies have reported such strong associations between psychosocial wellbeing and LBP. While several studies report statistically significant correlations between psychological factors and function, the correlation strengths tend to be relatively weak and potentially diluted by conflating biological and social factors [34, 35]. Other studies report no association between major psychopathology and the development of long-term (i.e., chronic) LBP. Overall, it is clear that psychological wellbeing is highly intertwined with LBP, though whether it has causative effects is less certain [43].

1.1.4. Study Factors

The diagnosis of LBP is a broad topic that encompasses many specific etiologies, which often makes it difficult to analyze because the context from which it is defined and investigated varies so much. For example, studies based on clinical data are likely to focus on individuals who sought medical treatment due to LBP, data from an insurance company is primarily concerned with individuals who applied for financial assistance. Some studies that recruited only patients with “well-documented” cases of LBP to provide a clear distinction between cases and controls [46]. The emphasis of study designs, the heterogeneity between subject populations, and publication bias all have the potential to influence study results; hence caution should be taken when drawing final conclusions [6].

Furthermore, the patient’s perception of LBP is believed to have evolved over time. As Robertson noted, there exists a direct link between rising LBP diagnoses with “the multiplication of health services, the improvement of diagnostics, [and] people perceiving pain in a different way” [14].

1.2. Introduction to Chronic Low Back Pain

When the source of LBP is readily identifiable, it is classified as being acute or pathology specific. However, up to 95% of LBP is classified as non-specific, meaning that there is no identifiable pathology associated with its cause [47, 48]. A particular type of non-specific LBP that causes patients, healthcare providers, and society in general much distress is chronic low-back pain (CLBP). A National Institute of Health Pain Consortium Research Task Force defined CLBP as “a back pain problem that has persisted at least three months and has resulted in pain on at least half the days in the past six months” [3]. This threshold of 3 months or 12 weeks has been widely used in past studies [22, 49-51], and is generally regarded as beyond the window of anticipated recovery. While most cases of acute LBP are resolved within that expected timeframe, there is a fraction that continues to have recurrent pain months and even years later that interfere with work and other

activities [4, 8]. The general prevalence of CLBP is estimated to be between 4-14% [21], and is most prevalent for individuals ages 35-65 [52].

Chronic LBP also entails a severe economic burden on society. Most of the economic resources associated with LBP are consumed by a minority of cases, usually in the form of long-term treatment and compensation benefits [14, 25-27]. Becker observed that patients suffering from CLBP on average have twice the direct and indirect costs of patients suffering from other types of LBP [53]. Hong and colleagues reported that the total healthcare costs for patients with CLBP were double that of matched controls [54].

There is disagreement as to what factors contribute the most to long-risk work absences. Rossingnol attributed primarily physiological issues (namely the location of the injury and the age of the patient) to be most predictive of long-term absences [26], while Robertson found socioeconomic influences to be more determinative of the results (e.g., job placement problems, psychiatric conditions, financial disincentive to work, and faulty medical management) [14].

In addition to the economic consequences to individuals and societies, CLBP can have serious implications to an individual's emotional health. Rainville and colleagues found "increased prevalence of depression, anxiety, substance abuse/dependence, somatization and personality disorders has been documented in patients with CLBP (30-65%) compared with the general population (5-17%)" [43]. Polatin also found higher rates of substance abuse, major depression, and anxiety disorder among a CLBP cohort than the general population [55].

1.3. LBP Treatments

Given the prevalence and multiple consequences of CLBP, it comes as no surprise that it has been the topic of significant research and medical interventions. A wide spectrum of potential diagnostic tests and treatments are available for patients. Studies have attempted to identify which treatment paradigm is superior to others, but without success. Only a handful of specific treatments have shown statistically significant benefits compared to others – and even those may lack clinical significance, long-term efficacy, and sufficient validation for general implementation [3, 14, 56]. It is likely that each treatment is best suited to a specific sub-set of patients. [57]. Unfortunately, a variety of sources (e.g., patient advocacy, professional concerns, increased perception to disability, and unrealistic marketing-driven expectations) often result in unrealistic expectations and medical interventions being applied beyond their scope of scientifically validated applications [14, 58]. It is therefore imperative to understand the aspects of different diagnostic methods and treatment paradigms, including their strengths and limitations. A review of the more commonly used diagnostic and intervention methods is described below.

1.3.1. Current Diagnostic and Intervention Methods

Imaging Techniques (MRI, Ct, X-Rays, etc.)

One of the most commonly used diagnostic techniques is imaging of the spine and surrounding tissue. Because it can assist clinicians identify structural irregularities in the spine it can help find causes for acute LBP. However, it is less efficacious in identifying the cause of CLBP. Past studies have found "no clear association between pain and identifiable pathology of the spine" in cases of CLBP [3]. Even if there is relevant information garnered from the image, it frequently only confirms what the clinician already suspected rather than providing new information [19]. Furthermore, not all structural irregularities identified in spinal images elicit pain. Positive findings of structural deformities are also common in individuals who do not experience LBP [2, 14, 58]. Deyo and colleagues found that using static images to inform treatment decisions for patients with CLBP did not improve outcomes [58]. Consequently, it is difficult to deduce optimal treatment paradigms based solely on static images of the spine [48, 59].

Opioids

Opioid use is an extremely common method of treating the symptoms associated with CLBP. Deyo and colleagues reported that the use of opioids increased by 108% from 1997 to 2004, even while inflation-adjusted prices increased by 431% during that same period [58]. However, the current consensus on the efficacy of opioids is under scrutiny. Deshpande reported that “more high quality studies are needed to address the benefits and risks of long-term opioid use in CLBP, their relative effectiveness compared with other treatments and to better understand which patients may be most suitable for this type of intervention” [60]. The benefits of opioids over nonopioid analgesics only slight, and individuals who rely on opioids for long-term management of CLBP experience persistent pain and a low quality of life [58, 61]. There are also several potential adverse side-effects related to opioid use, including hyperalgesia, hypogonadism, constipation, nausea, sedation, increased risk of falls and fractures, depression, sexual dysfunction, and potentially (and ironically) increased sensitivity to pain [58, 62]. Furthermore, the rate of deaths related to opioid overdoses has increased proportionally to the rate of opioid prescriptions. Overall, it is recommended that opioids be prescribed judiciously to individuals experiencing severe pain that is unlikely to be controlled by other methods and should be transitioned to other interventions when possible [58].

Spinal Injections

Deyo and colleagues report a 271% increase in spinal injections over seven years and a 629% increase in fees and charges during the same approximate period. However, despite the dramatic increase in spinal injection applications and costs, there appear to be no physiological improvements from spinal injections: multiple randomized experiments show that spinal injections do not decrease the rate of subsequent surgery. The only benefit is temporary pain relief, and only for axial pain [58].

Surgery

Studies highly encourage careful patient selection before opting to perform surgery. Spinal surgery is an aggressive form of treatment, but it does not necessarily produce better outcome for patients [58]. Keller and colleagues observed that patients in areas with low surgery rates had better treatment outcomes than patients from areas with high surgery rates. There were statistically significant differences observed in the Roland disability score, quality of life, and satisfaction [63]. Andersson observed that rate of LBP-related surgeries significantly differed between countries, and concluded the rate of LBP-related surgeries is more dependent on “cultural differences, differences in practice patterns, and the availability of health-care providers” than simply LBP prevalence [4].

This does not neglect the need for surgical intervention in appropriate cases. When there is a clear and severe source of pain – such as a nerve root compression – the rate of surgery success increases. However, the likelihood of a positive outcome decreases if there are less definite factors, such as a bulging disk [64]. Webster conducted a controlled study on 280 patients who sought treatment for LBP caused by disc herniation. The group was divided into three classes – those who clearly required immediate surgical intervention (67 patients), those who exhibited uncertain need for surgical treatment and were assigned a surgical intervention (126), and a third group that was assigned conservative treatment (87 – 17 of whom were operated on after conservative treatment proved insufficient). Surgery proved to be more effective after 1 year, but no statistically significant difference was observed between the groups after four years [65]. Overall, due to the options of less-dramatic alternatives and its highly invasive nature, surgery is considered

the last resort for treating LBP. However, in cases where it is necessary, surgery should not be significantly postponed because delaying needed surgery beyond 12 weeks could compromise the outcome [14].

Exercise

One intervention with a very low associated risk is physical activity. While it is still under investigation to determine the causal effects of exercise that assist patients, there is a plethora of evidence that physical activity is associated with better lifestyles and improved health [4, 14, 20, 43, 66-69]. Researchers propose four possible explanations as to how physical activity assists patients:

1. Reduces pain: Multiple studies have found exercises treatments to reduce back pain intensities, ranging from 10-50% efficacy [43]. Robertson suggested that the general effects of exercise include improved sleep, decreased stress, and improved attitude – offering patients an alternative method of mitigating pain other than relying on medication [14].
2. Improves physical function and general health: Multiple studies have shown that stretching improves trunk flexibility for patients with CLBP (when long-term compliance with a therapeutic is maintained) [43], while prolonged rest and recovery inhibit healing [14]. Exercise has the capacity to enhance spinal stabilization, increase muscle strength, restore posture, and improve neuromuscular control [68, 69].
3. Facilitates the process of overcoming fears: Rainville et al. observed that patients' attitude and beliefs highly affect patient outcomes, and that with repeated exposures to stresses, the human body and mind adapt through neurological desensitization, thereby reducing the pain experienced by patients with (c)LBP [43]. Fordyce et al. also recommended prescribing exercise in a quota-based manner (i.e., not subject to modification in response to pain) as part of a “fear-desensitizing process” [69].
4. Prevents the occurrence / recurrence of LBP: Multiple studies have observed that the prevalence of LBP is lower among healthier populations or postulated that exercise reduce the risk of LBP occurrence / recurrence [4, 14, 20, 43].

Despite its multiple benefits and low risks, exercise alone is not a complete solution for patients suffering from CLBP. Not all patients respond to conservative treatment, and even for those it assists it is not a complete solution. Therefore, “the role of exercise co-interventions must not be overlooked” [70].

1.3.2. Need for a Precision Medicine Technique

Despite the wide variety of potential treatment options, recent advancements in medical technology, and shocking increases in medical-related expenses (particularly in developed countries), CLBP is a growing issue. More individuals are reporting having CLBP and musculoskeletal disability. There are also significant increases in the resources being dedicated towards CLBP. Beneficiaries claiming Social Security Disability Insurance increased from 20.6% to 25.4% over the course of eight years, as the rate of disability for other conditions (e.g., circulatory, repository) has decreased. “Recent studies document a 629% increase in Medicare expenditures for epidural steroid injections; a 423% increase in expenditures for opioids for back pain; a 307% increase in the number of lumbar magnetic resonance images among Medicare beneficiaries; and a 220% increase in spinal fusion surgery rates” [58]. Other types of interventions - surgical, injections, pharmacologic, and nonpharmacologic alike – have also been applied at increasing rates. Regardless, the prevalence of CLBP symptoms and office visits attributed to LBP remain consistently high [3, 9, 14]. Unfortunately, the increased financial resources dedicated to treating CLBP is an overutilization of medical care and has led to increases costs rather than improved outcomes [14, 58].

This alarming trend indicates that current interventions are not effective enough. There are two potential conclusions that could be taken from this.

1. It could be that there simply does not exist a satisfactory cure for CLBP. Efforts should be dedicated towards prevention and developing a “chronic care model” to manage symptoms, educate in self-care, provide social support, and facilitate a return to work. Realistic expectations need to be set for what can be accomplished for patients rather than marketing false rhetoric of permanent and complete cures [58].
2. Rather than persisting in the current status quo, the basic science that drives CLBP should be investigated. Genetic, central nervous processing, environment, and psychological factors need to be reevaluated and further understood. New intervention techniques should be developed and rigorously tested [14, 58]. Further research should be conducted to develop a precision medicine technique that connects a patient to their optimal treatment paradigms [57], improving treatment outcomes, expediting recovery, and reducing financial costs [48].

There is likely an element of truth to both hypotheses: realistic expectations should be set for patients with CLBP, and there are also possible means of improving the efficacy of medical interventions. The solution to improving assistance for patients must be very comprehensive. It must include the promotion of healthy habits and prevention measures, it needs to incorporate the psychosocial components of CLBP as well as the physiological debilitation, it needs address the short-term need for reprieve and the long-term need for recovery, and it needs to be tailored according to each patient’s individual needs [57, 71]. Emphasis should be placed on restoring patients to functionality and work [58]. The motivation that inspires this work is to develop a potential precision medicine technique: motion-based phenotyping.

1.4. Motion-Based Phenotyping – a Promising Solution

Phenotyping is the process of classifying specimens according to their manifested, observable characteristics. Biomechanics is “a rich target for phenotyping [because it] represents the common final output through which all biopsychosocial constructs of back pain must pass” [44]. This is especially true of spinal mechanics due to its central role in performing physical activities. Patients intrinsically recognize motions and postures that trigger discomfort and compensate for degenerative spines with abnormal motions. “All biopsychosocial changes associated with LBP have the potential to modify how an individual tolerates, generates, balances, and responds to tissue loading, which in turn impacts how an individual with LBP executes a movement” [44].

Our primary objective in this application is to identify phenotypes of human spinal motion that are both characteristic of healthy spines and indicative of the presence of CLBP. It is our hypothesis that if we can identify an individual’s spinal-motion phenotype and convey that information to clinicians, that clinicians could then use that information to select (and potentially develop) the most relevant treatment paradigm to assist that patient.

1.4.1. Preliminary Evidence for Phenotyping

This phenotyping approach is highly analogous to other studies that have analyzed the relationship between gait and dysfunctions such as Parkinson’s disease [72], dementia [73], Alzheimer’s Disease [74], cerebral palsy [75], vascular burden [76], concussions [77], and musculoskeletal injuries [78]. Each of these ailments result in statistically significant alterations in gait mechanics, thereby making gait analysis an important tool for assessing patients’ conditions.

There is also substantial evidence that supports spinal-motion phenotyping. It has long been recognized that LBP alters motion. A plethora of studies have found differences in the motion between persons with and without (C)LBP [44]. Their findings report that individuals with LBP exhibited lower range of motions [79-81], smaller velocities [79, 81], weaker muscles [43], worse balance and proprioceptive sense [82], different

gait characteristics [83], and other functional tasks [83]. These differences in motion have been used to classify individuals as either having LBP or being LBP asymptomatic with as high as 94% accuracy [46].

Distinct pathologies of low back pain have been linked to specific changes in movement patterns [84]. Individuals with spinal instability are easily fatigued [85]. Cumulative microtrauma on the zygapophyseal joints cause individuals to avoid either excessive extension [86] or lateral bending to the afflicted side [87]. Proteoglycan decrease in the intervertebral discs result in reduced range of motion and nonspecific pain exacerbated pain by forward flexion [88-90]. Individuals with central stenosis in the vertebral and intervertebral foramina spend more time in flexion and avoid extension [91]. Patients with lateral stenosis in the vertebral and intervertebral foramina experience more pain from standing, walking, extension, side-bending, and rotation. [92]. It has been postulated that medical interventions may be enhanced by targeting these motion deficiencies [93]. This hypothesis has been supported by Barilay and colleagues, who report that following treatment, patients with LBP reported lower pain scores and exhibited improvements in motion characteristics (i.e., their motion was more similar that of a LBP asymptomatic cohort) [83].

1.4.2. Challenges to Phenotyping

Despite the promising indications and the enormous potential for motion-based phenotyping, there is yet to be precision medicine algorithms to guide treatment prescriptions for patients with CLBP in clinical practice [3, 57]. There are still significant challenges that need to be addressed before implementing a precision medicine phenotyping approach in a clinical setting, namely the following: (1) patients with CLBP represent a wide and heterogenous group, making it difficult to develop a generalized solution for the entire population; (2) CLBP is a multifactorial issue that involves many biopsychosocial aspects; and (3) the lack of precise, economic, and user-friendly motion-monitoring device [94].

Heterogenous Spectrum of CLBP

Low back pain is a broad term that encompasses a wide spectrum of ailments and a broad scope of severities. Chronic low back pain is an even more obscure diagnosis that heavily relies on self-reports rather than standardized medical tools [4, 21]. As such, each study must make judgement calls regarding which individuals represent the population suffering from CLBP. Some studies only investigate patients with well-documented LBP [46]. Other studies explicitly ignore severity or other qualifiers for being too restrictive [3, 17]. Most studies only investigate relatively small groups (e.g., 10-30 participants per group) [44]. All these effects make it difficult to make conclusions general to the entire population of patients with CLBP [6, 44].

Furthermore, it has been suggested that subgroups of patients suffering from LBP “exhibit nearly opposing biomechanical performance, which, if not accounted for, could diminish the ability to discriminate between those with LBP and without” [44].

Multifactorial Influences

Chronic LBP is described as nonspecific and idiopathic, meaning that it cannot be attributed to a recognizable pathology [3, 22]. Deyo and colleagues hypothesized that CLBP may be the effect of multiple biologic and behavior etiologies. Even if a specific pathoanatomic condition existed and could be identified, specific interventions for that condition may fail because it only accounts for one of the many underlying root causes [3].

In addition to the many potential physiological ailments that could result in CLBP, there is believed to be many psychological, genetic, socioeconomic, cognitive, and other factors involved as well [43, 48]. Several

studies have suggested that CLBP is “more socioeconomic than something that can be cured with knives, physiotherapy, and drugs” [14]. There has also been a significant increase in diagnostic health services in recent years, perhaps causing the population to perceive pain differently than before. This shift in perception makes it difficult to determine whether biological morbidity is actually on the rise or whether there is merely a heightened awareness of pain and symptoms that have always existed [95].

There is also evidence that LBP may be initiated as acute injuries, but then evolve into highly complex conditions involving functional changes in the central nervous system [3]. Christe and colleagues observed that individual who suffer from CLBP often demonstrate abnormal motion even when a specific task does not elicit pain, “implying a reorganization of motor tasks planning” [93]. Thus, dysfunctions that begin as recognizable pathologies morph into complex conditions that have far-reaching effects on the body’s nervous system and anatomical structure.

Need for objective Motion-Monitoring Techniques

The third major obstacle that is inhibiting the development of a precision medicine algorithm for treating patients with CLBP is the lack of objective, quantitative assessment techniques. Many clinicians will qualitatively and visually assess a patient’s condition and performance of different tasks, and then consider those assessments when prescribing a treatment paradigm for patients. Past studies have found this is only somewhat effective, and only when the clinicians are extensively trained to use a classification system [96]. Clinical inexperience and misdiagnosis can lead to delayed recovery and suboptimal use of medical resources [44]. Rather than rely on subjective observations, another possibility is to incorporate an objective motion-monitoring device. This could lead to improved efficacy in selecting the optimally suited treatments for patients according to their individual cases and symptoms.

1.4.3. Plan to Effectively Identify Phenotypes

In 2019, the National Institute of Health (NIH) launched the Helping to End Addiction Long-term (HEAL) initiative to combat the rising rates of opioid related deaths. Part of that initiative was the Back Pain Consortium (BACPAC) Research Program to reduce opioid dependence for managing CLBP symptoms. BACPAC is a multi-stage research program that involves multiple universities to better understand the science of CLBP, why patients respond differently to different interventions, and develop novel treatments and methods for linking patients to their optimal treatment paradigms. The overarching goal is to develop a precision medicine approach that can be applied in clinical settings and everyday activities [57]. This initiative is well-equipped to overcome the current challenges listed above in developing a precision medicine approach to CLBP.

First, multiple cohorts - comprised both of individuals who do and do not experience CLBP symptoms – will be recruited for the study at various research sites across the country. This will provide a broad and encompassing representation of the population who suffer from CLBP and their CLBP asymptomatic counterparts. The heterogeneous range of patients who suffer from CLBP and asymptomatic individuals who may be at risk of developing CLBP will be represented.

Second, data is thoroughly collected from study participants to account for the different biological, psychological, socioeconomic, physical characteristics, and demographics that have been identified to influence CLBP prevalence and severity. The incorporation of these features will enable researchers to better account for the multifactorial aspects of CLBP, which has the potential to reveal additional biologic-behavioral interfaces and improve our understanding and treatment of CLBP [3, 96].

Third, multiple BACPAC Tech Sites are working towards developing and validating innovative tools and technologies to better assess individuals' conditions. Multiple motion-monitoring technologies are being developed during this initiative [44].

1.5. Understanding Metrics of Wellbeing

A key step of being able to assist patients who suffer from CLBP is understanding patient wellbeing. The effects of CLBP and other ailments are often quantified using patient-reported outcomes (PROs). PROs are being implemented by healthcare providers with increasing frequency to inform clinical decisions [97]. There are PROs that quantify pain intensity, disability, anxiety, depression, physical activity, and more [97-103]. Although PROs are prone to biases due to self-assessment and unique individual perceptions, individual may therefore be a more important metric than other standards [104].

Substantial research has been conducted that evaluates the average PROs among patients suffering from different ailments [105-107], analyzes the change of PROs prior to and following intervention [108-114], identifies underlying factors to reduce the dimensionality of PROs [115, 116], and quantifies the correlation between different PROs among symptomatic patients [117-123]. However, to the authors' knowledge, there has yet to be a study that evaluates the moderating effects on the relationships between PROs. While the correlation between related PROs (such as disability and physical impairment) may naturally be assumed to be strong, confounding biopsychosocial factors may obscure the relationship when assessing patients with CLBP, and merit further investigation [124].

1.6. Motion-Capture Systems

An essential and major component of the BACPAC initiative is to monitor spinal motion. Spinal kinematics will be then used to inform research and clinical decisions. This approach has shown tremendous potential in past studies [43, 57]. An accurate and user-friendly motion-capture device is therefore needed for this research.

The highest standard of motion capture may be optical cameras with reflective markers. However, although they provide a high level of accuracy, they require significant cost, time, and training. Furthermore, motion-capture markers can only be implemented in a highly controlled environment, limiting the versatility and potential applications of this technology. There is a plethora of emerging technologies aiming to fill the need for adaptable and economic motion-capture devices [44]. One such device – the high deflection strain gauge (HDSG) – provides a particularly intriguing and innovative solution which merits further addition.

1.6.1. Background on Strain Gauges

Traditional strain gauges, though extremely tested and implemented in a variety of settings, are insufficient to meet the needs of biomechanical applications. Conventional strain gauges can only endure approximately 5% strain, after which the sensors become permanently deformed or fail altogether [125]. Hence the need for a highly elastic (up to 100% strain), robust (i.e., holds up over time and repeated applications), and biocompatible gauges. In addition to health and performance monitoring, it has been postulated that these sensors would have additional applications in robotics and entertainment technology [126]. Currently, there are two general classes of HDSG: capacitive and resistive.

- Capacitive strain gauges: Capacitive-based strain gauges operate on the principle of Poisson's ratio (as they are stretched, the conductive cross-sectional area diminishes). This type of strain gauge exhibits extremely stretchable strain properties and linear gauge factor analyses. However, there are major drawbacks that limit its efficacy in biomechanical applications, including "low gauge factors, unpredictable response due to unstable overlaps of the capacitive area, and capacitive interaction with the human body" [126].

- Piezoresistive strain gauges: In contrast to the capacitive strain gauge, piezoresistive strain gauges are generally comprised of a highly elastic base matrix (e.g., silicone), mixed with conductive nanoparticles [127]. Some of the drawbacks to piezoresistive strain gauges include creep, hysteresis, stress relaxation, temperature-influenced properties, and nonlinear gauge factors [125, 128-130]. However, they also demonstrate highly flexible material properties and a much higher gauge factor than the capacitive strain gauges (on the order of 10^3 - 10^4) [125]. They also provide the advantage of a relatively easy fabrication [128]. Carbon-based conductive materials, such as carbon nanotubes “have been extensively used as conductive fillers in wearable sensors because of their excellent electrical conductivity, low cost and potential for mass production, high chemical, and thermal stability, inherent flexibility, and ease of chemical functionalization” [128]. These are some of the key property characteristics necessary for biomechanical applications [131].

Overall, piezoresistive strain gauges have the advantage over capacitive strain gauges. The capacitive interactions with the human body make capacitive strain gauges an impractical tool, and the low manufacturing costs of piezoresistive strain gauges is ideal for widespread application. Despite the enormous potential for piezoresistive strain gauges for their biomechanical and other applications, there are still improvements needed for the sensors to achieve their optimal properties and performance. The primary challenge is the viscoelasticity of the sensor matrix. Past studies have identify the poor interfacial adhesion between the nanoparticles and elastic matrix as the source of the viscoelasticity [126]. The mechanical and electrical properties of the sensors are highly intertwined. Hence the electrical signal of the sensors exhibits significant hysteresis, signal drift, and other stress-dependent phenomena. The relationship between resistance and strain is dependent on how much the sensors have been elongated. Sensors with high tensile strength exhibit low hysteresis [128]. It is therefore imperative to understand both the mechanical properties and the electrical properties of these sensors to optimize performance. Past studies have used a variety of models (both mechanical and electrical) to investigate sensor properties.

- Material Models: Multiple materials models have been used in the past to describe viscoelastic behavior. One of the more commonly used is Burger’s model, which captures the elastic, viscoelastic, and viscoplastic responses of a material through a series of springs and dampers (see Figure 1.1a). However, it tends to oversimplify the response of viscoelastic materials and is unable to use a consistent set of parameters to model materials under different scenarios. The Konotou-Zacharatos (KZ) model, uses a similar approach but accounts for nonlinearities in model parameters (see Figure 1.1b). This has been proven to be more accurate for modeling nonlinear viscoelastic materials, such as polycaprolactone [132].

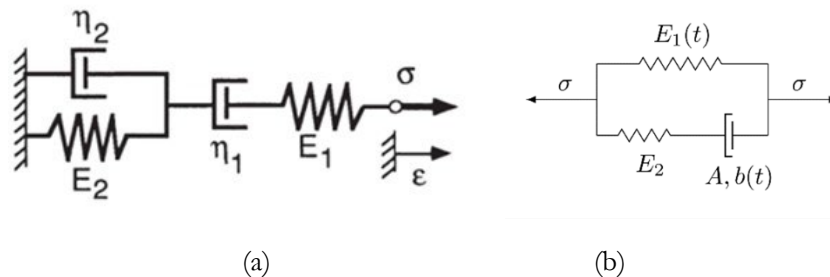


Figure 1.1 Depiction of (a) Burger's viscoelastic model and (b) the KZ model that accounts for nonlinear viscoelastic behavior. The Burger’s model captures fundamental viscoelastic behavior (E_2 , η_2), viscoplastic behavior (η_1), and elastic behavior (E_1). The KZ also captures these same aspects, but accounts for nonlinearities and time-dependencies in model parameters.

- **Electrical Models:** There have been multiple studies dedicated to developing a model that relates electrical signal to the load (either in terms of strain or stress) of piezoresistive strain gauges. These sensors operate on the principles of percolation theory and quantum tunneling. On a microscale, the silicon between conductive nanoparticles acts as a barrier to quantum tunneling. The quantum resistivity of the barriers is a function of the filler material properties and the distance between nanoparticles. As the sensor is stretched, the nanoparticles draw closer together, thereby decreasing the net sensor resistance [133]. The overall effect is that the sensors are piezoresistive in nature. Clayton's equation [133] describes quantum resistivity (ρ) a function of Planck's constant (h), electron charge (e), electron mass (m_e), barrier height (λ), and junction gap distance (s) as depicted in Equation 1.1.

$$\rho(s) = \frac{h^2}{e^2 \sqrt{2m_e \lambda}} e^{4\pi \sqrt{\frac{2m_e \lambda}{h}} s} \quad 1.1$$

Multiple studies observed an exponential decay, or bi-exponential decay, in resistance following an incremental increase / decrease in stress applied to the sensor (similar to the stress response of the material as predicted by the Burger's model) [128, 134-136]. Some of these models are explicitly restricted to modeling low-to-intermediate strains [128]. Other studies relied on empirical evidence to investigate the relationship between strain and resistance but fail to differentiate between the transient viscoelastic resistance and the steady-state quasistatic resistance [127, 137]. A model that accounts for both the quasistatic and dynamic responses of these sensors (such as the one described in Chapter 2) would be essential for implementing HDSG as biomechanical sensors and other desired applications.

1.6.2. BYU Strain Gauges

At Brigham Young University, such strain gauges have been developed. They are comprised of an Ecoflex 00-30 silicone matrix embedded with nickel coated carbon fibers and nickel nanostrands. The concentration of each material (by weight) for the sensor recipe is 64% silicone, 30% NCCFs, 5% NINs, and 1% surfactant. The nanoparticles and surfactants are mixed in the silicone matrix, then extruded into molds. The sensors are cured at 88°C under a vacuum pressure of 650 mmHG for 135 minutes, and then at 192°C for an additional 30 minutes.

These sensors have already been applied to several biomechanical applications, such as estimating knee kinematics [138], calculating ground reaction forces [139], measuring ligament strain [140], estimating range of joint motion [141], tracking pulse [142], and monitoring fetal movements [143]. The next application of using an array of these HDSG to identify spinal-motion phenotypes among patients with CLBP will likely undergo higher and repeated strains than in previous applications. Therefore, the need for a model that interprets electrical resistance to strain which accounts for the viscoelasticity is needed, as well as an optimized sensor to mitigate undesirable performance traits.

1.7. Dissertation Outline

1.7.1. Summary of Accomplishments

This research endeavor has a three-fold purpose. The first is to characterize and improve the performance of the HDSG described above in preparation to monitor spinal motion. The second is to understand how different components of wellbeing are related to each other and what the distinct components of wellbeing are. The third is to identify phenotypes of spinal motion, using the spinal kinematics collected using the HDSG described above, which have the potential to be clinically significant and inform a precision medicine technique for assisting patients who suffer from CLBP. The research conducted regarding these objectives is described in the subsequent chapters according to the following.

Chapter 2 describes the model that was developed to interpret strain as a function of resistance and time. This is the first model that the author knows of which accounts for the quasi-static and dynamic effects electrical responses due to sensor viscoelasticity. This work was published in 2022 in the *Sensors* academic journal [144].

Chapter 3 presents the development of a multilayered architecture to mitigate sensor viscoelasticity, improving the sensor performance under much higher strains. This work was presented at the 2023 Composites and Advanced Materials Expo Student Symposium and is currently being prepared for publication.

Chapter 4 describes three analyses that were conducted to better understand the relationship between CLBP and PROs. The first was to compare the average PROs of subjects with CLBP (i.e., cases) with the average PROs of subjects who do not experience CLBP (i.e., cases). The second was to evaluate the relationship between different PROs using linear regressions, accounting for the presence of CLBP as a potential moderating factor. The third was to identify the distinct components of wellbeing using an exploratory factor analysis on the PROs to identify latent factors (i.e., underlying dimensions which summarize the observed features). This work is currently being prepared to be submitted to *The North American Spine Society Journal* (“*NASSJ*”).

Chapter 5 presents the protocol for the BACPAC Research Program to identify phenotypes of spinal motion that will be used in future works. This includes the developing and validation of the SPInal Nanosensor Environment (SPINE Sense System) used to monitor spinal kinematics, the subject testing protocol, and the proposed data analysis methods that were developed to accomplish this task. This work was published in the 2023 *Pain Medicine* academic journal [145].

Chapter 6 presents the results from the protocol analysis described in Chapter 5. This work analyzes the relationship between spinal motion and different PROs, a machine learning model that predicts PROs as a function of demographics and spinal kinematics, an identification of phenotypes among subjects with and without CLBP, and the potential clinical application of phenotypes in treating CLBP.

1.7.2. Future Work

The follow-up from the BACPAC study will be the Biomarkers for Evaluating Spine Treatments Trial (BEST) program. The BEST study will be a multi-site, multiple assignment randomized trial to evaluate four potential interventions: acceptance and commitment therapy, duloxetine, evidence-based exercise and manual therapy, and enhanced self-care. Each participant will complete two randomly assigned 12-week treatments and periodically assessed [57]. Treatment efficacy will be evaluated by PROs [57] and spinal kinematics to reduce inter-clinician variability [44]. It is our hypothesis that these clinical experiments, facilitated by the phenotype analysis presented in this work and from other sites, will enable clinicians to select treatment paradigms individually tailored according to patient conditions. This in turn will improve treatment efficacy, improve the quality of life for the millions of patients suffering from CLBP worldwide, and save millions of dollars in medical resources worldwide every year.

CHAPTER 2 ACCOUNTING FOR VISCOELASTICITY WHEN INTERPRETING NANO-COMPOSITE HIGH-DEFLECTION STRAIN GAUGES

Sensor model published manuscript [144]. I hereby confirm that the use of this article is compliant with all publishing agreements.

Authors: Spencer A. Baker¹, McKay D. McFadden¹, Emma E. Bowden¹, Anton E. Bowden¹, Ulrike H. Mitchell², David T. Fullwood^{1,*}

¹ Department of Mechanical Engineering, Brigham Young University, Provo, UT 84062

² Department of Exercise Sciences, Brigham Young University, Provo, UT 84062

* Correspondence: dfullwood@byu.edu

2.0. Abstract

High deflection strain gauges show potential as economical and user-friendly sensors for capturing large deformations. The interpretation of these sensors is much more complex than it is for conventional strain gauges due to the viscoelastic nature of the strain gauges. This research endeavor developed and tested a model for interpreting sensor outputs that includes the time-dependent nature of strain gauges. A model that captures the effect of quasi-static strains is determined by using a conventional approach of fitting an equation to observed data. The dynamic relationship between strain and resistance is incorporated by superimposing dynamic components onto the quasi-static model to account for spikes in resistances that accompany each change in sensor strain and subsequent exponential decays. It is shown that the model can be calibrated for a given sensor by taking two data points at known strains. The resulting sensor-specific model was able to interpret strain gauge electrical signal during a cyclical load to predict strain with an average mean absolute error (MAE) of 1.4% strain, and to determine the strain rate with an average MAE of 0.036 mm/s. The resulting model and tuning procedure may be used in a wide range of applications such as biomechanical monitoring and analysis.

Keywords: high-deflection strain gauges; nanocomposites; modeling; viscoelasticity

2.1. Introduction

It has been postulated that surface-mountable high-deflection strain gauges can provide an economical and user-friendly solution in myriad motion-capture applications, such as human biomechanics and soft robotics. Conventional strain gauges can only endure approximately 5% strain, compared with potential skin strains of larger magnitudes; recently developed strain gauges, composed of conductive nanoparticles embedded in a silicone matrix, however, perform well at higher strains [125]. These sensors operate on the principles of quantum tunneling and percolation theory [133]. As the strain gauges are stretched, their electrical resistance decreases, causing the sensors to behave as inverse-piezoresistive sensors. Such sensors can also display a high sensitivity factor in the desired range of deformation during a typical quasi-static response [127, 146].

Interpreting the sensor output during multiple cyclic strains, however, is more complex than analyzing the output during quasi-static behavior. Due to the viscoelastic mechanical properties of the strain gauges, the gauge factor is dependent not only on the instantaneous strain, but also on previously applied strains, and on the recovery time since those applied strains [133]. The purpose of this research endeavor is to discover the time-dependent relationship between sensor strain and electrical response, accounting for the relevant

viscoelastic mechanical properties of the strain gauges. The uncovered relationships will be captured in an appropriate model, and the model performance during cyclical stresses and relaxations will be assessed.

Since deformation within the strain gauge largely happens in the polymer matrix, it could be assumed that a standard rheological model captures their mechanical response and provides valuable insights regarding the electrical behavior. Several models have been postulated to capture the viscoelastic mechanical behavior. Burger's model depicts the relationship between strain, strain rate, and resulting stress of viscoelastic materials; and Weibull's model predicts the strain relaxation of sensors after stresses are removed. [132, 147, 148] These two models provided valuable insight regarding the electrical behavior of the sensors under dynamic loading and relaxation conditions.

One application that motivates the current study is to detect and quantify spinal biomechanics by adhering an array of such sensors to a subject's lower back. The results of this study will potentially offer valuable insights when used as a diagnostic tool. For example, the most common diagnostic methods for identifying the source of low back pain employ static imaging (e.g., CT or MRI scans) to detect anatomical anomalies. It is difficult to pinpoint the etiology of chronic low back pain (CLBP) [59] using these methods because CLBP patients do not always exhibit clear anatomical anomalies in their spine [149]. Rather, their pain is the result of multiple psychological, social, and biological factors [4] that cannot be depicted in a scan. An alternative to using static diagnostic imaging is to analyze a patient's spinal motions. To execute this alternate method, a valid and reliable quantitative assessment tool is necessary in order to objectively assess and track spinal health [150]. Such a tool could be used for the objective monitoring of patient progress, i.e., improved movement patterns. In addition, it could also lead to the discovery of more efficient treatment paradigms for the millions of chronic low back pain patients worldwide. Furthermore, the information gleaned from the viscoelastic characterization of the sensors will be relevant to the application of strain gauges in other fields, such as applications in soft robotics, human-machine interfaces, and other biomechanical analyses [125, 129, 138, 140, 143].

2.2. Materials and Methods

The nanocomposite sensors are composed of Ecoflex 00-30 silicone with nickel-coated carbon fibers (NCCFs) and nickel nanostrands (NINs) mixed in the matrix. Ecoflex 00-30 Silicone was purchased from Smooth-On Inc., and the nanoparticles were purchased from Conductive Composites. The concentration of each material (by weight) for the sensor recipe is 64% silicone, 30% NCCFs, 5% NINs, and 1% surfactant. The nanoparticles and surfactants are mixed in the silicone matrix, then extruded into molds. The sensors are cured at 88°C under a vacuum pressure of 650 mmHG for 135 minutes, and then at 192°C for an additional 30 minutes.

In order to investigate how the strain gauge resistance responds to different loads, a series of tensile tests were conducted using an Instron 3345. The Instron was used to apply precise loads to the sensors and provide measurements of the sensor force and elongation during the loads. Polypropylene grips were applied to the sensor at either end, restricting elongation to the inner portion of the strain gauges (with an initial length of 20 mm). All tensile tests were conducted at room temperature. A pretension of approximately 0.1 N was applied to the sensors prior to the start of each tensile test to avoid initial slack. The sensor's electrical properties during these tests were also measured using a NIH 9215 data-acquisition device.



(a)

(b)

(c)

Figure 2.1 Depiction of (a) The high deflection strain gauges; (b) The strain gauge during a tensile test; and (c) A microscopic image of the sensors under a small load. During tensile tests (b), the sensor was secured between two polypropylene grips. The grips contained a copper metal interior coating to facilitate measuring the strain gauge's electrical resistance at different loads.

2.2.1. Model Development

Due to the viscoelastic nature of the strain gauges, the resistance is dependent on the load applied to the strain gauge and the time that has elapsed since the load has been applied, making the electrical behavior highly nonlinear. A series of tensile tests were therefore conducted to understand and interpret the response of the sensors under different loading conditions and the time following the loading transition.

2.2.1.1. Experimentation

The first tests investigated the mechanical strength of the sensors, specifically to determine the (potentially rate-dependent) linear region of the stress-strain diagram. Guedes found that above certain stress levels, a viscoelastic material's response becomes highly intricate and difficult to model [132]. Our studies have confirmed that beyond the linear region of the nano-composite strain gauges, the electrical output also becomes increasingly complex. The strain gauges were pulled at a constant rate until failure at three strain rates – 0.05mm/s, 0.5mm/s, and 5.0mm/s, which encompassed the expected rates of human skin stretch during motion. The data from these tests were used to generate stress-strain diagrams. The (rate-dependent) elastic modulus of the sensors was estimated as the average derivative of stress with respect to strain within the first 10% strain. The linear region of the stress-strain diagram was calculated on the same basis as estimating 0.2% yield strain in a typical material [147]. Subsequent analysis of the sensor's electrical properties targeted strains within or near the linear region of the stress-strain diagram.

To observe the sensor's response at different elongations, we programmed the Instron 3345 to apply incremental displacements of 0.5 mm (i.e., 2.5% strain increments). After each incremental strain, the sensor was held steady for a period of five seconds to allow initial recovery of stress and resistance in the sensors. This process was repeated until the sensors reached an elongation of 15% strain, after which the sensors were incrementally relaxed in reverse order, at the same rate, back to their original length. This process was repeated for ten cycles. To account for the rate-dependency of the viscoelastic materials [126], the experiment

was repeated at multiple strain rates as before: 0.05mm/s, 0.5mm/s, and 5.0mm/s. Each test was conducted with three strain gauges at each strain rate.

2.2.1.2. Quasi-Static Model

The resistance response of the sensors during deformation involved an initial spike, or overshoot, in resistance relating to the initial change in strain [126], followed by an exponential decay towards a steady-state asymptote. Hence, the strategy for relating the strain imposed on the gauge with the resultant sensor resistance was as follows:

1. Determine a functional relationship between sensor strain and sensor resistance that approximates the steady-state behavior, based upon tabulating and interpolating experimental data.
2. Incorporate the short-term resistance peaks (“spikes”) and subsequent decay into the model based on observations of how strain magnitude and strain rate affect resistance spike magnitude and decay rate.

The quasi-static model captured only the effect of strain (under approximately static conditions) on a sensor’s resistance. Electrical data were collected from the tensile tests at each incremental strain after transient electrical behaviors had dissipated for five seconds. Spline fit curves were implemented to interpolate between the data points ϵ_i and R_i and achieve a relationship between strain and resistance (see Eq 2.1).

$$R = f(\epsilon) = \text{spline}(\epsilon_i, R_i, \epsilon) \quad 2.1$$

As stated previously, sensor resistances operate on the principles of percolation theory and quantum tunneling. This implies that the resistance is highly dependent on the distribution of nanoparticles on a microscopic level [125]. During the manufacturing process, the concentration of nanoparticles embedded in the silicone matrices is approximately uniform. However, even slight variation in the distribution of nanoparticles can have significant effects [133]. The static-strain model $f(\epsilon)$ is therefore specific to each sensor. However, the general trends for all sensors are likely to be similar.

Gauge factor (or sensitivity factor) is defined as the relative change in resistance with respect to strain [125]. High gauge factors provide higher strain resolution. The gauge factor was calculated by taking the derivative of the static model (Eq 2.1) with respect to strain, dividing it by the sensor resistance at its unstretched length, and dividing the product by strain (see Eq 2.2).

$$GF = \frac{\Delta R/R_0}{\epsilon} = \frac{f'(0)/\epsilon}{\epsilon} \quad 2.2$$

Previous studies have found that rubbers “exhibit an appreciable change in their mechanical properties resulting from the first extension” [151] due to the Mullins effect. Initial sensor tests indicate that the strain gauges’ electrical properties during preliminary strains also significantly differ from the electrical properties during later strains. Therefore, during cyclic stresses and relaxations, the first stress-and-relaxation cycle(s) served to precondition the strain gauge pass any initial viscoelastic phenomena that caused inconsistent electrical behavior. In order to determine how many preconditioning cycles were necessary to achieve consistent electrical behavior, the steady-strain model (Eq 2.1) was derived using data from the first, second, third, and fourth cyclic strain cycles. These models ($\hat{f}(\epsilon)$) were used to predict the steady-state strain-resistance relationship for the remainder of the ten stress-relaxation cycles. The mean average error (MAE) of the predictions were used to evaluate model performances and determine how many stress-relaxation cycles were necessary for preconditioning.

2.2.1.3. Dynamic Model

The dynamic strain model accounts for the transient spikes that were ignored in the steady-state strain model. Previous studies have attributed these spikes to viscoelastic stress relaxation [126]. Every time the sensor is pulled or relaxed to a new strain, the internal sensor stresses cause a “change [in] the distance between several [conductive] nanomaterials” [125], resulting in a resistance spike. By this explanation, the sensor’s electrical behavior under dynamic conditions will be heavily influenced by the sensor’s viscoelastic mechanical properties.

For a given applied (macroscopic) strain, the time dependent distance between filler particles will relate strongly to the stress localization in the soft polymer between the ‘hard’ particles, and the subsequent stress relaxation over time. Hence, the magnitude of the resistance spike will presumably be inversely related to the increase of internal sensor stresses. Time dependence of stress and strain in a typical polymer is commonly modeled via the Burger’s rheological model (see Figure 2.2). This model predicts a rate-dependent increase in stress during application of the macro strain, followed by an approximately exponential decay during the stress-relaxation phase. This view motivates the superposition of rate-dependent spikes and subsequent exponential decays in resistance on top of the quasi-static resistance model. The data collected from the incremental strain tests were used to estimate the relative increase in resistance (\mathcal{S}) following an incremental strain step under different strains and strain rate conditions (e.g., if the sensor’s resistance under static conditions is 100Ω and the sensor resistance including the spike is 200Ω , the relative resistance spike magnitude \mathcal{S} is equal to one).

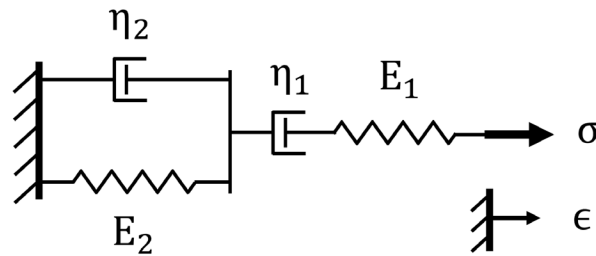


Figure 2.2 Burger's rheological model of viscoelastic materials. The spring and damper in parallel (E_2 and η_2) capture the sensor’s viscoelastic behavior, the spring in series (E_1) models the elastic behavior, and the damper in series (η_1) accounts for the viscoplastic behavior.

During a series of stepwise strain changes applied to the sensor, once the sensor reaches its new macroscopic strain, the internal stresses relax, causing the resistance spike to dissipate. Weibull’s equation describes viscoelastic strain recovery as an exponential decay transition [147]. Preliminary experimental data indicated that the transient mechanical and electrical behavior followed a similar dissipation rate. The time constant (λ) of this exponential decay was estimated from experimental data using MATLAB’s gradient-based optimization algorithm *fminunc*. The criterion for the optimal λ was the predicted stress relaxation response that minimized the sum squared differences between the predicted stresses and the observed stresses. The λ constants were tabulated by strain rate and strain magnitude and were used to predict the rate of resistance spike dissipation.

2.2.1.4 Combined Model

Using the steady-state strain-resistance model (Eq 2.1) and the viscoelastic-dependent parameters (\mathcal{S} and λ), an equation was developed that predicts the sensor response during transitions between strain levels (see Eq 2.3). The model is a function of the quasi-static resistance-strain relationship ($f(\epsilon)$), the resistance spike

magnitude (S), the stress-relaxation coefficient (λ), and the time since the previous resistance spike occurrence ($t - t_s$).

$$R = f(\epsilon) * [1 + S e^{-\lambda(t-t_s)}] \quad 2.3$$

2.2.2 Model Validation

The model was evaluated with a series of tensile tests, during which different strains and strain rates were applied to the sensors. The model performance was evaluated by calculating the r-squared correlation between the observed and predicted response as well as the mean absolute error (MAE) of the model predictions. Three validation tests were conducted to assess the model accuracy.

- Quasi-Static Interpretation: The static-strain resistance model (Eq 2.1) was used to interpret the sensor resistance under static conditions to predict the sensor strain.
- Sensor Output Predictions: The combined static and dynamic-strain resistance model (Eq 2.3) was used to predict sensor resistance as a function of a known strain and strain rate.
- Biomechanical Application: The combined static and dynamic-strain -strain resistance model (Eq 2.3) was used to interpret sensor strain and strain rate during a tensile test that imitates cyclical biomechanical function.

As stated previously, the static-strain model (Eq 2.1) for each sensor is unique due to the variation in the microscopic distribution of nanoparticles in the silicone matrix, and the resistance response during the first stress-relaxation iteration(s) is significantly different than during subsequent repetitions. The first cycle(s) therefore served to precondition the sensors. After preconditioning was complete, the steady-state strain model (Eq 2.1) was calibrated by measuring the sensor resistance at 0% strain and 15% strain. The data point taken at 0% strain was collected after the transient spike had dissipated. The resistance spike at 15% strain had not yet dissipated when the resistance was measured. Instead, the steady-state strain resistance was estimated by dividing the sensor reading by $(1 + S)$. A template of the static strain resistance was obtained from the incremental strain tensile tests, which was scaled and shifted using the two data points to represent the static-strain response of the sensor of interest. The dynamic model parameters (spike magnitude coefficients S and spike decay coefficients λ) were obtained from the incremental strain experiments described above. The model was then used to analyze and interpret the output from the stress-relaxations cycles following the calibration cycle (see Figure 2.3).

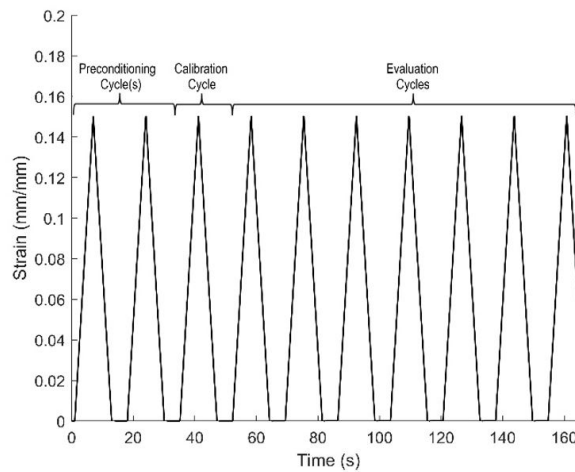


Figure 2.3 Depiction of the strain profile that the tensile tester applied to a sensor, and which cycles constitute preconditioning, calibration, and evaluation stress-relaxations.

2.2.2.1. Quasi-Static Interpretation

The second validation test evaluates the model's ability to interpret strains under approximately quasi-static conditions. After the sensors were preconditioned, and the static-strain model was developed as described above, the sensors were pulled to a series of random strains between 5-15% strain (strains were selected using a uniformly distributed random number generator). The sensors were held at each randomized strain for five seconds, and then relaxed back to the original length. The minimal resistance during the static period was extracted from each repetition and compared the static-strain model (Eq 2.1). This reading was used to interpret sensor strain. A total of ten stress-relaxation cycles were conducted (including preconditioning cycles). These tests were conducted at a strain rate of 0.5 mm/s and repeated with 10 strain gauges.

2.2.2.2. Sensor Output Predictions

The first validation test conducted analyzes the model's ability to predict strain gauge resistance during a known strain and strain rate. Following preconditioning and calibration cycles, the sensors were pulled to 15% strain, immediately relaxed to initial length, and held for five seconds. This process was repeated until 10 stress-relaxation cycles were completed. Using the dynamic-strain model (Eq 2.3) and the known strain and strain rates, the sensor resistance for the evaluation stress-relaxation cycles was predicted. These tests were conducted at rates of 0.05mm/s, 0.5mm/s, and 5.0mm/s. Three sensors were tested at each strain rate.

2.2.2.3. Model Evaluation during Simulated Biomechanical Application

The intended purpose of the high deflection strain gauges is to monitor biomechanical motion. The final evaluation test analyzed the model's ability to interpret elongations such as would be typical during repetitive biomechanical activities. Random strain rates between 0.05 and 5.0mm/s were selected for this evaluation (using a logarithmically distributed random number generator). Strain magnitudes for the analysis were selected between 5 and 15% strain (using a uniformly distributed number generator). The sensors were preconditioned (at the strain rate that was randomly selected) and calibrated using the methods described above to obtain the dynamic-strain model (Eq 2.3). After this, the sensors were repeatedly pulled to the randomly selected strain at the randomly selected strain rate. The dynamic-strain model was used to estimate the sensor strain magnitude by tracing the resistance values to the nearest strain. The strain rate was estimated by dividing the estimated strain magnitude by the time required to reach the maximum strain.

2.3. Results

2.3.1. Model

From the strain to failure diagrams, it was found that the linear portion of the stress-strain curve did not significantly vary between strain rates (see Table 2.1).

Table 2.1 The average yield strain from sensors pulled at 5.0 mm/s, 0.5 mm/s, and 0.05 mm/s. Notice that the linear strain range of the stress-strain diagram was not significantly affected by strain rate.

Strain Rate (mm/s)	Linear Strain (percent)
5.00	11.26
0.50	12.35
0.05	12.41

These results provided us with an initial indication of the linear range of the stress-strain diagram. Subsequent characterization tests of the sensor's electrical and mechanical properties were limited to strains near the linear stress-strain region.

2.3.1.1. Quasi-Static Model

During the incremental strain tests, both the transient and ‘steady-state’ (i.e., the post-spike) response of the sensors were observed. For the preliminary sensor model, we desired to capture only the effect of steady-state strains on the sensor’s electrical resistance. This was accomplished by collecting data points at each incremental strain level (Figure 2.4a) after the transient spike had dissipated (Figure 2.4b). The resulting stress-strain relationship and sensitivity factor are depicted in Figure 2.4c and d.

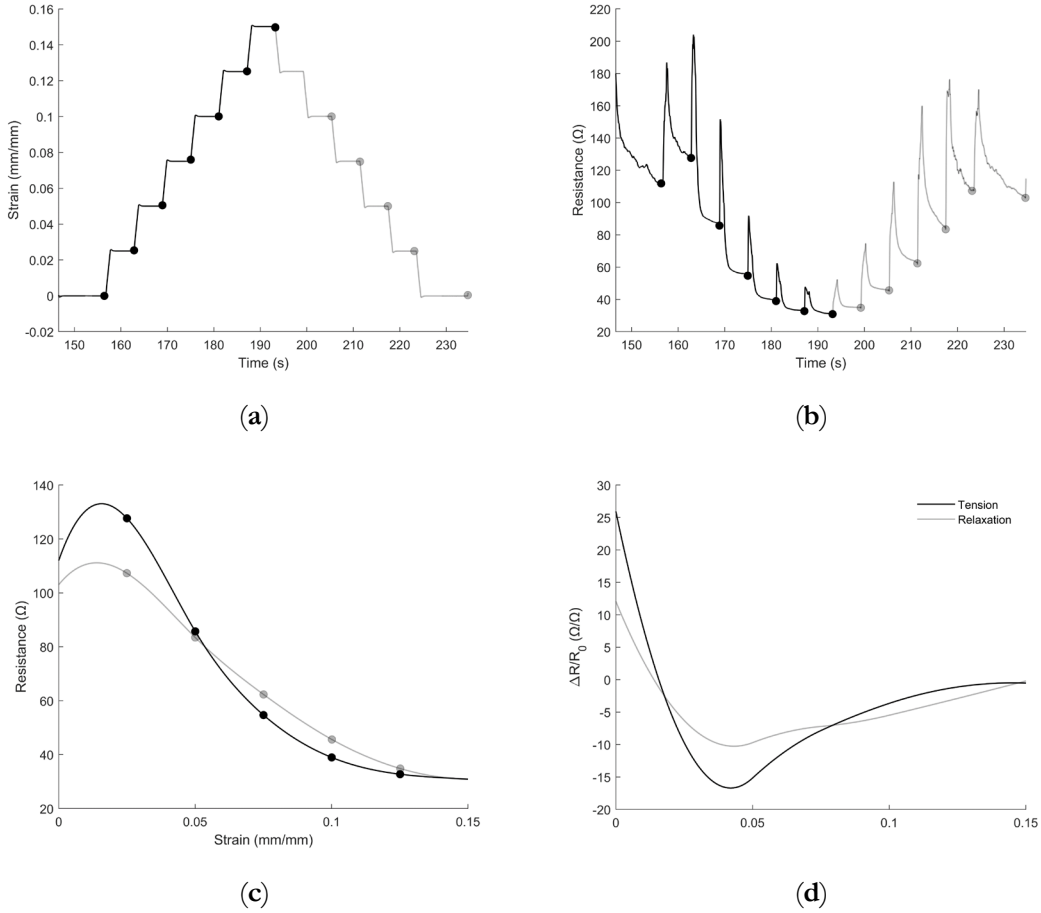


Figure 2.4 (a) The strain profile of an incremental strain test (black line indicates the sensor performances as it is being pulled in tension, and the gray line indicates the sensor performance as it is being relaxed; dots represent the points at which empirical data was collected from the resistance test after the transient spike had dissipated for all sub-figures). (b) The electrical response from the sensors over time as the strain gauges were pulled to different incremental strains. (c) The strain-resistance relationship interpolated from the tensile tests. (d) The gauge factor (relative change in resistance with respect to strain). Spline fit curves were used to interpolate the resistance of the sensor under static conditions between the empirical points. The derivative of the spline fit curves over the spline fit depicts the relative sensitivity of the sensor at different strains.

Using the resistance data points collected during static strains after the resistance spike had dissipated, we determined the strain-resistance relationship by interpolating between data points with polynomial fit curves (see Equation 2.4, Table 2.2).

$$R = f(\epsilon) = c_0 + c_1(\epsilon - \epsilon_0) + c_2(\epsilon - \epsilon_0)^2 + c_3(\epsilon - \epsilon_0)^3, \epsilon_0 < \epsilon \quad 2.4$$

Table 2.2 Coefficients for equation in Eq 4 to describe the strain-resistance relationship during tension.

ϵ_0	c_0	c_1	c_2	c_3
0	1.468 E6	-1.793 E5	4.520 E3	1.383 E2
0.025	1.468 E6	-6.906 E4	-1.697 E3	1.622 E2
0.05	3.629 E5	4.120 E4	-2.394 E3	9.940 E1
0.075	-6.710 E4	1.399 E4	-1.014 E3	5.963 E1
0.10	-8.356 E4	8.941 E3	-4.400 E2	4.194 E1
0.125	-8.356 E4	2.674 E3	-1.496 E2	3.522 E1

The critical strain is defined as the point after which the sensor response becomes monotonic (the strain after which the resistance will only increase / decrease with additional strain) [146]. The critical strain for these sensors is approximately 1.5% strain.

The gauge factor is highly nonlinear. The optimal performance of the sensor occurs at approximately 7-8% strain, after which the magnitude of the gauge factor decreases.

We observed that the resistance of the sensors during the first cycles exhibited significantly different behavior than during the following cycles as well due to primary creep (see Figure 2.5). The model is not intended to capture this highly transient behavior; hence it is calibrated against data from a subsequent cycle. As stated previously, steady-state strain-resistance models $\hat{f}(\epsilon)$ (Eq 2.1) were generated using data collected during the first, second, third, and fourth stress-relaxations cycles to predict the static-strain response of the sensor for the remainder of the ten stress-relaxations cycles. The resulting mean absolute errors (MAEs) are shown in Table 2.3.

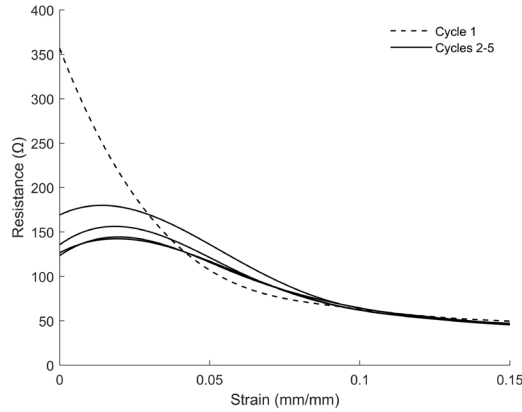


Figure 2.5 Depiction of the strain-resistance relationship during the first five stress-relaxation cycles.

Table 2.3 The steady-state strain-resistance model (Eq 1) was estimated using the first, second, third, and fourth cycles. The resulting mean-squared error of this model (in Ohms) was used to determine how many cycles were needed for preconditioning purposes.

Strain Rate (mm/s)	$\hat{f}(\epsilon)_1$ MAE (Ω)	$\hat{f}(\epsilon)_2$ MAE (Ω)	$\hat{f}(\epsilon)_3$ MAE (Ω)	$\hat{f}(\epsilon)$ MAE (Ω)
0.05	8.51	8.50	5.69	4.64
0.5	17.92	15.18	7.38	5.05
5.0	16.79	11.16	6.40	6.51

It was observed that the MAE generally decreased with each additional preconditioning cycle. However, it was also desirable to develop the static-strain model with as few cycles as possible to maximize the predictive power of the model (e.g., if three preconditioning cycles were necessary, the model would be calibrated during the fourth stress-relaxation cycle and will only be capable of predicting the resistance of the sensor during the fifth stress-relaxation cycle and beyond). The largest reduction in error occurred between $\hat{f}(\epsilon)_2$ and $\hat{f}(\epsilon)_3$. The first two stress-relaxations cycles were therefore utilized for preconditioning the sensors, and the third cycle was used for calibrating the steady-strain resistance model (Eq 2.1).

2.3.1.2. Dynamic Model

During each transition from one strain level to the next, the sensor exhibited a transient resistance spike. The spike magnitude was defined as the increase of resistance from its static-strain resistance (see Figure 2.6). From the incremental strain tests, the increase in resistance under each strain and strain rate condition were obtained. The average S parameters are depicted in Table 2.4.

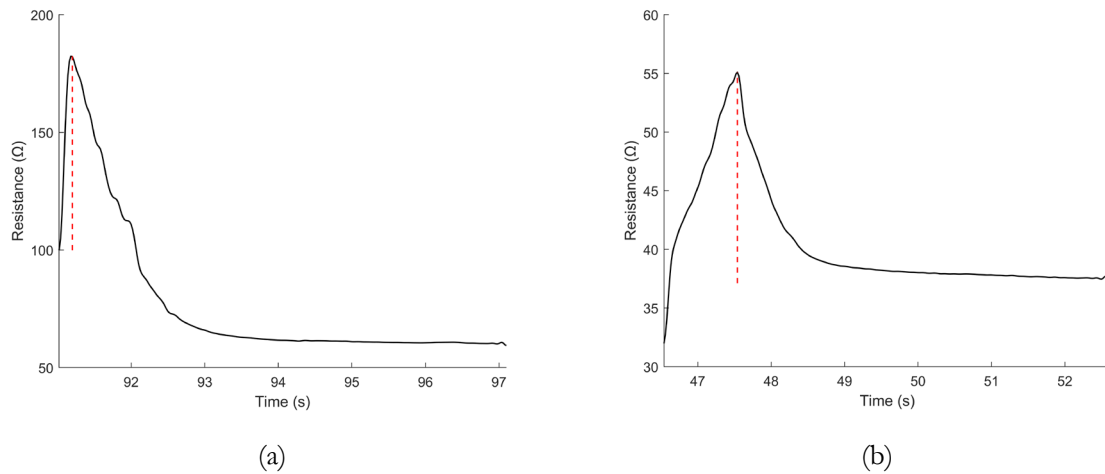


Figure 2.6 The sensor electrical response following (a) an incremental strain step of 0.5mm and (b) following an incremental relaxation step of 0.5mm. The solid black lines indicate the sensor resistance. The dotted red lines indicate the peak of the resistance spike during the transition between strains.

Table 2.4 The spike magnitude, S , (in units of Ω/Ω) was found to be dependent on strain rate. At higher strain rates, the magnitude of the resistance spikes increased. Notice that at low strains, the spike magnitudes are significantly smaller, most likely due to sensor buckling.

Strain Rate (mm/s)	Strain (Percent)						
	0	2.5	5.0	7.5	10.0	12.5	15.0
0.05	0.182	0.187	0.263	0.319	0.230	0.264	0.214
0.5	0.429	0.534	0.673	0.785	0.700	0.566	0.449
5.0	0.915	0.981	1.192	1.358	1.173	0.899	0.751

As expected, strain changes at higher strain rates results in higher resistance spikes. As discussed earlier, if the resistance spike relates to localized and short-lived stress levels between conductive particles, these observations correlate with Burger’s rheological model relating stress to strain and strain rate in viscoelastic materials. Similarly, the stress relaxation behavior of the sensors demonstrated a strong correlation with the resistance spike dissipation (see Figure 2.7). This observation validated our hypothesis that both can be approximated as an exponential decay with time constant, λ , such as is done in Weibull’s model that captures the strain recovery of viscoelastic materials. The time constant, λ , was found to be both rate and strain dependent. The average lambda values observed in the sensors under a variety of strains and strain rates are depicted in Table 2.5 (one outlier was discarded from the data).

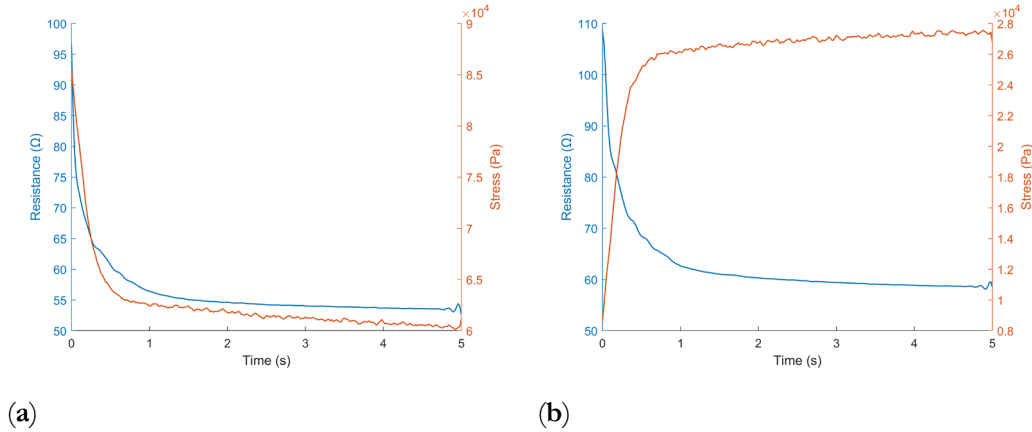


Figure 2.7 Stress relaxation (orange) and transient resistance response (blue) during stress relaxation following an incremental step in tension (a) and following an incremental step in relaxation (b).

Table 2.5 The time constant, λ , (in units of s^{-1}) was found to be rate and strain dependent. At higher strains and strain rates, the sensors exhibited a faster transient response. Notice that at low strains, the stress relaxation constants are significantly lower, possibly due to strain gauge buckling.

Strain Rate (mm/s)	Strain (Percent)						
	0	2.5	5.0	7.5	10.0	12.5	15.0
0.05	0.433	0.718	0.778	0.804	0.818	0.815	0.736
0.5	0.875	1.914	1.979	2.011	2.089	2.220	1.641
5.0	1.121	4.390	3.178	4.051	4.176	4.231	3.391

2.3.1.3. Combined Model

The aim of this study is to provide a model that relates measured resistance to skin strain during a set of cyclical exercises performed by a human subject. The quasi-static and dynamic components of the model described in the previous sections are combined into the final model by taking the following steps. For a given sensor, two preconditioning stress and relaxation cycles from 0 to 15% strain (at any strain rate) are applied to the sensors to mitigate Mullins effects, and a third stress and relaxation cycle is used to calibrate the sensor-specific model. The quasi-static model (Eq 2.1) is fitted to these data points to depict the relationship between static strains and resistance. For the initial sensor used in this study, the parameters of this model are given in Table 2.4; for a different sensor, the curve given by Eq. 2.4 and Table 2.4 is shifted based upon two data points taken at strain of 0 and 0.15.

The parameters for the dynamic component of the model (Eq 2.3) are then obtained by incorporating the resistance spike and exponential decay rate parameters (S and λ) from Table 2.4 and Table 2.5 (which remain

constant for all sensors made by the same route). This model can then be used to predict and interpret sensor output during any sequence of static and dynamic loading conditions.

2.3.2. Model Validation

2.3.2.1. Quasi-Static Model Performance

The model's ability to interpret strains under static condition was evaluated by preconditioning and calibrating 10 sensors. The strain gauges were pulled to a series of randomly selected sequenced strain changes, and the strain was estimated using the quasi-static model described above (Eq 2.1); note that the original sensor used to calibrate the model is not included in the 10 test sensors. The quasi-static sensor model, along with its strain predictions and measured strains are depicted in Figure 2.8a. The results from all ten sensors, comparing the randomly selected strain to the model's estimation is depicted in Figure 2.8b. The static-strain model evaluated achieved an MAE of 1.6% strain for all the sensors tested and r-squared score of 0.64 (see Figure 2.8b). It was observed, however, that the prediction error varied for each sensor – MAE for each individual sensor ranged between 0.5 and 4.4% strain. Resistance measurements outside the model range were neglected. As seen in Figure 8a and 8b, the model tended to overestimate the magnitude of the quasi-static strains. It was observed that the quasi-static strain-resistance relationship generally drifted downward (i.e., the sensor would exhibit a lower resistance for a given strain than it had during prior strains at the same magnitude). This is consistent with observations in other investigation of viscoelastic sensors [137] and is likely due to viscoplastic deformation as described in the Burger's model.

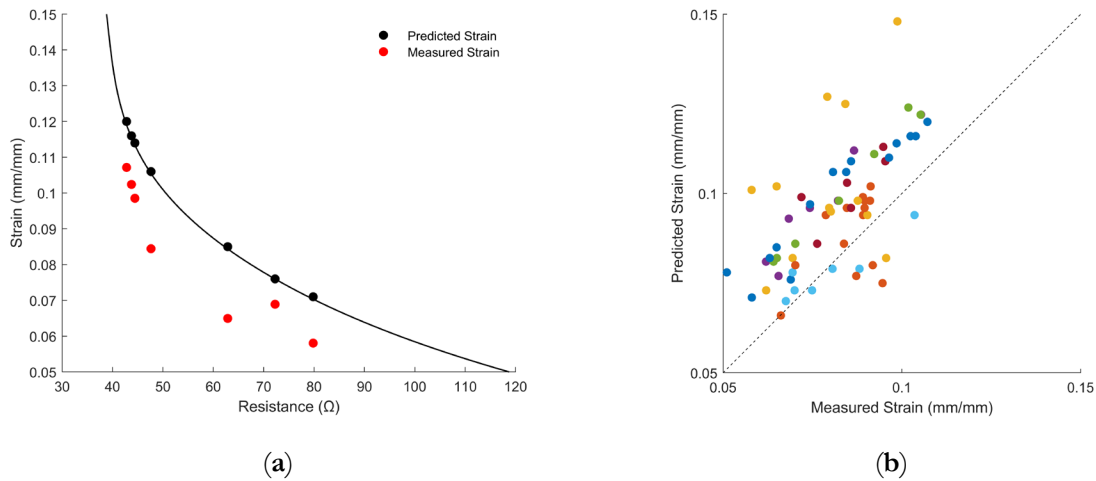


Figure 2.8 (a) The quasi-static strain model (black line), the model prediction at the randomly selected strain points (black dots), and the actual strains (red dots) for a single sensor. Vertical distances between black and red line represent the model error. (b) Scatterplot of the randomized strains (x-axis) compared to the model prediction (y-axis) for all 10 sensors (each strain gauge is indicated by a different color). Predictions that fall on the dotted black line are exactly accurate.

2.3.2.2. Dynamic Model Performance

The full model was then used to predict the time-dependent strain from the resistance measured during the random sequence of strain changes mentioned in the previous section. When predicting the resistance values of sensors pulled from 0 to 15% strain at low to intermediate strain rates (0.5mm/s or slower), the model achieved r-squared values of greater than 0.9 (see Table 2.6). For all strain rates, the model captured the general trends in the resistance data exhibited by the viscoelastic sensors, but the MAE increases slightly for faster rates (Figure 2.9).

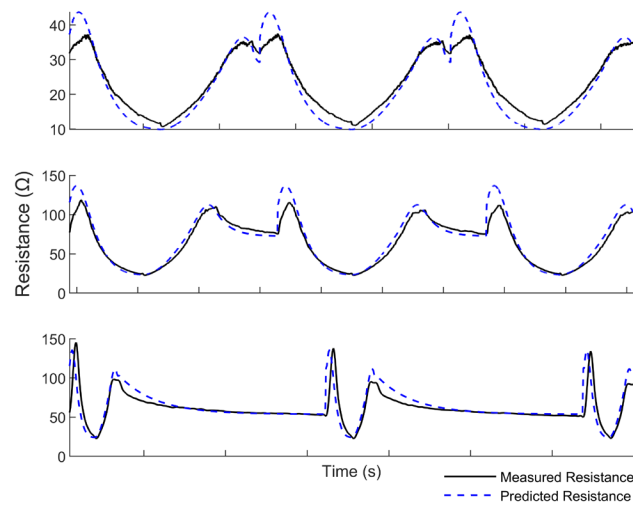


Figure 2.9 The predicted resistance value (dotted blue line) compared to the true sensor resistance (black line) during the validation test. The top plot was conducted at a rate of 0.05 mm/s, the middle plot was the validation test conducted at a rate of 0.50 mm/s, and the bottom plot was the validation test conducted at a rate of 5.0 mm/s.

Table 2.6 Model application test results (r-squared and mean-averaged error) conducted at each different strain rates.

Strain Rate (mm/s)	R ²	MAE (Ω)
0.05	0.96	5.00
0.50	0.96	4.03
5.00	0.80	8.59

2.3.2.3. Model Evaluation during Simulated Biomechanical Application

As stated previously, one of the most important potential applications of the strain gauges is to provide estimate of biomechanics (e.g., range of motion, velocity, etc.). The sensors were therefore tested in a broad envelope of strains and strain rates to evaluate how the model interprets strain and strain rate during potential biomechanical activities. The strain gauges were preconditioned, calibrated, and then pulled to randomly selected strains (between 5 and 15%) at randomly selected strain rates (between 0.05 mm/s and 5.0 mm/s) on the Instron machine to imitate the range of expected strains and strain rates that a sensor would undergo during a repetitious, biomechanical applications. Ten sensors were evaluated during this application. The dynamic-strain model achieved an MAE of 1.4% strain when used to predict strain and an MAE of 0.036 mm/s when used to predict strain rate; the corresponding r-squared values for predicted strain magnitude and strain rate are 0.80 and 0.99, respectively (see Figure 2.10). Two sensors were ignored that exhibited resistance readings outside the range of the model.

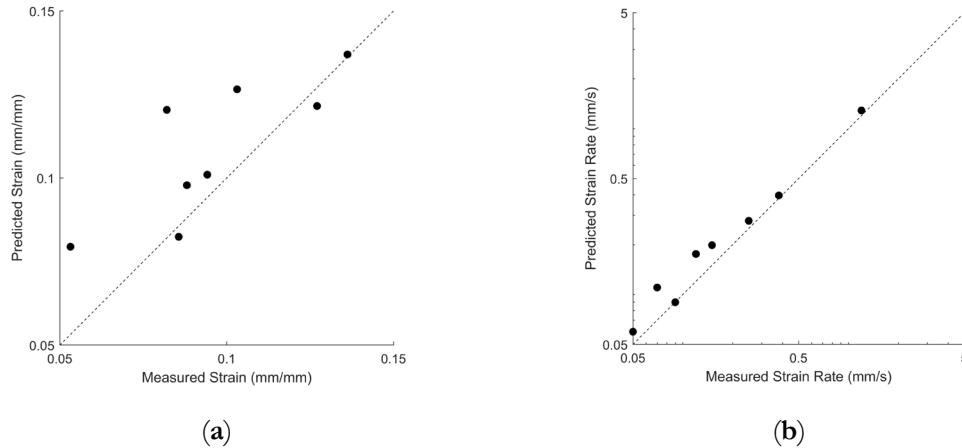


Figure 2.10 (a) Scatterplot of the true strain compared to the predicted model strain for different sensors, each pulled to a random strain (between 5 and 15% strain). (b) Scatterplot of the true strain rate of each sensor compared to the predicted strain rate, pulled at a random strain rate between 0.05 and 5.0 mm/s. Each sensor is represented by a single scatter point.

2.4. Discussion

The present work investigates the output of high deflection, resistance-based strain gauges. The findings from this research concurs with previous works that viscoelastic sensors exhibit highly nonlinear outputs [125, 126, 137] builds on these findings by quantifying the relationship between strain and resistance under quasi-static and dynamic conditions during cyclical strains. The quasi-static relationship between resistance and strain of high-elongation viscoelastic sensors (Eq 2.1) was determined by fitting an equation to the observed data of a single sensor. The model was subsequently calibrated for other sensors by taking two resistance data points at known strains and shifting the fitted curve to the new points. The dynamic relationship between strain and resistance, which is heavily influenced by the sensor's viscoelastic properties, was then superimposed onto the quasi-static model to account for the resistance spikes and their subsequent dissipation (Eq 2.3).

The resulting model was validated in a variety of tests to determine its ability to correctly interpret both quasi-static and dynamics strains of sensors from resistance measurements. When used to interpret static strains, the model achieved a MAE of 1.6% strain. The model prediction of sensor output of dynamic strain applications captured the general trends of the viscoelastic resistance behavior and achieved high accuracy at low to intermediate strain rates (MAE values of 5.00Ω , 4.03Ω , and 8.59Ω at elongation rates of 0.05 mm/s, 0.50 mm/s, and 5.0 mm/s, respectively). The model interpretation of dynamic strains was able to estimate strain magnitude with an MAE of 1.4% strain and strain rate with an MAE of 0.036 mm/s. These validation tests provide an estimate of the model's ability to predict and interpret a wide range of strains and strain rates that encompass the expected sensor loads potential applications.

The intended purpose of the model is to interpret spinal biomechanics from an array of sensors adhered to a patient's lower back. The findings from this endeavor will be valuable in the analysis of the strain gauge outputs to extract biomechanical features from the subject's spinal motion (e.g., range of motion, velocity, etc.). This innovative motion-monitoring technique may be used by clinicians to objectively assess a patient's spinal movement patterns. This in turn could be used to monitor movement changes and progress and to help identify the optimal treatment paradigms for millions of chronic low back pain patients worldwide. Additionally, these findings provide a foundation for interpreting all viscoelastic, resistance-based sensors, which can be used in other applications.

Because this model was restricted to the linear region of the stress-strain diagram where the strain gauges exhibited a predominately elastic and viscoelastic response, the effects of viscoplasticity on the electrical output were neglected. However, this model does account for nonlinear response with respect to load and time. Future iterations of the model could improve performance by further quantifying the relationship between viscoplasticity and sensor resistance, which would become increasingly relevant to interpreting sensor outputs with additional stress and relaxation cycles (i.e., with additional stress and relaxation cycles, the effects of viscoplastic creep become more pronounced in the sensor output).

Future research can also be conducted to fine tune the sensor recipe to achieve desired material properties and model parameters (e.g., reducing the nanoparticles to expedite resistance spike dissipation). Additional investigation into preconditioning methods may lead to more effective methods and improved model performance.

There were slight instrumentation errors during tensile tests at high strain rates (the incremental strain tests pulled the sensors by increments of 0.6mm rather than 0.5mm). This may have affected the specific parameters used for estimating the sensor resistance being tested at a strain rate of 5.0mm/s. However, the general trends observed, model performance, and conclusions regarding the effect of viscoelasticity on a strain gauge's electrical output are still valid for the resistance-based sensors.

Funding Information: This research was supported by NIH grant UH3AR076723.

Conflicts of Interest: The authors declare no conflict of interest.

CHAPTER 3 MULTI-LAYERED ARCHITECTURE FOR IMPROVED NANO-COMPOSITE BIOMECHANICAL SENSORS

Spencer A. Baker¹, Thomas B. Andrews¹, Jaydn Christensen¹, Tyler A. Hutchinson¹, Hailey E. Jones¹, McKay D. McFadden¹, Ulrike H. Mitchell², Anton E. Bowden¹, David T. Fullwood¹

¹Department of Mechanical Engineering, Brigham Young University, Provo, Utah

²Department of Exercise Sciences, Brigham Young University, Provo, Utah

Corresponding to dfullwood@byu.edu

Acknowledgements: Research reported in this publication was supported by the NIH HEAL Initiative under award number NIAMS UH3AR076723. The content is solely the responsibility of the authors and does not necessarily represent the official views of the National Institutes of Health.

3.0. Abstract

Conventional strain gauges are a valuable sensing technology used in a variety of fields but are limited in their applications due to their low strain capacity. In contrast, high deflection strain gauges are capable of much larger deflections and are therefore more suitable for specialized applications such as biomechanics or soft robotics. One type of high deflection strain gauges is piezoresistive sensors, which are composed of nanoparticles embedded in silicone, and are therefore economic to manufacture and exhibit large gauge factors. However, combining stiff nanoparticles with a soft silicone matrix leads to high stress concentrations and a highly non-linear time-dependent electrical response to strain that is difficult to simulate, and therefore interpret.

This paper proposes a multi-layered sensor architecture, whereby silicone support layers regulate the mechanical response of the internal sensor, leading to a more repeatable and predictable electrical signal. The multilayer strain gauge exhibits 60% less signal drift than the stand-alone sensor under high strain. It also results in strain measurements with 60% more accuracy. The application of this multi-layered compound may be used to facilitate new biomechanical discoveries, including a reliable method of identifying the optimal treatment paradigm for each patient suffering from chronic low back pain, improving outcomes for millions of patients worldwide.

Keywords: nanocomposites, viscoelasticity, modeling

3.1. Introduction

Many of the advances in the medical field are the result of innovative sensing technology. It has been postulated that skin-mounted strain gauges would provide significant contribution to this field as an economical means of capturing biomechanics. Strain gauges offer numerous advantages over other motion-capture techniques, such as cameras that track reflective markers, which require expensive equipment, complex set-up, and controlled environments. Although conventional strain gauges are unsuited for biomechanical application due to their limited strain capacity (approximately 5%), the development of high-deflection strain gauges in recent years has led to promising new solutions [125].

While conventional strain gauges, which rely on metals and semiconductors, high deflection strain gauges are governed by different by very different mechanisms. Capacitive-based strain gauges operate on the principle

of Poisson's ratio: as they are stretched, the conductive cross-sectional area diminishes. This type of strain gauge exhibits extremely stretchable strain properties and linear gauge factor analyses. However, there are major drawbacks that limit its efficacy in biomechanical applications, including "low gauge factors, unpredictable response due to unstable overlaps of the capacitive area, and capacitive interaction with the human body" [126]. Piezoresistive strain gauges, on the other hand, are generally comprised of a highly elastic base matrix (e.g., silicone), mixed with conductive nanoparticles [127]. These sensors exhibit highly flexible material properties and a much higher gauge factor than the capacitive strain gauges (on the order of 10^3 - 10^4) [125]. They also provide the advantage of a relatively easy fabrication [128]. However, the electrical signals from these high-deflection strain gauges are highly influenced by their time-dependent, viscoelastic material properties. At large strains, the mechanical properties become increasingly non-linear due to the stress concentrations between the stiff nanoparticles in the soft matrix. Furthermore, the local stress concentrations lead to accelerated creep of the material and accompanying drift of the sensor response. This results in complex electrical signals that are difficult to simulate and interpret, in terms of accurate strain values [144]. The objective of this research is to ameliorate the drawbacks of current high deflection strain gauges via a novel multi-layer architecture that increases linearity of response and reduces creep. By providing a supporting structure of pure silicone around the strain gauges, the proposed multi-layered architecture mitigates the drawbacks of the high-contrast composite, and results in enhanced characteristics and better performance as a sensor material.

The specific application which inspires this research is monitoring and analyzing the spinal motion of patients suffering from chronic low back pain using an array of the high deflection strain gauges [145]. Past studies have found that spinal motion patterns correlate with functional limitations associated with the condition that causes the pain [152]. Additional spinal motion research may lead to the identification of phenotypes, which could assist clinicians identify the optimal treatment paradigm for each patient suffering from chronic low back pain [44]. It is our hypothesis that the improved performance of the multi-layered sensor will render even more accurate spinal-motion estimates and improve the identification of phenotypes, which in turn may have the potential to link millions of patients to their optimal treatment worldwide [57, 145]. Furthermore, this multi-layer architecture may offer similar improvements to high-deflection strain gauges in other fields, including soft robotics, human-machine interfaces, and more [125].

3.2. Materials and Methods

Silicone has very linear mechanical properties. The nanocomposite strain gauge requires both the linear, elastic properties of silicone and the conductive properties of the metallic nanoparticles to perform its intended function. However, as stated previously, it has been found that the elasticity of the silicone matrix is greatly inhibited by the stress concentrations due to the nanoparticle filaments.

3.2.1. Nanocomposite Sensors

The conventional strain gauge design from Brigham Young University [127] are composed of an Ecoflex 00-30 silicone matrix (64% of the composite by weight) with nickel-coated carbon fibers (30%) and nickel nanostrands (5%) embedded in the matrix with surfactant (1%). The sensors are cured under vacuum at 88 °C for 135 minutes, followed by a flashing period of 192 °C for an additional 30 minutes (see Figure 3.1a).

The multi-layered architecture is designed to provide a support structure for the conventional sensors and modify the mechanical response. The proposed design is comprised of a conventional nanocomposite strain gauge encased in a layer of pure silicone prior to flashing. A lower layer of silicone is allowed to cure for 60 minutes in a mold, after which the strain gauge is laid on this layer, and an upper layer of silicone is poured over the gauge, and the mold is closed. The entire structure is then flashed at 192 °C for 30 minutes (Figure 3.1b-c).

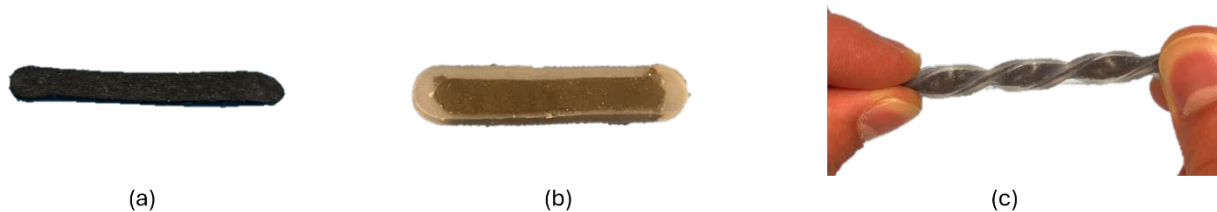


Figure 3.1 A depiction of (a) the conventional nanocomposite sensor and (b) the multi-layered sensor in a relaxed state and (c) the multi-layered sensor under combined torsion and tensile strain.

The following experiments were conducted to evaluate the effects of the multi-layered architecture on

1. The mechanical properties of the viscoelastic strain gauges,
2. The electrical signal of the viscoelastic strain gauges under quasistatic and dynamic conditions, and
3. The sensor performance in a simulated biomechanical application.

3.2.2. Viscous Properties

Past endeavors have shown that polymers, such as our sensors, exhibit three types of mechanical properties – elastic, viscoelastic, and viscoplastic. We hypothesized that the multi-layered architecture would mitigate the viscoplastic creep of the nanocomposite sensors and lengthen the linear region of the multi-layered nanocomposite sensors. The regulated mechanical properties would in turn facilitate more consistent and interpretable electrical signals, especially at high strains.

The mechanical properties of the single-layered sensors, the multi-layered sensors, and pure silicone in the form of the conventional single-layered sensor were evaluated and compared. Samples of each type of sensor were tested on the Instron tensile tester to measure performance during a strain to failure test and a cyclic loading test up to 75% strain. Viscoelasticity was quantified as the work done on the strain gauge material during a stress and relaxation cycle (i.e., the integration of the force over distance). Viscoplasticity was quantified as the difference between the work done on the strain gauge material during the first stress and relaxation cycle and each subsequent cycle (i.e., if the work done on the material was the same for each cycle, it would indicate that the material was completely viscoelastic and exhibited no viscoplastic deformation).

3.2.3. Electrical Signal

The electrical signals of the nanocomposite sensors were evaluated, with and without the multi-layered architecture. Past studies have developed a model to relate electrical resistance to strain for the viscoelastic sensors. The model was comprised of (1) the quasistatic model which related strains under stationary conditions to resistance and (2) the dynamic model which related stress relaxation to resistance as a function of time. The full electrical response of the sensors was obtained by superimposing the quasistatic and dynamic models. The model was developed by testing the sensors during 10 incremental stress and relaxations cycles with maximum strains of 15% (see Figure 3.2a). The quasistatic response of the model was evaluated by reading the sensor resistance during the incremental strain tests after the sensor had been held at each strain for a period of for a specified duration, thus allowing the transient spikes to dissipate (see Figure 3.2b). A spline curve was fit to interpolate the quasistatic resistance at all strains (see Figure 3.2c) and evaluate the relative change in sensor signal with response to strain (see Figure 3.2d). The dynamic response was

evaluated by examining the relative increase in resistance during the transitions between strains and using the stress-relaxation exponential decay factor to account for the transient spike dissipations (see Figure 3.2e-f). [144].

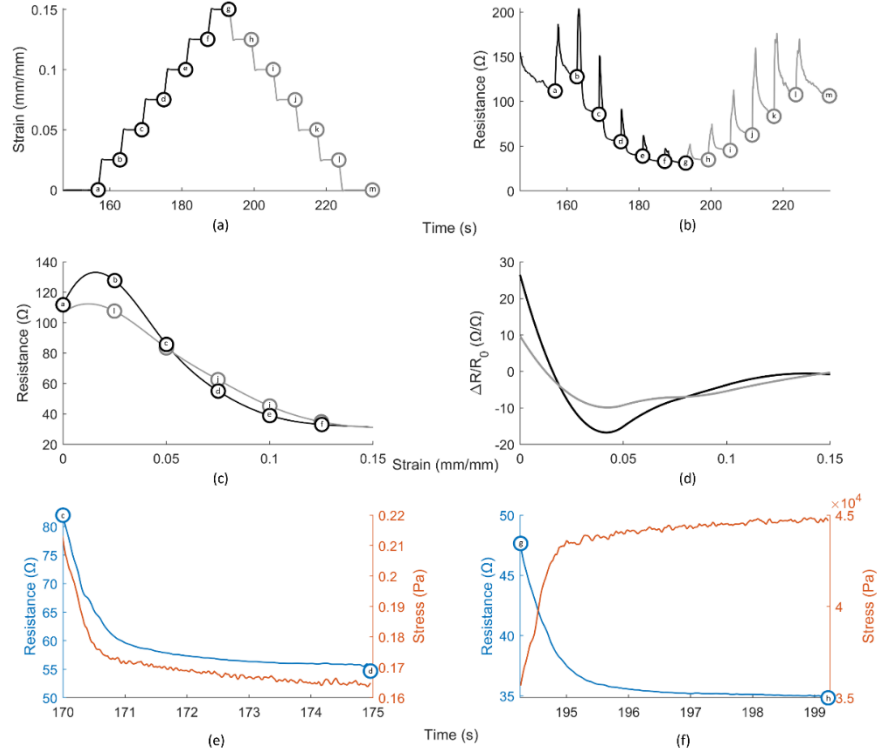


Figure 3.2 Findings from previous study, in which (a) incremental strains were applied to a sensor, (b) the sensor output was captured, (c) a quasistatic model was developed ignoring transient outputs, (d) the relative signal (in terms of $\Delta R/R_0$) of the sensor at different strain levels, (e-f) the relationship between resistance while the sensor is held at a constant strain [144].

Equations that describe the quasistatic, dynamic, and composite models are described below. The resistance as a function of quasistatic strain (R_s) is a spline fit curve taken from sensor readings (R_i) at different steady-state strains (ϵ_i) (Eq 3.1). The resistance of the sensor under dynamic conditions (R_d) is described as a transient resistance spike (S) which decays exponentially with respect to time (t) after the dynamic strain occurs (t_s) with a time constant of λ (Eq 3.2). The composite model (R) is a superposition of the quasistatic and dynamic models (Eq 3.3).

$$R_s = f(\epsilon) = \text{spline}(\epsilon_i, R_i, \epsilon) \quad 3.1$$

$$R_d = S \exp(-\lambda(t - t_s)) \quad 3.2$$

$$R = f(\epsilon) * [1 + S \exp(-\lambda(t - t_s))] \quad 3.3$$

This methodology was implemented in this endeavor, but the strain gauges were exposed to much more rigorous conditions. Both the single- and multi-layered nanocomposite sensors were tested up to 50% strains. Data was collected from four samples of each sensor type.

3.2.4. Sensor Performance

To evaluate and compare how well the sensors would perform during their intended uses, the single-layered and multi-layered strain gauges were used to predict strain levels from a simulated biomechanical application. The sensors were preconditioned, and models were fitted to the sensors using a linear interpolation at the 0 and 50% strain points. The sensors were then pulled to ten strains – randomly selected between 10 and 40% strain – and used to interpret the strains to which they were pulled. This is intended to imitate the intended biomechanical applications and obtain an estimate of how reliable the sensors will perform.

3.3. Results

3.3.1. Viscous Properties

It was observed that the multi-layered architecture mitigated the sensor stresses and exhibited a lower modulus of elasticity, which remained more consistent at higher strains and much more similar to silicone (Figure 3.3a). It was also observed that by adding a multi-layered architecture, the sensors still exhibited viscoelasticity (as can be observed by the energy absorbed the single- and multi-layered sensors in Figure 3.3b). However, when the strain gauges were exposed to multiple high strains and relaxations, it was observed that the multilayered sensors experienced significantly less viscoelastic deformation. Viscoplastic deformation was quantified as the difference between the energy absorbed by the material the initial cycle and the energy absorbed during cycles 2-5, as depicted in Figure 3.3c.

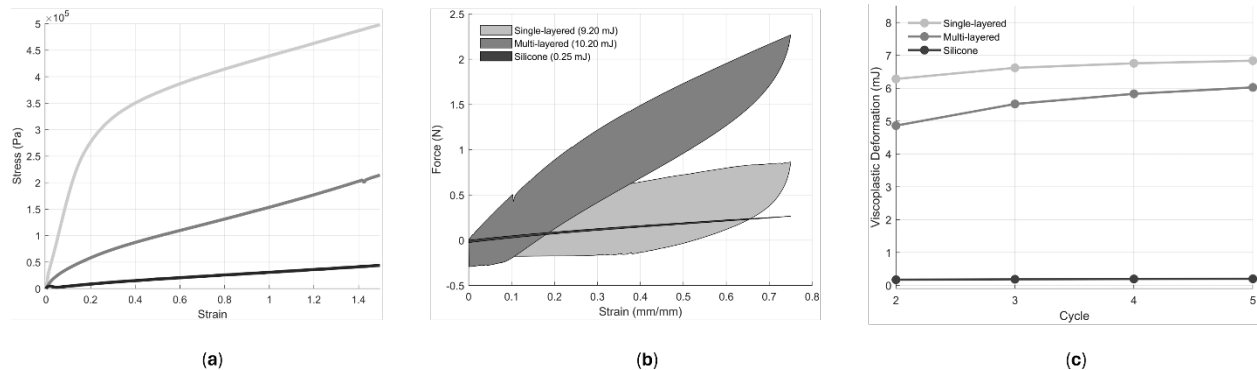


Figure 3.3 (a) The stress-strain diagram for single-layered nanocomposite sensor (light gray) and the multi-layered strain gauge (dark gray) and pure silicone (black) pulled at a constant rate of 3.0 mm/s. (b) Force vs strain during a cyclic test between 0 and 75% strain, depicted for a silicone sensor (black), conventional sensor (light gray), and multilayered sensor (dark gray). Notice that during the recovery, the multilayered sensor recovers more than the conventional sensor (the sensor buckles at approximately 15% strain rather than 20% strain). (c) the viscoplasticity of the different strain gauges during repeated cyclic loads, quantified as the energy absorbed and not recovered by the material.

Unsurprisingly, these effects also greatly influenced the electrical signals of the sensors during the cyclic tests.

3.3.2. Electrical Signal

As observed in past studies, the first stress-relaxation cycle exhibited significantly different mechanical and electrical properties [144], presumably due to the Mullins effect [151]. The first cycle therefore served to precondition the sensors and was ignored in the electrical signal processing.

3.2.1 Quasi-static model

The quasistatic response of the model (see 3.1) was evaluated by sampling the sensor resistance during the incremental strain tests after the sensor had been held at each strain for a period of one second (thus allowing the transient spikes to dissipate). The spline fit curve, using the methodology described in Section 2.2, are depicted below in Figure 3.4.

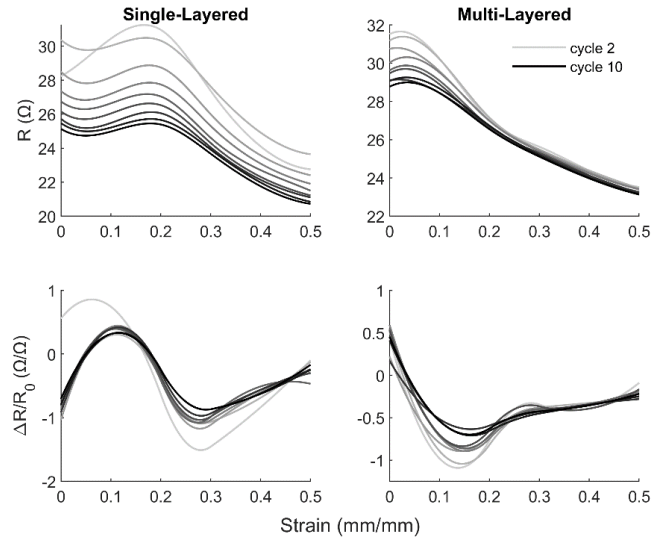


Figure 3.4 Comparison of the resistance-strain relationship (top) and the relative signal change at different strains (bottom) of the single-layered sensors (left) and the multi-layered sensors (right) during tension. The shade of each line indicates the cycle performed (darker shades represent later cycles).

The monotonic region (i.e., the region during which the resistance only decreased with increased strains) was approximately 18-50% strain for the single-layered sensors, while the monotonic region for the multi-layered sensors was approximately 5-50% strain. It was also observed that the variation in sensor resistance was much lower for the multi-layered sensors than the single-layered sensors (see Table 3.1).

Table 3.1 Summary of the relative variation in sensor readings as a percentage of the average sensor resistance, $100 * \frac{stdev(R_\epsilon)}{average(R_\epsilon)}$, at each strain level for the single- and multi-layered sensors for the four samples taken of each and the perfect drift-reduction.

Strain (percent)	Single-Layered Drift	Multi-Layered Drift	Drift Reduction (percent)
0	4.52	2.78	38.5
10	4.78	1.52	68.2
20	4.21	1.35	67.9
30	3.24	1.37	57.7
40	2.85	1.24	56.5
50	2.75	0.71	74.2

3.2.2 Dynamic model

The parameters of the dynamic model (see Eq 3.2) were determined by analyzing the change in resistance as the strain gauge was transitioned between quasistatic strains (see Figure 3.5).

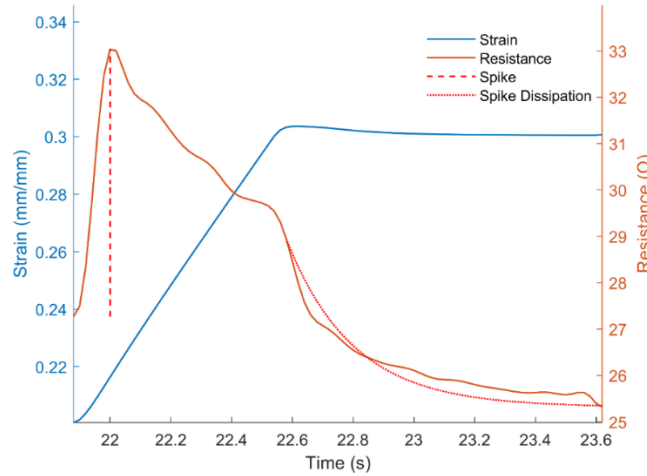


Figure 3.5 Depiction of the strain profile (blue) and corresponding resistance (orange). The spike magnitude is indicated by the dashed red line and the spike dissipation under constant strains is estimated as an exponential decay with a time constant of λ .

The parameters for the spike magnitude, \mathcal{S} , are summarized in Table 3.2. Note that the multi-layered sensors exhibited higher resistance spikes than the single-layered counterparts, especially at strains below 20 percent. However, at higher strains, the spike magnitudes were very similar.

Table 3.2 Summary of the resistance spikes, in percent increase in sensor resistance $100 * \left(\frac{\Omega}{\Omega}\right)$, after an increase / decrease in strain, for the single- and multi-layered strain gauges.

Strain (percent)	Single-Layered	Multi-Layered
0	6.36	31.43
10	7.57	33.91
20	13.85	29.69
30	20.24	23.45
40	17.14	18.29
50	14.45	14.23

The rate of resistance spike was estimated by applying an exponential resistance spike decay choosing a coefficient that minimized the squared difference between the observed and estimated resistances using Matlab's *fminunc* function. This method was repeated for estimating the exponential decay coefficient for stresses, λ_{σ} , for the single-layered and multi-layered sensors.

The λ values for the strain gauges were both dependent on the strain magnitude and the sensor architecture (the multi-layered sensors had higher coefficient values than the single-layered counterparts).

Table 3.3 A summary of the spike exponential decay coefficients (λ) and stress relaxation coefficients (λ_σ) for the single- and multi-layered strain gauges. The stress relaxation coefficients were ignored when the initial stress was less than or equal to zero.

Strain (percent)	Single-Layered λ	Single-Layered λ_σ	Multi-Layered λ	Multi-Layered λ_σ
0	3.23	~	4.75	~
10	3.31	~	5.11	4.51
20	3.40	~	6.83	4.71
30	4.96	4.63	8.32	4.70
40	4.74	4.62	7.28	4.68
50	5.83	4.39	6.33	4.38

3.3.3. Sensor Performance

A multi-layered and single-layer sensor were both tested to evaluate their ability to interpret strain levels as a function of electrical signal at ten randomly selected strains. The mean absolute error of the prediction for the single-layered sensor was 14.99 percent strain, while the mean absolute error of the multi-layered sensor was 4.77 percent strain (see Figure 3.6).

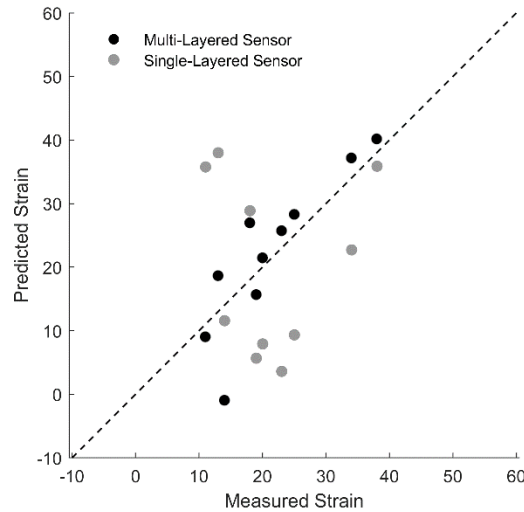


Figure 3.6 A summary of the strain interpretation performance for the multi-layered sensor (black) and the single-layered sensor (gray). Any dot that falls on the slanted black line is correct, and the mean absolute error is the vertical distance between a dot and the slanted dashed line.

3.4. Discussion

It was observed that high-deflection, nanocomposite strain gauges exhibited significantly different material and electrical properties when reinforced with a multi-layered silicone architecture. It was observed that the multi-layered architecture mitigated internal stresses at high strains and made the strain gauges less prone to buckling during cyclic strains.

The change in material properties also resulted in notable differences in the electrical signal. One of the key improvements of the multi-layered sensors was that of signal monotonicity (i.e., that the resistances changes only in one direction – either increasing or decreasing – with additional strain) [146]. The multi-layered sensors exhibit a much larger monotonic region, which is likely be related to the region at which the strain gauges were under tension.

A previous study hypothesized that the resistance spikes and dissipation were correlated with internal stresses [144]. The resistance spikes of the multi-layered sensors were significantly larger than the resistance spikes of the single-layered sensors at low strains. It is presumable that this is also due to the multi-layered architecture which prevented the strain gauge from buckling at low strain levels, thereby resulting in larger changes in stress per incremental strain at low strains.

It was also found that rate of spike dissipation (λ) was higher for the multi-layered sensors than the single-layered sensors. The λ values for the single-coated sensors were very similar to the rate of dissipation of internal stresses after an incremental strain (λ_{σ}). However, the λ values of the multi-layered strain gauges were slightly higher than the λ_{σ} values, indicating that the resistance spikes dissipate faster than the internal stresses for the multi-layered sensors. It's possible that the multi-layered architecture causes an expedited recovery along the interface with the nanocomposite sensor, and therefore an accelerated spike dissipation, while the stresses of the internal nanocomposite continue to dissipate as a similar rate as the single-layered strain gauges.

It is important to note that this study refers to stress as the measured forced divided by the nominal cross-sectional area of the single- and multi-layered strain gauges. Force measurements during the Instron tests for the multi-layered sensors were larger than the force measurements for the single-layered sensors, but the but the cross-sectional area was more than five times larger due to the added thickness and width, resulting in lower net stresses. Additional studies ought to consider differentiating between the average cross-sectional stress and local stress concentrations, particularly at the interface between the multi-layered architecture and the internal nanocomposite sensor.

Overall, the multi-layered sensors were able to interpret strain levels with much higher accuracy than the single-layered counterpart during extremely high-strain applications. The enhanced performance of the high-deflection strain gauges will facilitate more accurate spinal motion monitoring and improved phenotype identification for patients suffering from chronic low back pain. This will assist clinicians to prescribe treatment paradigms according to each patient's individual case and improve outcomes for millions worldwide [44].

CHAPTER 4 CORRELATIONS OF PATIENT REPORTED OUTCOMES AMONG PATIENTS WITH CHRONIC LOW BACK PAIN AND CONTROLS

The following manuscript is being revised for submission to *The North American Spine Society Journal* "NASSJ" academic journal. I hereby confirm that the use of this article is compliant with all publishing agreements.

Spencer A. Baker^a, Kelsey A. Clark^b, Andrew K. Gibbons^a, Maxwell F. Rogers^a, Anton E. Bowden^a, Ulrike H. Mitchell^b, David T. Fullwood^{a,*}

^a Department of Mechanical Engineering, Engineering Building, Brigham Young University, Provo, UT 84602, USA

^b Department of Exercise Sciences, Brigham Young University, 15 Field House Dr, Provo UT 84604, USA

* Corresponding author. *Email Address:* dfullwood@byu.edu

4.0. Abstract

Background Context: Chronic low back pain (CLBP) is a prevalent ailment that has been associated with many physiological, psychological, social, and economic consequences. There is a plethora of available patient-reported outcomes (PROs) that quantify the effects of CLBP on the different aspects of an individual's well-being, some of which are highly correlated with each other, but it is currently unknown whether CLBP is a moderating factor in the relationships between PROs.

Purpose: (1) Assess the effects of CLBP on various legacy and PROMIS patient-reported outcomes (PROs). (2) Evaluate the relationship between PROs in the context of CLBP. (3) Identify a concise set of features to summarize multiple PROs.

Study Design: Cross-sectional study.

Patient Sample: 233 subjects, 133 of whom experience CLBP.

Outcome Measures: Pain Intensity, Oswestry Disability Index (ODI), General Anxiety Disorder 2 (GAD), Pain Catastrophizing Scale 6 (PCS), International Physical Activity Questionnaire Metabolic Equivalent Task (IPAQ MET) minutes / week, PROMIS Pain Interference 4a, PROMIS Physical Function 6b, PROMIS Sleep Disturbance 6a, PROMIS 4-item Depression, and PROMIS 4-item Anxiety.

Methods: Welch T-tests were used to compare the scores from cases (individuals who experience CLBP) and controls (individuals who are CLBP asymptomatic). Linear regressions, accounting for presence of CLBP as a binary variable, were fitted to evaluate the relationship between different reported outcomes. An exploratory factor analysis was conducted to identify a concise set of factors summarizing the variance in the PROs.

Results: Case participants reported a lower quality of life in terms of Pain Intensity, ODI, PROMIS Pain Interference, General Anxiety, Pain Catastrophizing, PROMIS Physical Function, PROMIS Anxiety, and PROMIS Depression than control participants. Strong correlations were observed between several PROMIS metrics with Pain Intensity and ODI ($|r|$ ranging 0.83-0.91). CLBP was a significant moderating variable in these relationships. Moderate to strong correlations were observed between PROMIS metrics with PCS and GAD ($|r|$ ranging 0.35-0.81). Small correlations were observed between PROMIS metrics and IPAQ MET minutes / week ($|r| < 0.28$). Most of the variance from the PROs included in this study can be attributed to five latent factors: (1) Pain and Physical Limitations and (2) Psychological Distress, (3) Physical Activity, (4) Sleep Deprivation, and (5) Pain Catastrophizing.

Conclusions: PROs that quantify physiological and psychological well-being are strongly related to each other. When monitoring patient well-being and progress, researchers should account for the biopsychosocial effects of CLBP by including control subjects to make evaluations against a baseline.

Keywords: Patient-reported outcomes, PROMIS, moderating factor, regressions, biopsychosocial, chronic low back pain, lumbar spine

4.1. Introduction

Pain mitigation is one of the primary components of nearly every medical intervention [1]. One of the most common health ailments, which has even been deemed “the nemesis of medicine” [2], is low back pain (LBP). Studies have estimated the lifetime prevalence of LBP of the general population between 50-80% [10-12]. Not only is LBP prevalent, but it also has the potential to be very severe. It is known to cause functional limitations and reduced quality of life [8], and has even been identified as the leading cause of disability worldwide [16, 17].

When LBP persists beyond or recurs after three months, it is characterized as chronic (CLBP) [3]. Approximately 10% of LBP cases will develop into CLBP [153], which has been associated with direct and indirect medical costs, reduced physical activity, decreased quality of life, anxiety, and depression [21, 43, 55, 154].

The effects of CLBP and other ailments are often quantified using patient-reported outcomes (PROs). PROs are being implemented by healthcare providers with increasing frequency to inform clinical decisions [97]. Substantial research has been conducted that evaluates the average PROs among patients suffering from different ailments [105-107], analyzes the change of PROs prior to and following intervention [108-114], identifies underlying factors to reduce the dimensionality of PROs [115, 116], and quantifies the correlation between different PROs among symptomatic patients [117-123]. However, after an exhaustive review of the literature it appears there are few current studies that investigate PRO correlations using data from subjects with and without CLBP [107], and none that considered the moderating effects of CLBP on the relationship between PROs. While the correlation between related PROs (such as disability and physical impairment) may naturally be assumed to be strong, confounding biopsychosocial factors may obscure the relationship when assessing patients with CLBP, and merit further investigation [124]. Chronic pain is a complex, multifactorial phenomenon that differs from transient, acute pain. This is due to the prolonged nature of chronic pain that alters the biopsychosocial sensation of pain. Over an extended period of time, the psychological, social, emotional, and behavioral consequences of pain intertwine to characterize pain perception and clinical manifestations [155, 156]. Imaging studies have shown that individuals suffering from chronic pain exhibit changes in the central nervous system synapsing that may influence the feeling of pain [157], independent of the pain stimuli itself [156]. Furthermore, the ability to self-regulate and adapt is an important resource to coping with pain and distress. However, this resource can be fatigued by prolonged conditions. As individuals who experience chronic pain are depleted of their ability to self-regulate, they also experience other exacerbated biopsychosocial comorbidities [158]. These key differences must be thoroughly understood in order to provide more effective medical intervention for patients suffering from chronic pain [156]. This study therefore seeks to fill the current knowledge gap regarding how different aspects of well-being (as quantified by PROs) relate to each other for individuals who suffer from CLBP, and how these relationships differ for individuals who experience either no LBP or mild transient LBP (which most of the population will experience at some point). This was done by performing the following analyses:

- (1) Quantify the difference in PROs between the cases (study participants who suffer from CLBP) and the controls (participants who do not experience CLBP symptoms).

- (2) Evaluate the correlation between the relatively new PROMIS metrics with more established PROs and investigate the moderating effects of CLBP on these correlations.
- (3) Identify the latent factors (i.e., underlying dimensions which summarize the observed features) of the PROs data via an exploratory factor analysis to identify the distinct aspects of well-being.

The PROs of interest in this work include several commonly used and thoroughly validated questionnaires (referred to in this study as legacy PROs) and the relatively new Patient-Reported Outcomes Measurement Information System (PROMIS) Short Forms metrics. These measurements encompass the PROs collected by the Back Pain Consortium Research Program [159] and additional metrics. A brief description of each PRO is as follows:

- Pain Intensity: Low-back pain intensity was measured using a numeric rating scale from 0-10 (0 representing ‘no pain’ and 10 representing the most severe pain possible). Pain mitigation is one of the primary purposes of nearly every medical intervention [1]; and low-back pain is also one of the most frequent causes for hospitalizations, physician visits, and medical consultation [21, 104]. It is a vital metric to consider when assessing patient well-being.
- Oswestry-Disability Index (ODI): Spine-related disability was measured using the widely used ODI metric [98]. The ODI metric has been thoroughly vetted and is frequently used as the gold standard for quantifying disability related to LBP [118, 160] and has shown strong experimental reliability when evaluating patients with chronic pain [104].
- General Anxiety Disorder 2 (GAD): General anxiety disorder is an ailment in which an individual suffers from a generic worry. It is not caused by current stressful events in an individual’s life, though stress can aggravate the condition [161]. The GAD-2 questionnaire is used to identify depression of mood over a two-week period, and has shown acceptable accuracy in past studies [162].
- Pain Catastrophizing Scale 6 (PCS): Pain catastrophizing is “an exaggerated negative orientation towards actual or anticipated pain experiences”, which past studies have found to be associated with higher pain intensities [163]. The PCS-6 is designed to capture three psychological components of catastrophizing: helplessness, rumination, and magnification [164].
- Short Form International Physical Activity Questionnaire (IPAQ): Self-assessed physical activity in the week prior to subject participation in the study was estimated in terms of Metabolic Equivalent Task (MET) minutes per week. Previous studies have compared IPAQ scores to objective metrics of physical activity, and found it to be moderately reliable for estimating vigorous physical activity [99] but an uncertain metric for evaluating total aerobic activity [99, 100]. However, due to the innately subjective nature of patient-satisfaction, an individual’s self-perception of physical activity may be more valuable than precise estimations of activity [104].
- Patient-reported outcomes measurement information systems (PROMIS) metrics: PROMIS scores are “a set of person-centered measures that evaluates and monitors physical, mental, and social health in adults and children” [101]. Past studies have evaluated PROMIS metrics and concluded them to be “efficient, flexible, and precise” [97]. Questionnaire responses for each PROMIS metric are used to calculate T-scores, which are intended to achieve a normal distribution with a mean metric score of 50 and a standard deviation of 10 for the general population [102, 103]. Past studies have found that PROMIS metrics T-scores are less prone to floor effect, easier to implement in clinical settings, and more comprehensive than other metrics such as the ODI [118, 120]. The short-form PROMIS metrics implemented in this research included the PROMIS Pain Interference 4a, PROMIS Physical Function 6b, PROMIS Sleep Disturbance 6a, PROMIS 4-item Depression, and PROMIS 4-item Anxiety.

4.2. Methods

4.2.1. Data Collection

Two cohorts of subjects were recruited for this study – individuals who suffer from CLBP and control subjects who do not experience CLBP symptoms [145]. The control group was recruited via flyers to the local community. The group that was CLBP symptomatic was recruited from individuals who are already scheduled for physical therapy relating to CLBP. Participants were between the ages of 35 and 65 (which is the age range with the greatest CLBP prevalence [153]). For purposes beyond the scope of this work, it was required that all participants be capable of standing and moving without an assistive device and be eligible for an MRI scan. As stated previously, CLBP is a persistent ailment that affects a subset of the population [21], but nearly every individual will experience an acute episode of LBP at some point [10]. Hence, the “control” population and the “case” population tend to be very heterogeneous, often making it difficult to differentiate between the effects of varying severities of CLBP and with those of intermittent acute LBP [44]. In order to mitigate this issue, past studies have recruited only individuals with well-documented cases of LBP [46]. In our study, an important aspect was to avoid conflating the effects of persistent CLBP and the symptoms of severe transient LBP symptoms or other acute ailments. Therefore, the exclusion criteria for participants in the control group were current or history of treatment for lumbar spine pain, known scoliosis, and LBP pain intensity of greater than 2.5 on a scale of 0-10. The CLBP had to be primarily axial (as opposed to radiating, as seen in radiculopathy), persistent for at least three months prior to the study, and the Pain Intensity score had to be at least 2.5 on a scale of 0-10. Individuals with knee or hip surgery were excluded from the study for both cases and controls. See also Figure 4.1.

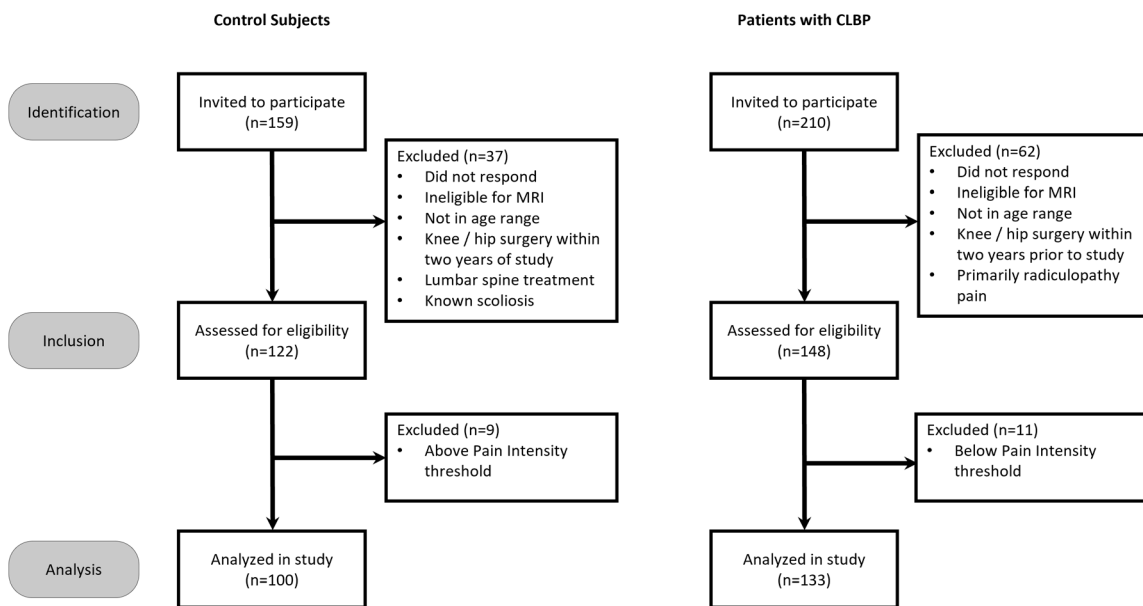


Figure 4.1 Individuals who were invited to participate in study and met eligibility criteria.

A total of 233 subjects were recruited for the study – 133 who experienced CLBP symptoms and 100 subjects who served as controls. Participant demographics are summarized in Table 4.1.

Table 4.1 Summary of the subject demographics, in terms of the average values and standard deviation (stdev), for the study participants.

Demographic	Control Subjects	Subjects with CLBP
Number of subjects	100	133
Age [Stdev] (yrs)	47.8 [7.5]	49.0 [8.8]
Height [Stdev] (cm)	174.3 [9.5]	172.2 [18.0]
Weight [Stdev] (kg)	79.5 [15.9]	85.2 [20.2]
BMI [Stdev] (kg/m ²)	26.1 [4.5]	28.3 [6.1]
Sex at Birth (Female / Male)	43 / 57	64 / 69

All demographic data and PROs were collected using an electric survey sent to the study participants. (the IPAQ questionnaire was included in the study shortly after it was initiated, hence the IPAQ MET minutes / week scores for the first 30 participants are missing from this study). The participant responses were de-identified, then uploaded to the Back Pain Consortium Data Portal [159], along with other features of interest, to be used in ongoing and future research initiatives [57].

4.2.2. Data Processing

It has been observed that IPAQ MET scores are prone to overestimations [165]. Past studies have warned that including extreme outliers in a dataset can lead to spurious findings [166], so can the removal of outliers without due cause and documentation [167]. To mitigate both risks, subsequent statistical tests including the IPAQ MET scores were conducted twice. The first analyses were conducted after filtering extreme outliers in the IPAQ responses (i.e., z-scores > 3, which is slightly more aggressive than the recommendation by Tabachnik and Fidell [168]) and reported. The second analysis was conducted including the entire dataset. The effects of including the entire dataset in the analyses were noted.

Several of the analyses performed in this study assume the data have a normal distribution. While the PROMIS metrics are designed to achieve a normal distribution [102, 103], the other PROs of interest in this study were not designed with the intention of achieving any particular spread. The skewness of the PRO distributions was quantified using Python's *skew* function to calculate the Fisher-Pearson coefficient. Significant skewness (designated in this study as having a Fisher-Pearson coefficient outside the bounds of -1 to 1, which indicates right- and left-skewness respectively) was mitigated by transforming the data prior to conducting statistical analysis.

4.2.3. Data Analysis

Several statistical analyses were conducted to achieve the aims described in the Introduction. In each test, a p-value of less than 0.05 was considered statistically significant, after accounting for multiple comparisons using the Holm correction factor.

Aim One: Comparison of PROs from Cases and Controls

Welch T-Tests were used to evaluate the differences of the PROs distributions between the cases and controls. The p-value of the comparison of Pain Intensity between the two groups was not calculated (calculating this statistic would have been improper due to the inclusion-exclusion criteria – individuals with a Pain Intensity below 2.5 were excluded from the cases, and individuals with a Pain Intensity were excluded from controls).

Aim Two: Correlations between PROs

The second objective of this study was to evaluate the strength of the correlation between legacy PROs (Pain Intensity, ODI, GAD, PCS-6, and IPAQ MET Minutes/Week) with the PROMIS metrics (Pain Interference, Physical Function, Sleep Disturbance, Depression, Anxiety), and test whether CLBP is a moderating factor in the relationships. Linear regressions were employed to quantify the strength and statistical significance of the correlations (after skewness has been corrected for, when necessary). The linear regression models were of the following forms:

$$y = \beta_0 + \beta_1 x \quad 4.1$$

$$y = \beta_0 + \beta_1 x + \beta_2 \delta_{CLBP} \quad 4.2$$

$$y = \beta_0 + \beta_1 x + \beta_2 \delta_{CLBP} + \beta_3 x \delta_{CLBP} \quad 4.3$$

$$y = \beta_0 + \beta_2 \delta_{CLBP} \quad 4.4$$

In each equation, y represents one of the five legacy PROs and x represents one of the five PROMIS metrics, for a total of 25 regressions analyses performed.

- In Eq 4.1, the simplest form of linear regression is considered. The β_0 coefficient represents the y-intercept and the β_1 coefficient represents the slope depicting the average effect on the dependent variable y per unit increase in the independent variable x . In this model, the relationship between the legacy and PROMIS PRO is independent of the presence of CLBP.
- In Eq 4.2, the additional coefficient β_2 represents the difference in y-intercepts between cases and controls. CLBP status is indicated by δ_{CLBP} , which has a value of 1 for subjects who suffer from CLBP and a value of 0 for control subjects. The nature of the relationship between PROs (i.e., the slope of the regression) in this model is the same for both cases and controls, but the presence of CLBP is associated with an offset of the dependent variable.
- In Eq 4.3, the β_3 coefficient represents the difference in slope for the y-intercept between cases and controls, indicating that the nature of the relationship between PROs (i.e., the slope) is altered by the presence of CLBP and therefore differs for the two groups.
- In Eq 4.4, the dependent variable y is estimated using the average value for the two groups. This model is applicable when the average value of the legacy PRO (y) differs, but the legacy PRO and PROMIS score (x) are not related to each other.

The most appropriate equation to model the relationship between the PROMIS metric, legacy PRO, and the effect of CLBP was determined using the logic displayed in the decision tree in Figure 4.2.

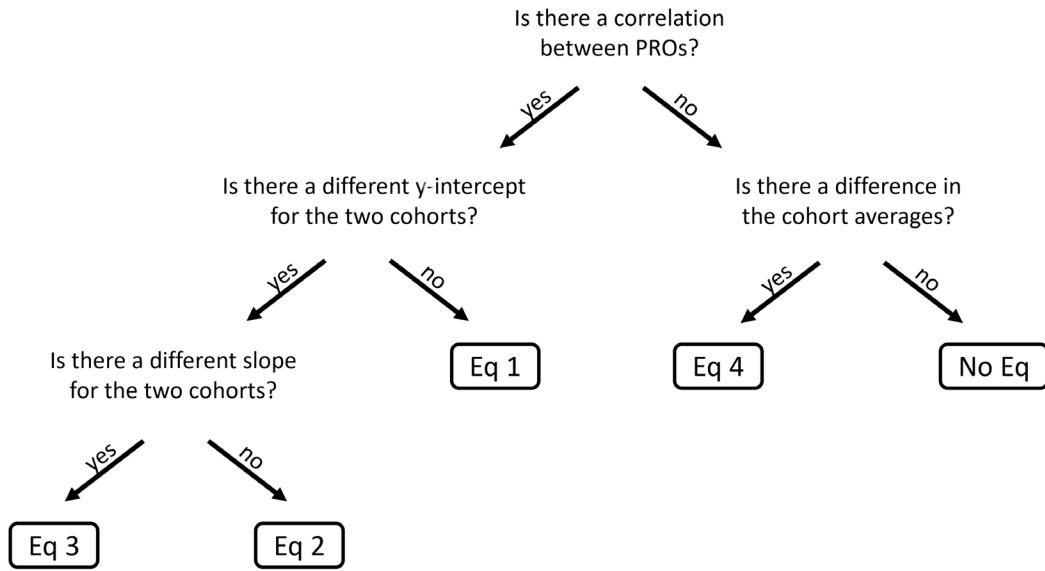


Figure 4.2 Decision tree indicating the process for selecting whether a relationship between the legacy and PROMIS PRO exists, and if so in what manner the presence of CLBP influences the relationship.

To reduce the risk of Type I Error, each additional model feature was added incrementally after the base model was proven statistically significant (Eq 2 was not considered unless Eq 1 was proven statistically significant, and Eq 3 was not considered unless Eq 2 was proven statistically significant). At each decision tree node, the F-statistic and corresponding p-value was calculated to determine the statistical significance of the additional model feature (Eq 4.5).

$$F = \frac{(R_P^2 - R_Q^2)/(P - Q)}{(1 - R_P^2)/(n - P - 1)} \sim F_{P-Q, n-P-1} \quad 4.5$$

R_P^2 – The variance explained by the model with P features.

R_Q^2 – The variance explained by the model with Q features.

P, Q – The number of variables in the regression models being compared (Eq 1 and Eq 4 have one variable, Eq 2 has two variables, and Eq 3 has three variables). When testing the statistical significance of Eq 1 and Eq 4, $Q = R_Q^2 = 0$.

n – The number of datapoints observed.

The strength of the correlations was evaluated using the Cohen cut points for the absolute values of the Pearson's correlation coefficients r ($|r|=0.10-0.30$ is considered small, $|r|=0.31-0.50$ is considered moderate, and $|r|>0.50$ is considered large [165, 169]).

Aim 3: Identify Distinct Components of Well-Being

The third aim of this analysis was to uncover the minimal set of independent theoretical constructs that could account for the observed trends in the PRO data (including both the legacy and PROMIS metrics). These constructs are comprised of latent factors, which are unobservable independent variables that are either causally related to or associated with the observed variables. Latent factors are essentially linearly independent

hidden components that summarize the variance in the raw data. In contrast, however, to the original PROs, there is no covariance between latent factors. We utilized a machine learning algorithm to identify these latent factors through an Exploratory Factor Analysis (EFA) [170].

Prior to analysis, the z-scores of each observed PRO were calculated so that each would have an equal weight in the EFA. The PROMIS metric z-scores were calculated according to the theoretical distribution by subtracting 50 and dividing by 10 [103]. Other PRO z-scores were calculated using Python's *zscore* function (after mitigating skewness when necessary).

The latent factors were identified by conducting a principal component analysis on the z-score data and applying a varimax rotation, which maximizes the variance explained by each original component by a single factor. This process was repeated multiple times to determine how many resultant latent factors were needed to capture at least 50% the variance in each of the original z-score data. I.e., the first EFA analysis identified a single latent factor, the second EFA analysis identified two latent factors, etc., until the resultant latent factors identified could account for at least 50% of the variance in every PRO z-score data.

The Coefficients of Determination were calculated between the PRO z-scores and the resultant latent factors to provide an interpretation of the factors.

4.3. Results and Discussion

A summary of the Fisher-Pearson coefficients for each PRO investigated in this study (prior to and post transformation) are recorded in Table 4.2.

Table 4.2 Summary of the data collected and the normality skewness before and after transformation (~ in the after-transformation column indicates that no transformation was applied, and the Fisher-Pearson coefficient remained constant).

PRO	Fisher-Pearson (before transformation)	Transformation Applied	Fisher-Pearson (after transformation)
Pain Intensity	0.178	None	~
ODI	1.005	Square-root	0.001
IPAQ MET Minutes / Week	3.106	Square-root	0.685
PROMIS Pain Interference T-Score	0.148	None	~
PROMIS Physical Function T-Score	-0.095	None	~
PROMIS Sleep T-Score	0.189	None	~
PROMIS Depression T-Score	0.726	None	~
PROMIS Anxiety T-Score	0.599	None	~

It was noted that the ODI and IPAQ MET minutes / week scores were both right-skewed. This was mitigated with a square-root transformation, (in both cases, this was the minimal transformation needed to achieve a Fisher-Pearson coefficient within the range of -1 to 1 while maintaining as much of the original data characteristics as possible).

4.3.1. Impact of CLPB on Well-Being

Boxplots were used to visually depict the differences in the PRO scores between cases and controls in Figure 4.3.

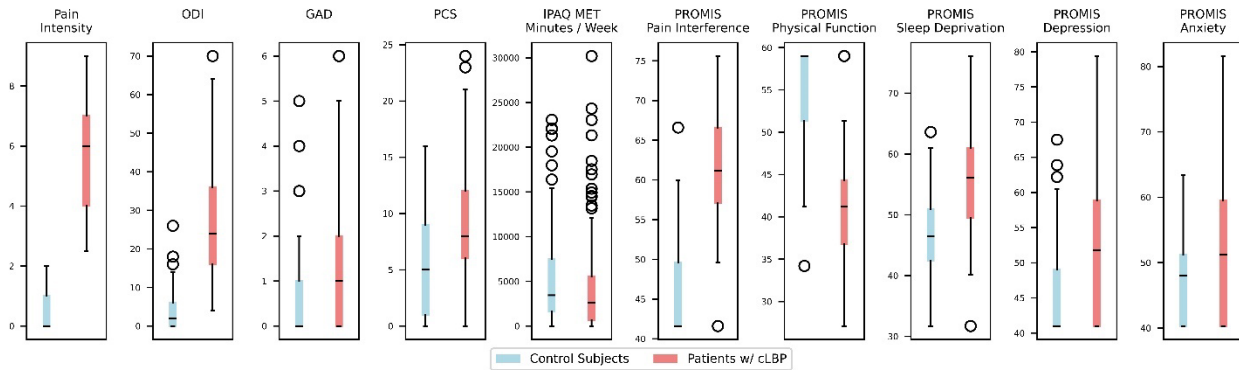


Figure 4.3 Boxplots contrasting the PRO values between controls (blue) and cases (red). The raw data collected (prior to the transformation to achieve normal sample distributions) are depicted here.

A summary of the results from the Welch T-tests is recorded in Table 4.3.

Table 4.3 Summary of the Student T-tests to evaluate the difference in PRO among the control and case groups (group averages and standard deviations are reported in terms of the raw data, and the t-statistic and corresponding p-values are reported in terms of the normalized dataset when necessary to satisfy the assumptions of a Welch T-test).

PRO	Control Cohort Mean [Stdev]	Cohort w/ CLBP Mean [Stdev]	t-statistic	Adjusted p-value
Pain Intensity	0.59 [0.74]	5.45 [1.52]	-30.61	N/A**
ODI	3.57 [4.83]	27.41 [15.32]	-19.85	0.000*
GAD	0.63 [1.04]	1.56 [1.75]	-5.01	0.000*
PCS-6	5.54 [4.53]	9.50 [5.79]	-5.85	0.000*
IPAQ MET Minutes / Week	5648 [5758]	4678 [5958]	1.72	0.087
PROMIS Pain Interference	44.84 [5.71]	61.56 [6.99]	-20.07	0.000*
PROMIS Physical Function	55.34 [5.61]	41.29 [7.10]	16.91	0.000*
PROMIS Sleep Deprivation	46.12 [7.24]	55.78 [8.36]	-9.43	0.000*
PROMIS Depression	45.86 [6.89]	42.46 [9.45]	-6.17	0.000*
PROMIS Anxiety	47.16 [7.09]	51.98 [9.44]	-4.45	0.000*

* Statistical significance was observed in the comparison

** The p-value of the Pain Intensity comparison was not calculated due to the threshold criterion involving this metric

It was observed that individuals who reported experiencing CLBP symptoms also reported PROs that reflect a statistically significant lower quality of life in terms of ODI, GAD, PCS, PROMIS Pain Interference, PROMIS Physical Function, PROMIS Depression, and PROMIS Anxiety. A stark difference in the Pain Intensity scores between the two cohorts was also observed. These findings are consistent with results from past studies that employed similar metrics [106, 107].

There was no statistically significant difference in the IPAQ MET Minutes / Week scores of the cases and controls, neither after removing outliers nor when considering the entire dataset. Several previous reported works have evaluated the role of CLBP on self-reported or measured physical activity, sometimes with conflicting results. Several review articles have reported a similar conclusion that CLBP may either prompt normal or increased physical activity (i.e., an ignore and persist approach) [171] or reduced physical activity consequent to fear avoidance [150, 152], depending upon other psychosocial factors. Consequently, there may exist sub-groups of patients with CLBP who exhibit reduced, altered, or increased physical activity, and the contrasting effects of the different sub-groups appear to negate each other when evaluating patients with CLBP as a whole [172, 173].

While evaluating the PRO scores from study participants, this study also afforded the opportunity to evaluate one of the purported advantages of the PROMIS metrics, namely, robustness against flooring effects. While the distribution of PROMIS metric scores in this study affirmed that flooring effects did not occur (consistent with past investigations [123]), a significant number of controls subjects reported the same lower value for PROMIS Pain Interference and PROMIS Depression, resulting in some of the same negative effects as flooring.

4.3.2. Relationships Between Reported Outcomes

The resulting correlations between PROs were generated and depicted as shown in Figure 4.4. The type of regression is indicated by the line(s) of best fit on each subplot. Relationships best described by Eq 4.1, 4.2, 4.3, and 4.4 are indicated by a single purple line of best fit, two parallel purple lines of best fit, and two non-parallel lines of best fit, and two horizontal dashed lines of best fit, respectively.

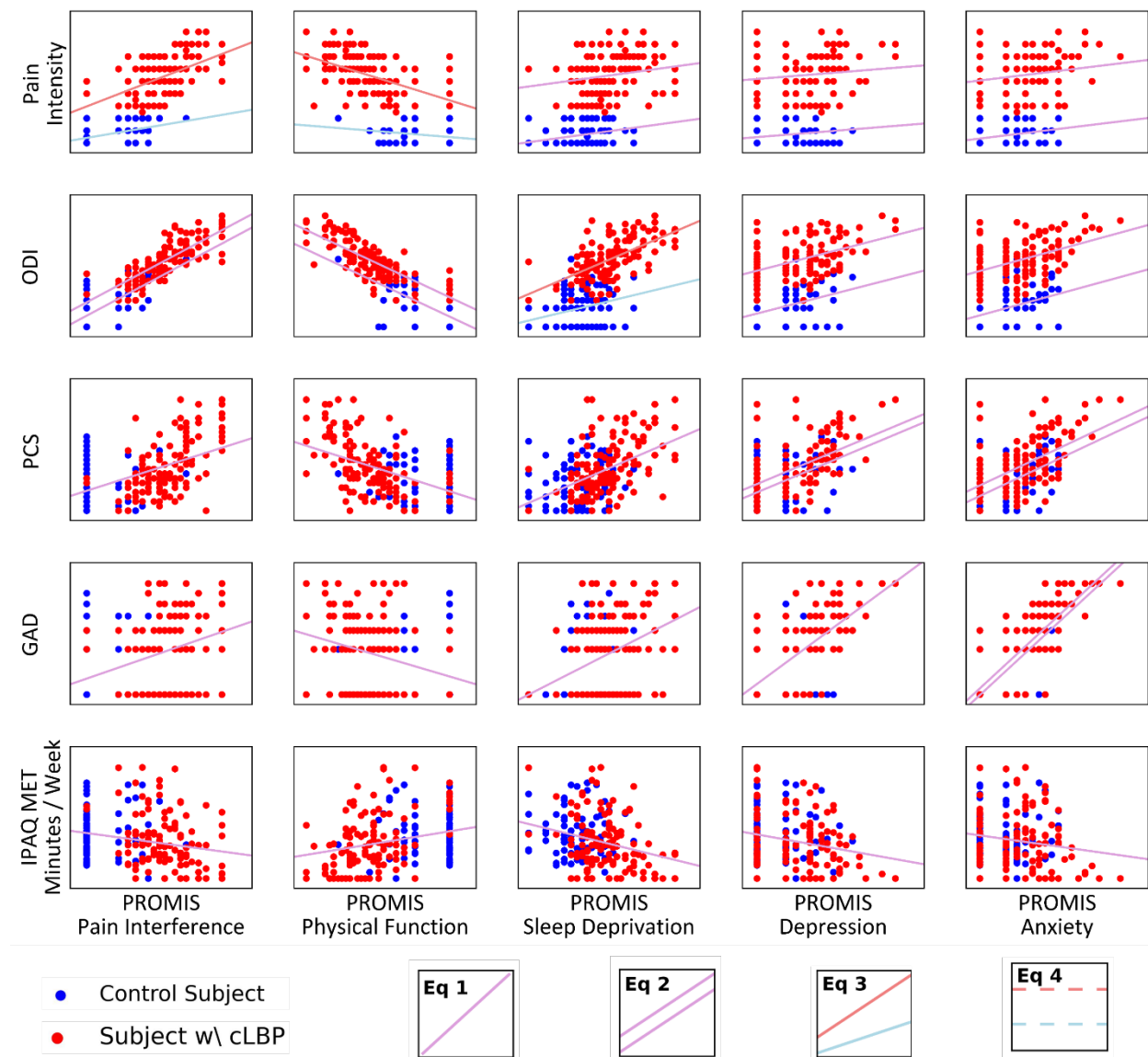


Figure 4.4 Scatterplots and the respective line of best fit (when applicable) depicting the relationship between the different PROs for subjects who experience CLBP symptoms (red) and asymptomatic subjects (blue).

The different model parameter values, statistical test results, and the absolute value of the Pearson's correlation coefficient ($|r|$) from the regressions are summarized in Table 4.4.

Table 4.4 Summary of the model parameters and overall p-values and $|r|$ values for each PRO combination correlation. Note that the interaction terms (β_2 and β_3) indicate the difference in the y-intercept and slope from the baseline values (β_1 and β_2). If no statistically significant model was found to depict the relationship, the statistically insignificant parameters from Eq 4.1 were reported.

Legacy PRO	PROMIS T Score	β_0	β_1	β_2	β_3	Adjusted p-value	r
Pain Intensity	Pain Interference	-1.874	0.055	-0.367	0.070	0.000	0.913***
	Physical Function	2.218	-0.029	7.890	-0.083	0.000	-0.906***
	Sleep Deprivation	-1.102	0.037	4.513		0.000	0.88***
	Depression	-0.505	0.024	4.709		0.000	0.881***
	Anxiety	-1.005	0.034	4.704		0.000	0.884***
ODI	Pain Interference	-5.815	0.160	1.009		0.000	0.910***
	Physical Function	10.124	-0.158	1.456		0.000	-0.909***
	Sleep	-1.434	0.060	0.524	0.046	0.000	0.852***
	Depression	-1.863	0.070	3.224		0.000	0.832***
	Anxiety	-1.957	0.070	3.343		0.000	0.833***
PCS	Pain Interference	-7.073	0.273			0.000	0.510***
	Physical Function	22.413	-0.309			0.000	-0.523***
	Sleep Deprivation	-8.062	0.307			0.000	0.503***
	Depression	-9.434	0.327	1.798		0.000	0.600***
	Anxiety	-10.759	0.346	2.290		0.000	0.627***
GAD	Pain Interference	-0.910	0.030			0.000	0.405**
	Physical Function	2.121	-0.029			0.000	-0.354**
	Sleep Deprivation	-1.179	0.037			0.000	0.436**
	Depression	-2.172	0.059			0.000	0.675***
	Anxiety	-2.803	0.069	0.148		0.000	0.808***
IPAQ MET Minutes / Week	Pain Interference	107.843	-0.860			0.003	-0.222*
	Physical Function	5.770	1.170			0.000	0.276*
	Sleep Deprivation	127.155	-1.284			0.000	-0.283*
	Depression	111.710	-1.021			0.003	-0.232*
	Anxiety	99.133	-0.764			0.018	-0.167*

* small correlation strength ($|r|$ is between 0.10 - 0.30)

** moderate correlation strength ($|r|$ is between 0.30 - 0.50)

*** large correlation strength ($|r|$ is between 0.50 - 1.00)

The relation between the back-specific legacy PROs (Pain Intensity and ODI) with the PROMIS metrics that inquire as to an individual's general physiological well-being (PROMIS Pain Interference and Physical Functionality) demonstrated a strong correlation. Moderate to strong correlations were also observed between the legacy metrics that evaluate psychological well-being with the PROMIS metrics. These findings are consistent with observations from past investigations [94, 118, 123, 160, 163]. A novel finding from this study is that the presence of CLBP is a significant moderating factor in several of these correlations (i.e., the regression model for case participants had differing slopes and / or y-intercepts than the regression model for control participants). Specific observations regarding the relationships between PROs include the following.

- PROMIS metrics with Pain Intensity: Large positive correlation strengths were observed between Pain Intensity with PROMIS Pain Interference, PROMIS Sleep Depression, PROMIS Anxiety, and PROMIS Depression for both cohorts, and a negative correlation with PROMIS Physical Function. The presence of CLBP altered the y-intercept in each of these cases – individuals with CLBP reported higher pain intensities for any average PROMIS score, e.g., individual with higher PROMIS Sleep Deprivation scores reported higher Pain Intensity scores for both cohorts, but at any given Sleep Deprivation score, the cases reported higher Pain Intensities than their control counterparts. Furthermore, the presence of CLBP had an interactive effect on the slope of the correlation for the cases of Pain Interference and Physical Function: the slopes of the relationships were steeper for cases than controls. This indicates that on average, a step increase of Pain Interference and Physical Function reported a more dramatic change in pain intensity for cases than controls.
- PROMIS metrics with ODI: Similar trends were observed between the PROMIS metrics and ODI scores. Increases in Pain Interference, Sleep Deprivation, Anxiety, and Depression as measured by the PROMIS metrics were associated with increases in disability as measured by ODI. Increases in PROMIS Physical Function were associated with decreases in ODI. The presence of CLBP was again a significant moderating factor that influenced the y-intercept in each of these correlations. Cases had higher ODI scores on average than controls who reported similar PROMIS metrics. Furthermore, the presence of CLBP also had an interactive effect on the slope of the relationship between PROMIS Sleep Deprivation and ODI – increases in Sleep Deprivation scores were associated with a more dramatic increase in ODI scores for cases than controls.
- PROMIS metrics with PCS: Large correlation strengths were observed between the Pain Catastrophizing metrics with the PROMIS metrics. For the PROMIS metrics that evaluate Pain Interference, Physical Function, and Sleep Deprivation, the presence of CLBP was not a significant moderating factor in the relationship. E.g., the relationship between Pain Interference and Pain Catastrophizing followed the same trend for both cohorts. However, CLBP was a significant moderating factor in the correlations for PROMIS Depression and PROMIS Anxiety. In both relationships, the presence of CLBP was associated with a higher y-intercept. E.g., increases in PROMIS Depression were associated with increases in Pain Catastrophizing for both cases and controls, but for a given PROMIS Depression score, cases on average had a higher Pain Catastrophizing score than controls.
- PROMIS metrics with GAD: Moderate to large correlation strengths were observed between General Anxiety with the PROMIS metrics. The presence of CLBP was considered a moderating factor only in the relationship with PROMIS Anxiety, in which cases had a higher y-intercept than controls.
- PROMIS metrics with IPAQ Minutes per Week: Statistically significant small correlations were observed between the PROMIS metrics and individuals' IPAQ MET Minutes per Week ratings. IPAQ MET Minutes / Week demonstrated a negative correlation with Pain Interference, Sleep Deprivation, Depression, and Anxiety. A moderate positive correlation with Physical Function. These observations were consistent when outliers were removed from the dataset and when all observations were included. Past studies have also found physiological and psychological benefits to physical activity [174-177]. Future studies may find stronger correlations between physical activity

and reported outcomes by using objective activity measurements rather than self-reports activity [99, 100].

The presence of CLBP significantly influenced the relationship between PROs for several of the relationship. Future studies that examine the correlation between PROs ought to also consider the interaction effects of whether study participants are diagnosed with an ailment that can impact the relationship between patient-reported metrics.

4.3.3. Distinct Components of Well-Being

From the EFA analysis, a total of five latent factors were required to account for at least 50% of the variance in the original PRO z-score data. The latent factors were identified, and the Pearson’s correlation coefficient (r) between the latent factors and PROs was calculated. The first factor demonstrated a strong correlation with Pain Intensity, ODI, PROMIS Pain T-score, and a strong negative correlation with the PROMIS Physical Function T-score. Due to its strong correlation with PROs that describe an individual’s physiological limitations, this latent factor was labeled “Pain and Physical Limitations”. The second factor identified demonstrated a strong correlation with PROMIS Depression T-score, PROMIS Anxiety T-score, and the General Anxiety Disorder metric, and was consequently labeled “Psychological Distress”. The final three latent factors nearly replicated the PROMIS Sleep Deprivation, IPAQ MET Minutes / Week metrics, and Pain Catastrophizing 6 scores. These were subsequently named “Sleep Deprivation”, “Physical Activity”, and “Pain Catastrophizing”. See Figure 4.5a, Table 4.5. These findings coincide with the correlation of determinations observed between the original features (see Figure 4.5b).

Table 4.5 Summary of the Pearson’s correlation between the original PROs of interest and the identified latent factors.

PROs	Pain and Physical Limitations	Psychological Distress	Physical Activity	Sleep Deprivation	Pain Catastrophizing
IPAQ MET Minutes / Week	-0.099	-0.059	0.983	-0.077	-0.064
Pain Intensity	0.905	0.152	0.022	0.098	0.091
ODI	0.875	0.274	-0.079	0.217	0.142
PROMIS Pain Interference	0.906	0.234	-0.077	0.156	0.121
PROMIS Physical Function	-0.878	-0.184	0.145	-0.173	-0.174
PROMIS Depression	0.442	0.265	-0.121	0.833	0.149
PROMIS Anxiety	0.284	0.791	-0.157	0.112	0.183
PROMIS Sleep Deprivation	0.186	0.893	-0.059	0.067	0.199
GAD	0.174	0.894	0.064	0.160	0.081
PCS	0.309	0.409	-0.096	0.148	0.838

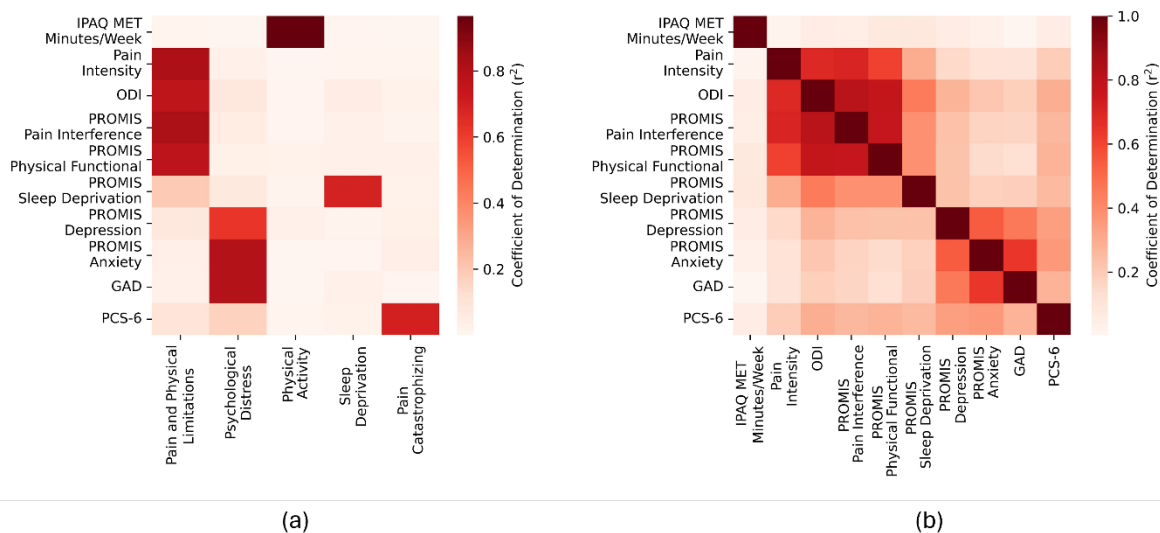


Figure 4.5 (a) The correlation of determination between the five factors identified -Physiological Ailment, Psychological Ailment, Sleep Deprivation, Physical Activity, and Pain Catastrophizing- with the original features PROs of interest and (b) and the correlation of determination between the PROs of interest.

In summary, there are several PROs designed to quantify physiological well-being (Pain Intensity, ODI, PROMIS Pain Interference, and PROMIS Physical Function) that are highly correlated with each other, as are PROMIS metrics and GAD scores that quantify psychological well-being. However, PROMIS Sleep Deprivation, IPAQ MET Minutes / Week, and the Pain Catastrophizing Scale were relatively independent of the other PROs investigated in this study and appear to represent distinct components of well-being.

4.3.4. Limitations

There were certain limitations in this study. The sample size was relatively small and was recruited by a single institution. Due to CLBP being a very heterogeneous ailment, caution should be taken before generalizing results to a population [6, 44]. Because the subjects were being recruited as part of a larger, ongoing study, inclusion criteria for the study required that the subjects be eligible to receive an MRI scan and perform a variety of functional motions [145], which may have deterred individuals with metal implants or more severe CLBP symptoms from participating. Additional studies that collect data from control subjects may be of value to further develop this line of work. An additional, innate limitation of any PRO is that all self-assessments are prone to biases: e.g., past investigations have observed that self-reported physical activity is generally higher than objective activity measurements [165], and self-reported pain intensity is associated with direct observations of pain behavior but influenced by several moderating factors [178]. However, many studies consider individual's self-perception as a vital (and sometimes superior) metric of back pain due to its highly subjective nature [21, 104, 179].

4.3.5. Conclusions

There is a plethora of PROs that are frequently used in clinical settings, and several of them show strong correlations with each other. However, from the PROs in this study there were five generalized and independent dimensions of well-being identified: Pain and Physical Limitations, Psychological Distress, Sleep Deprivation, Physical Activity, and Pain Catastrophizing.

It was observed that CLBP is associated with worse quality of life in terms of Pain and Physical Limitations, Psychological Distress, Sleep Deprivation, and Pain Catastrophizing. Although it is a common supposition that individuals with CLBP would be less active than their asymptomatic counterparts, CLBP was not

associated with a decrease in Physical Activity in this study. This finding is consistent with reports from past studies [171, 180]. There is stronger evidence, however, that individuals with CLBP exhibit different motion patterns than controls during specified tasks [150, 152]. Furthermore, the relationships between the PROMIS metrics with IPAQ MET Minutes / Week were relatively weak. This implies that while the total time an individual spends in physical activity is an important metric, it may be more vital to consider the quality of physical activity (i.e., the range of motion, proper technique, etc.).

Another key finding, which was also the primary motivation of the investigation, was that PROs take on different meanings according to an individual's experience with CLBP. Unsurprisingly, there were strong relationships observed between the PROMIS metrics (which quantify how much pain limits activities and common tasks) with the legacy PROs of Pain Intensity and ODI (which quantify more of how much pain is being experienced by an individual) for both cases and controls. However, at any given PROMIS score, cases reported higher Pain Intensity and ODI scores than their controls counterparts on average. This indicates that cases experience higher pain levels than even their control counterparts who report similar same functionality (i.e., PROMIS) scores. While this study cannot infer a causal relationship based on observational data, it does highlight the important distinction between pain being experienced by an individual and pain hindering an individual's ability to perform tasks. This finding re-emphasizes the need to develop new techniques to assist individuals with CLBP to manage their symptoms, even if those symptoms cannot be eliminated [156].

These findings provide important context for interpreting PROMIS and legacy PROs in future clinical investigations. This in turn may enable clinicians to more effectively monitor patient progress compared to the baseline of asymptomatic subjects, make more quantitative assessments of patients, and perhaps eventually contribute to the objective selection of treatment paradigms according to patient needs [44].

CHAPTER 5 WEARABLE NANOCOMPOSITE SENSOR SYSTEM FOR MOTION PHENOTYPING CHRONIC LOW BACK PAIN: A BACPAC TECHNOLOGY RESEARCH SITE

Published manuscript regarding data analysis protocol for BACPAC [145]. I hereby confirm that the use of this article is compliant with all publishing agreements.

Co-authors: Spencer A Baker, BS,¹ Darci A Billmire, BS,¹ R Adam Bilodeau, PhD,¹ Darian Emmett, BS,¹ Andrew K Gibbons, BS,¹ Ulrike H Mitchell, PhD, PT,¹ Anton E Bowden, PhD, PE,¹ David T Fullwood, PhD¹

¹Brigham Young University, Provo, Utah

Correspondence to: David T. Fullwood, PhD, Engineering Bldg., Campus Dr, Provo, UT, 84062, 350N EB, Tel: 801-422-6316, Email: dfullwood@byu.edu

Funding sources: This research was supported by NIH grant UH3AR076723.

Conflict of Interest: Dr. Bowden and Dr. Fullwood own equity in Sensable Technologies, a company that licenses the underlying sensor technology described in this paper from BYU for tracking human biomechanics in other applications.

5.0. Abstract

Chronic low back pain (CLBP) is a prevalent and multifactorial ailment. No single treatment has been shown to dramatically improve outcomes for all CLBP patients, and current techniques of linking a patient with their most effective treatment lack validation. It has long been recognized that spinal pathology alters motion. Therefore, one potential method to identify optimal treatments is to evaluate patient movement patterns (i.e., motion-based phenotypes). Biomechanists, physical therapists, and surgeons each utilize a variety of tools and techniques to qualitatively assess movement as a critical element in their treatment paradigms. However, objectively characterizing and communicating this information is challenging due to the lack of economical, objective, and accurate clinical tools. In response to that need, we have developed a wearable array of nanocomposite stretch sensors which accurately capture the lumbar spinal kinematics, the SPINE Sense System. Data collected from this device are used to identify movement-based phenotypes and analyze correlations between spinal kinematics and patient-reported outcomes.

The purpose of this paper is twofold: first, to describe the design and validity of the SPINE Sense System; and second, to describe the protocol and data analysis towards the application of this equipment to enhance understanding of the relationship between spinal movement patterns and patient metrics, which will facilitate the identification of optimal treatment paradigms for CLBP.

Keywords: Chronic low back pain; Machine learning; Phenotypes; Clusters; Spinal motion; Optimization

5.1. Introduction

Low back pain (LBP) is a prevalent ailment. In the United States alone, it is estimated that 80% of the population will experience a back problem at some point in their lives [10], and that at any given time 31 million Americans are suffering from LBP [181]. Not only is LBP common, but it also has the potential to be

very severe. Back pain is the single leading cause of disability [17]. Treating back pain imposes a significant economic cost as well. In the United States alone, over \$100 billion are annually lost from treatment costs and productivity losses associated with LBP [182]. Unfortunately, the increased costs of treating lower back pain have not mitigated the issue [58].

The ineffectiveness of LBP treatments is due in part to the limitations in current diagnostic techniques. The most common diagnostic methods employ static imaging (e.g., CT or MRI scans) to detect anatomical anomalies. However, it is difficult to pinpoint the etiology of chronic and other types of non-specific low back pain (CLBP) using these methods [59]. Virtually all static images are acquired with the patient lying down or standing, failing to capture the dynamic aspect of lower back pain which could be critical to the diagnosis. Furthermore, many patients suffering from CLBP do not exhibit clear anatomical anomalies in their spine [149]. Rather, the pain is the result of myriad psychological, social, and biological factors [4]; additionally, many subjects who exhibit anatomical anomalies do not experience corresponding symptoms, indicating that anatomical anomalies are often unrelated to the underlying cause of the subject's pain [183]. In summary, it is very difficult to prescribe treatments that will resolve the underlying cause of CLBP because those underlying causes might have been resolved, or in case that they are still present, cannot be captured with static images or existing biomarkers.

Several methods and many studies have attempted to identify linkages between patients and their most effective treatment paradigm. One intriguing approach is to evaluate patient motion patterns (i.e., movement phenotypes). It is well known that individuals with acute and chronic back pain move differently than asymptomatic controls, a phenomenon that potentially becomes more pronounced the longer the symptoms last [184-186]. Patients intrinsically recognize motions and postures that cause pain and alter their position accordingly. Usually, a reduction in spinal range of motion in uniplanar [81, 187] and multiplanar directions [188] is involved. Biomechanists, physical therapists, chiropractors, and surgeons each utilize a variety of tools and techniques to assess and interpret qualitative movement changes as a window to understanding potential mechanical and neurological sources of low back pain, and as a critical element in their treatment paradigm. It is therefore reasonable to postulate that motion-based phenotyping of CLBP could be valuable in finding effective treatment options [189] and in evaluating patients' rehabilitation progress. Past studies that have investigated phenotyping as a means to identify optimal LBP treatments, and have found that while several classifications methods show promise, the margin of improved treatment outcomes currently fall short of clinical significance [96]. These and related studies often rely on qualitative assessments of LBP symptoms [190] or highly trained individuals [191] to classify patients according to their respective phenotypes, making these methods liable to misdiagnosis due to either the subjective nature of the assessment [96, 192] or clinical inexperience [44].

Overall, the identification of LBP classes—particularly those that account for spinal-motion phenotypes—is a concept that shows enormous potential, but is stymied by the lack of cost-effective, objective, and accurate tools that are compatible with the clinical setting. A valid and reliable quantitative assessment tool is therefore necessary to objectively measure and monitor spinal motion [150] in order to identify and analyze said phenotypes. Our BACPAC Technology Research Site team has addressed this challenge through the use of unique, inexpensive, elastomer-based nano-composite piezoresponsive sensors. Specifically, we have integrated these sensors into a SPInal Nanosensor Environment (SPINE Sense System), which provides an objective, quantitative platform for diagnosis, monitoring, and follow-up assessment of movement changes associated with CLBP. The raw data that are collected from the subjects are comprised of electrical signals from an array of these piezoresponsive sensors that are optimally arranged on the skin of the lower back. These sensors measure local skin strains, which, in turn, correlate with the kinematic motion of the lumbar spine [193, 194]. This method of using externally mounted sensors offers advantages over alternative kinematic-measuring methods, such as percutaneous skeletal trackers or radiographic imaging, which either

involve invasive tools or extended exposure to radiation [193]. It is also a more economical solution than other motion-capture techniques such as optical cameras, which require expensive equipment and elaborate set up. These sensors have already been used in several biomechanical applications, such as estimating knee kinematics [138], calculating ground reaction forces [129], measuring ligament strain [140], estimating range of joint motion [141], tracking pulse [142], evaluating upper limb posture [195], and monitoring fetal movements, [143] with promising results.

To make this technology applicable to biomechanical phenotyping of the spine, our laboratory has engaged in multiple phases. The overall purpose of this paper is to describe the completed and promising phases of our work.

- In Section 2, we will describe our completed work focused on the design and development of our SPINE Sense array, along with our experiments that describe the validity, reliability, and usability of our equipment to capture spinal kinematics objectively.
- Section 3 presents the current step of our BACPAC study, describing our current human subject testing protocol.
- Section 4 describes how the data collected from this protocol will be analyzed to leverage spinal kinematics to determine to what extent they are related to patient-reported outcomes (PROs) and how they can be leveraged to identify dominant motion phenotypes. Some preliminary findings from the early stages of data collection are also presented in this section. It is expected that the outcomes from these analyses will lead to enhanced diagnostics, patient monitoring, and eventually to more effective clinical treatment paradigms [44].

These three phases of research and development are depicted in Figure 5.1.

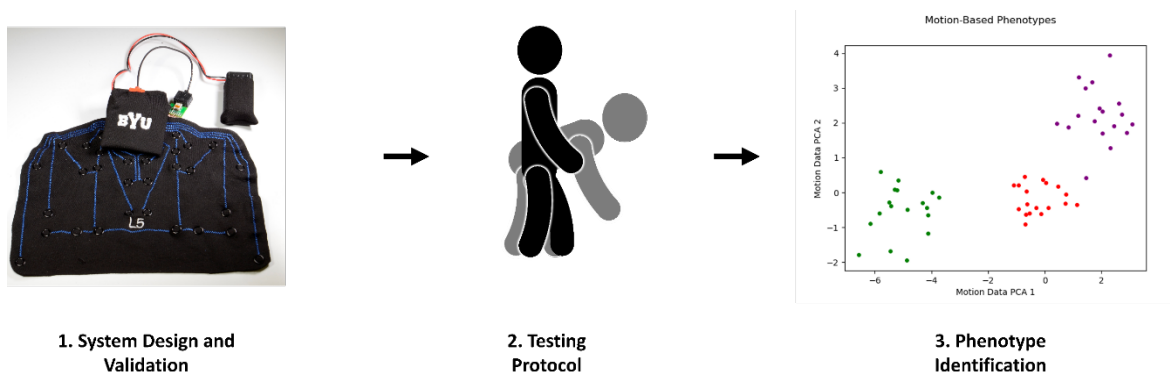


Figure 5.1 Overview of methodology to identify and analyze movement-based phenotypes among symptomatic and asymptomatic subjects by (1) developing and validation system design (2) collecting data from symptomatic and asymptomatic subjects during several single-planar and multi-planar spinal motions, and (3) analyzing the spinal motion data to identify and interpret different motion-based phenotypes among subjects.

5.2. System Design and Validation

The primary objective of this article is to present the protocol that is being used to collect spinal motion data from control participants and participants with CLBP subjects and the proposed methods to analyze those data to determine the correlation between spinal motion and PROs. We previously reported on the development of the SPINE Sense System which is used to effectively monitor spinal motion. A brief recap of the elements of that design will follow (see also references [194, 196-198] for additional information).

- **Array Design:** To obtain the clearest reading from the sensors and an accurate estimation of spinal kinematics, the skin-mounted strain gauges were optimally placed on the lines of maximum extension (LoME) of the skin.
- **Array Implementation:** A prototype of the strain gauge array to be used in clinical applications was presented to prospective users. The usability of the system was evaluated, and suggestions were recorded to improve future iterations of the design.
- **Electronics Design:** A key aspect of the system was to provide patients and clinicians with a user-friendly device that can monitor spinal motion. An app was designed to collect and store the data in an efficient manner and provide the users with an intuitive interface.

5.2.1 Array Design

In previous endeavors, skin-mountable nanocomposite sensors (composed of nickel nano strands and nickel coated carbon fibers embedded in a silicone matrix) have been developed by researchers at Brigham Young University [127]. In this endeavor, these sensors are being used to detect the skin strain in the area of the lumbar spine to obtain an estimate of the underlying spinal kinematics (related studies have also used skin-mounted sensors to obtain estimates of knee [131] and spinal motions [199]). In order to extract an accurate estimate of spinal kinematics, the sensors must be strategically placed to detect skin stretch during different motions. Specifically, we desire to estimate the primary kinematics of the spine, which are comprised of flexion-extension along the sagittal plane, lateral bending (left and right) along the coronal plane, and axial rotation (clockwise and counterclockwise) along the axial plane [200, 201]. In a related study, researchers seeking to optimize the placement of skin-mounted motion capture markers to estimate knee kinematics approached this task by placing sensors along the lines of maximum extension (LoME) during different motions [202], which facilitated accurate knee kinematic estimations along multiple degrees of freedom [131].

In order to determine the LoME, spinal motion and skin elongation data were extracted during a motion-capture experiment [203]. Data were collected from 28 subjects. This sample size was selected to provide sufficient distinguishing power, accounting for differences between genders and other subject demographics, and is consistent with or exceeds the sample sizes used in related studies [193, 199]. A summary of the subject demographics of the participants in this study are shown in Table 5.1.

Table 5.1 Summary of the subject demographics in motion-marker study (the average of each demographic and the corresponding standard deviation of the motion capture participants)

Demographic	
Age (years) [stdev]	25.3 [9.2]
Height (cm) [stdev]	176.5 [8.4]
Weight (kgs) [stdev]	73.6 [14.24]
BMI (kg/m ³) [stdev]	23.5 [3.3]
Sex (M/F)	15 / 13

Participants were asked to perform three repetitions of several single-planar and multi-planar motions. Skin stretch at different areas of the low back was measured during these motions via an array of 36 reflective markers on subjects' lower backs (see Figure 5.2) and tracked using a 10-camera motion capture system.

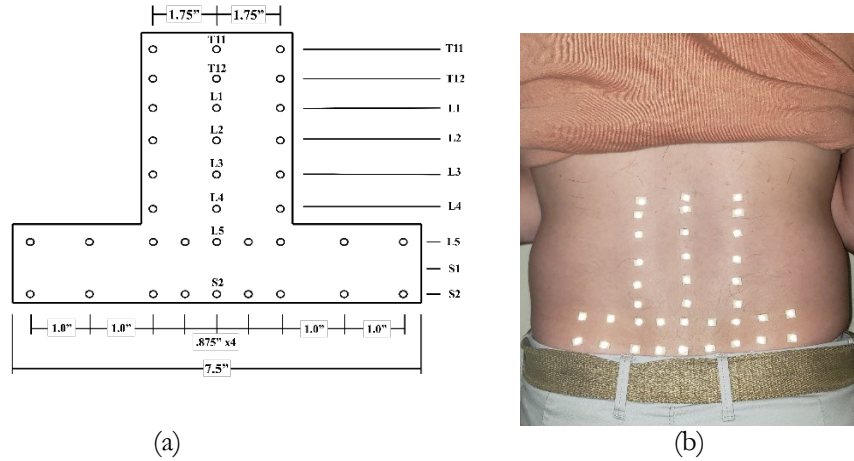


Figure 5.2 (a) Placement of reflective markers for motion-capture study and (b) the markers on a subject's lower back. The skin stretch during different spinal motions was estimated by calculating using the distance between markers.

The engineering strain ($\Delta L/L_0$) was calculated between the adjacent reflective markers during each motion. The LoME for each of the six single-planar motions (flexion, extension, lateral bending left, lateral bending right, axial rotation left, axial rotation right) were identified (see Figure 5.3a). Strain gauge locations were chosen to capture the clearest signal of spinal motion along specific spinal degrees of freedom by considering the LoME and the strain limitations of the gauges (see Figure 5.3b); four sensors were selected to primarily capture flexion-extension (marked by blue), six sensor locations were chosen to detect lateral bending motion (marked by red), and six sensors were placed to optimally capture axial rotation motion (marked by green).

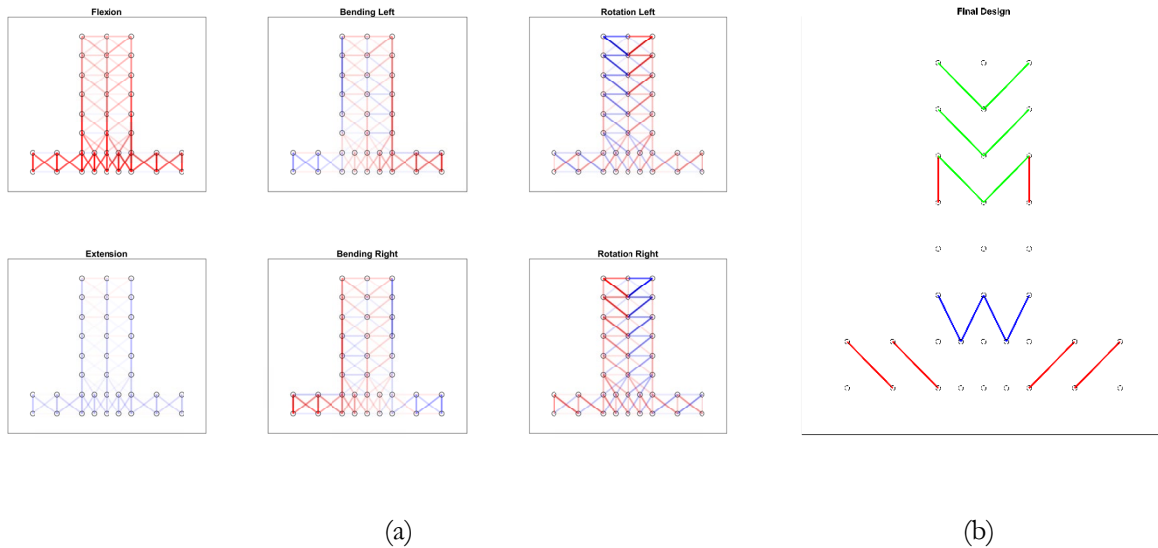


Figure 5.3 Summary of the extension magnitude for (a) each single-planar motion – higher magnitudes of extension indicated by darker shades of red and higher magnitudes of compression indicated by darker shades of blue – and (b) the result array design. The reflective markers are indicated by the circles, following the placement depicted in Figure 5.2.

The array design was evaluated by its ability to differentiate between different spinal movements in a support vector classification model. The model input was the maximum skin strain between reflective markers included in the final design (Figure 5.3b) for each subject-motion combination. The output was the model prediction of which spinal motion was performed. The spinal motions considered in the evaluation included

single-planar movements (lateral bending left, lateral bending right, flexion, extension, axial rotation left, and axial rotation right) and multi-planar movements (flexion-left, flexion-right, extension-left, and extension-right). Data from 20 subjects were randomly selected for training the model, and the data from the remaining 8 subjects were selected for evaluating the model. This process of training and testing the model was repeated 10 times. The model achieved an average of 90% classification accuracy (see Figure 5.4). Ten other designs (randomly generated placements of the 16 strain gauges) were also evaluated using the same methods for comparison, which achieved an average of 76% classification accuracy. None of the random designs achieved greater than 83% accuracy. From this evaluation, we validated that skin stretch can be a reliable metric for evaluating different spinal motions, and that the quality of data for inferring spinal kinematics may be optimized by placing markers along the LoME of the lumbar spine.

True Class	BendL	174	1	12	26	12			3					76.3%	23.7%
	BendR		202	2	5	16				3				88.6%	11.4%
	Ext	7	11	179	10	4								84.8%	15.2%
	ExtL	17	2	10	134	3						8		77.0%	23.0%
	ExtR	6	4	13	7	160							9	90.4%	19.6%
	Flex						186	15	13					98.9%	13.1%
	FlexL	4					38	188						81.7%	18.3%
	FlexR		12				18		202					87.1%	12.9%
	RotL									240				100.0%	0.0%
	RotR										240			100.0%	0.0%
		83.7%	87.1%	82.9%	73.6%	82.1%	76.9%	91.3%	92.7%	96.8%	96.4%				
		16.3%	12.9%	17.1%	26.4%	17.9%	23.1%	8.7%	7.3%	3.2%	3.6%				
		BendL	BendR	Ext	ExtL	ExtR	Flex	FlexL	FlexR	RotL	RotR				
		Predicted Class													

Figure 5.4 Confusion matrix, depicting the true class of exercise being performed by a subject and the corresponding predicted class, using the skin strains captured by the optimized strain gauge array design as predictors in a machine learning classification model. Predictions along the diagonal represent accurate exercise classifications.

During desired applications, the strain gauges must be applied to the lumbar spine to capture skin strains and estimate spinal kinematics. One option is an adhesive layer to hold the strain gauges to the lower back (such as kinesiology tape, which is commonly used in athletics and biomechanical applications). A validation test was conducted to compare the skin strain under normal conditions and when kinesiology tape is applied to the lumbar spine. It was determined using a finite-element model that although an adhesive layer diminishes the strain magnitude, general strain patterns during motion were not significantly affected [204]. This finding further validated the use of kinesiology tape to adhere the strain gauges to the spine, and further emphasizes the need to place sensors along the LoME to obtain the clearest signal possible.

Finally, a validation test was performed to evaluate the device's ability to estimate spinal kinematics. The array of the 16 sensors was adhered to the lumbar spine of a cadaver specimen. The specimen was supported using a harness and manually manipulated in a series of spinal motions along the sagittal plane. The flexion of the cadaver spine was measured using an electromagnetic tracking system, adhered to the L1-S1 functional

spinal units via bone pins. A lasso regression model was developed to predict spinal motion as a function of sensor readings root-mean squared error of less than 10% (for full details, see [194]).

5.2.2. Array Implementation

Once the array was designed and its ability to capture spinal motion was shown, its usability in the context of clinical practice was assessed. A prototype of the SPINE Sense System – composed of the 16 nanocomposite sensors adhered to kinesiology tape with a scripted explanation about how the device is used including its integration with its smartphone application (see Figure 5.5) – was presented to 32 potential users of the device including clinicians and patients with CLBP [196].



Figure 5.5 The vertebral motion tracking system of 16 nanocomposite sensors (two are visible from underneath the cover in the lower right side) on kinesiology tape with stitched wiring.

Reviewers were asked to fill out the System Usability Scale, which is a common validated industry standard to evaluate the general usability of a system [205]. The System Usability Scale score is from 0-100 – a score above a 68 indicates a device that is intuitive to use [206]. The mean value of our study usability score was 72, which is considered above average. A more comprehensive breakdown of the results is presented in Table 5.2. It was concluded from these results that the device is usable and attractive to clinicians and patients who are potential users of the device.

Table 5.2 System Usability Scale scores from clinicians and patients.

Item	Clinicians	Patients	Total
Participants	19	13	32
Mean Score	70.79	73.85	72.03
Standard Deviation	13.74	6.69	11.51

The reviewers were also asked open ended questions about the design of the device and given the opportunity to voice ideas, questions, and concerns regarding the design of the device. Common feedback and comments about the design of the device included the following:

- The easy application and flat compact design of the device was common positive feedback received.
- The simplicity of the system of its use with a smartphone application was also well received amongst the potential users.
- Some concerns and questions included the concerns of the device only coming in one size, the duration of adherence, and ease of removal.
- There was also a concern about the tackiness of the kinesiology tape with recommendations of other commonly preferred athletic tapes.

5.2.3 Electronics Design

The electronics portion of the system, required to read data from the 16 strain gauges, was designed to be minimal in both size and complexity to facilitate a national clinical study and obtain consistent results across investigation sites. A custom printed circuit board assembly (PCBA) was designed and fabricated with a 16-channel switcher to cycle through all the sensors and sample at a rate of 800 Hz. This PCBA measures 54.61 mm x 50.8 mm (2.15 in x 2 in) and is 4.6 mm (0.181 in) tall at its highest point, with a mass of 12.00 g. The planar, lightweight design enables it to be tucked into a small fabric pouch mounted to the sensor array, without disturbing the subject being tested, adding significant weight, or impacting the motion of the sensor array during exercises. Custom cables using the micro-HDMI connection standard further reduce the size, weight, and complexity of the system. This provides a flexible 17 channel (16 sensors & common ground) connection between the array and the custom PCBA (see Figure 5.6).



Figure 5.6 (a) Custom PCB for reading the resistance across all 16 piezoresistive sensors and (b) integration of PCB with final SPINE Sensor System.

The board is powered by a standard 9V alkaline battery (nominal mass 45 g), which is readily available across the country. The battery is connected to the custom PCBA using a small power cable and wire (for a total system mass of 64 g), so that the battery can be mounted off to the side of the test subject, while providing multiple hours of charge to the PCBA. A user-friendly switch and LED system allows the clinician to know (a) the board is powered on and (b) the battery has a good charge and/or needs to be replaced. This simple system reduces the possibility of failure on the part of the electronics and custom PCBA due to battery/charging concerns.

To extract and record sensor readings from the device, a smartphone app was developed for Android® smartphones, and is currently available on the Google Play® app store. The app has an easy-to-use interface, designed to reduce options or confusion for the clinician.

5.3. Subject Testing Protocol

Using the SPINE Sense System developed as described above, data are acquired from two cohorts (150 healthy, 150 symptomatic) of participants during clinician-guided diagnostic movements, in order to provide a

sufficient body of data to identify major spinal movement deviation phenotypes. Subjects are between 35-65 years old. This is the age range with the greatest prevalence of CLBP [153]. Demographic characteristics (sex, age, BMI) are approximately matched across the two cohorts. Data gathering will occur at BYU, along with various partner BACPAC sites, such as University of Pittsburgh, UCSF, OSU, and Harvard. The symptomatic cohort is recruited from individuals who are already scheduled for physical therapy for complaints of CLBP. The exclusion criteria for asymptomatic participants are current or history of lumbar spine pain for which treatment was sought at any point during the participant's lifetime ('treatment' is defined as having seen a physiotherapist, chiropractor, osteopath, or medical doctor for the condition), known scoliosis and inability to receive MRI (e.g., metal or electrical implants, claustrophobia or possible pregnancy). In addition, all participants (symptomatic and asymptomatic) must be able to assume a vertical position and move without an assistive device. Participants are screened for exclusion criteria, and after consent is given, receive our standardized diagnostic movement examination and are scheduled for their MRI.

With the participant in standing position the spinous process of L5 is palpated and marked. The participant then transfers onto a treatment table into prone position. The lower back is sprayed with a commercially available pre-tape spray adhesive and the array is attached as depicted in Figure 5.7.

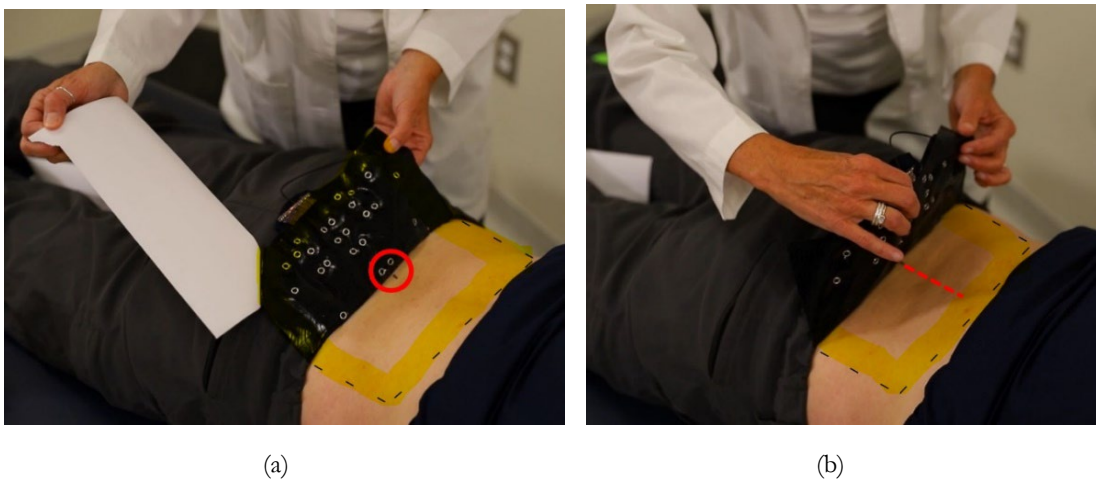


Figure 5.7 The SPINE Sense System is placed to the lower back using the L5 spinal process unit as a to guide the placement (a) and is aligned vertically on the lower back (b). The kinesiology tape adherence is reinforced on the edges (depicted in yellow in the figures above) using pre-tape spray.

After the array is adhered, the participant is ready to begin the spinal motion tests. Each movement is performed six times with a two-second break between repetitions. The clinician demonstrates each movement, and the participant is allowed to practice the movement once. Participants are instructed to perform the motions to the extent possible without inducing pain. The 'SPINE Sense' app, available on Play Store, is used to guide the clinician and participant through the spinal motion tests. Once the app is connected to the PCBA via Bluetooth (Figure 5.8a), it requests basic biometric data along with a de-identified subject ID (Figure 5.8b). Then, it provides a sequential series of one-click-one-action buttons that first demonstrates the spinal motion for the participant, initiates the recording of data as the subject then performs six repetitions of the movement, and stops recording the data and downloads them via Bluetooth from the PCBA (Figure 5.8c). Once the data are downloaded, the app continues to the next motion. After all spinal motions are completed and confirmed by the clinician, the app uploads the data to a cloud server via WiFi or cellular internet to be accessed by the researchers for analysis (Figure 5.8d).

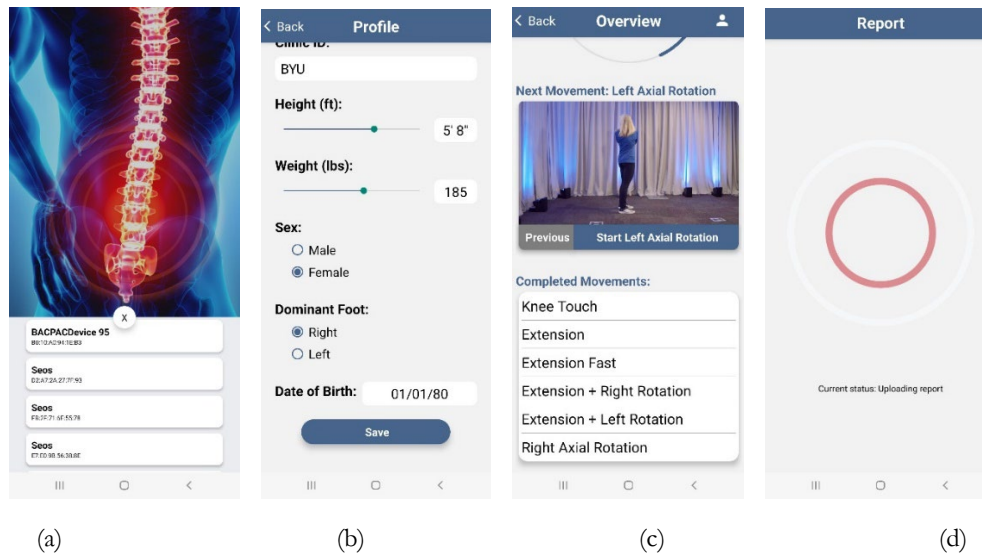


Figure 5.8 Summary of the SPINE Sense App during the different stages of motion capture. The clinician or participant (a) opens the app, (b) enters participant demographic information, (c) is guided through the series of spinal motions to perform, and (d) uploads data to the cloud server.

Our project involves classic uniplanar movements (flexion, extension in the sagittal plane, rotation in the transverse plane and side bending in the frontal plane), but also combination of those (flexion and extension with rotation) and a functional sit-to-stand motion. Further details of each movement and the order in which they were performed, are listed below:

1. Knee Touch: the participant is instructed to round their lower back and reach with their hands to the respective knees from an upright position.
2. Extension: The participant extends their spine in the sagittal plane as far as comfortably possible.
3. Extension Fast: The participant extends their spine similarly, but as fast as comfortably possible.
4. Extension-Right: The participant extends their spine in the sagittal plane while rotating it in the transverse plane to their right.
5. Extension-Left: The participant extends their spine in the sagittal plane while rotating it in the transverse plane to their left.
6. Rotation-Right: The participant crosses their arms over their chest and rotated their spine in the transverse plane towards their right side while maintaining pelvis position (facing anteriorly).
7. Rotation-Left: The participant crosses their arms over their chest and rotates their spine in the transverse plane toward their left side while maintaining pelvis position (facing anteriorly).
8. Side Bending-Right: The participant flexes their spine to their right in the frontal plane while maintaining a forward-facing trunk orientation.
9. Side Bending-Left: The participant flexes their spine in the frontal plane to their left while maintaining a forward-facing trunk orientation.
10. Flexion-Right: The participant flexes their spine and hips in the sagittal plane while rotating the spine in the transverse plane to the right.
11. Flexion-Left: The participant flexes their spine and hips in the sagittal plane while rotating the spine in the transverse plane to the left.
12. Up and Go: The participant sits on a short stool and rises, without the assistance of their hands, and walked two steps forward.
13. Flexion: The participant flexes their spine and hips in the sagittal plane as far as comfortably possible (slight flexion of the knees is allowed).
14. Flexion Fast: The participant flexes their spine similarly, but as fast as comfortably possible.

After the motion tests are complete, the SPINE Sense System is removed with the help of paper towels and baby oil. The duration of the test, including the don and doff of the SPINE Sense System, is approximately 15 minutes [44].

As reported in the Anchor paper, the BACPAC Minimum Dataset is used as patient reported outcomes [57]. Briefly, the assessment consists of 19 questions/questionnaires that investigate demographics and pain location (radicular/ non radicular and if it is widespread), pain intensity, pain duration and frequency, pain interference, pain catastrophizing, pain somatization, physical function, sleep, depression, anxiety, substance use and opioid use. In addition, our site added a physical activity questionnaire [99]. Participants are requested to complete the questionnaire during the week prior to the motion-capture study.

5.4. Data Analysis

After the PCBA uploads the electrical signal from the 16 piezoresistive strain gauges measured during the set of exercises, the data will be processed and analyzed. This section will present the methods that used to analyze said data. Results from early stages of subject testing will also be presented as a preview of anticipated findings.

High deflection strain gauges are a relatively new innovation, and the interpretation of such is a complex task due to the nonlinear output of the sensors [125]. Past studies have used a variety of curve-fitting analyses and machine learning algorithms to extract biomechanical information from the skin-mounted strain gauges [131, 207-209]. For the purposes of this research, a model that accounts for the viscoelastic material properties of the sensors was developed to extract stretch magnitude and strain rate (for full details, see [144]). Additional metrics, such as asymmetry of motion, will be extracted by comparing the calibrated sensor outputs on mirror sides of the sagittal plane. These metrics will be calibrated for each participant using the knee touch motion performed during the first stage of subject testing to account for inter-subject variations of subcutaneous tissue and anthropologies. The metrics will then be used to run two general analyses:

1. Biomechanical Analysis: Analyze the relationship between spinal kinematics and PROs.
2. Phenotype Analysis: Cluster participants by similarity of motion patterns and demographics, identify dominant features of each cluster (i.e., the motion-based phenotype), and investigate correlation between phenotype and PROs.

The Biomechanical Analysis will provide a conceptual understanding of how and to what extent spinal kinematics correlate with patient well-being, and the Phenotype Analysis will provide clinicians and patients with information that may facilitate the prescription of more effective treatment paradigms.

5.4.1. Biomechanical Analysis

One objective of this research endeavor is to quantify the extent to which spinal kinematics correlate with different PROs. Past studies have attempted to differentiate between the motion of subjects with chronic and acute low back pain from the motion of asymptomatic subjects, with promising results as described below [46, 93, 210, 211]. This research endeavor will complement previous findings and make further contributions to this topic by analyzing spinal kinematics during a broader range of motions and testing the correlation between spinal kinematics and additional patient-reported metrics. These tests will be accomplished by (1) identifying features of interest that may correlated with PROs and (2) running a series of statistical tests to investigate the correlation.

5.4.1.1. Features of Interest

Two obvious biomechanical features relating to CLBP are spinal range of motion for a given exercise and the velocity at which the exercise is performed. Previous studies have found that patients with CLBP have statistically lower ranges of motion and velocities in certain exercises than control subjects [46, 210]. It is

expected that the range will change with pathology. However, there are few other specifically identified biomechanical features that have been correlated with CLBP phenotypes in a quantifiable way. Two recently studied attributes of patient motion include time-of-rise [93] and jerk level (rate of change of acceleration during a given motion) [211].

In order to provide guidance for the identification of features of the SPINE Sense data, a recent study was undertaken by the BACPAC Technology Site at Brigham Young University using participants with CLBP and control subjects who did not suffer from CLBP, that followed the same set of exercises described above (5.3. Subject Testing Protocol). The participants were fitted with three inertial measurement units (IMUs) on the sacrum, L4, and C7 spinal segments. Kinematics including acceleration, angular velocity and jerk were recorded and are currently being analyzed for motion features that most clearly identify CLBP (e.g., features with high variance across the subject set).

Other potential metrics available from the SPINE Sense system include asymmetry of motion, a range of other derivative metrics from strain, time, and surface shape features of the back (such as angular velocity, back curvature, etc.), as well as changes in metrics with repeated exercises (such as variance and gradients).

5.4.1.2. Statistical Tests and Regression Models

Statistical tests will evaluate the difference between the spinal motion subjects with CLBP and asymptomatic subjects, as well as the motion of subjects who do and do not take opioids. Student t-tests are ideal for this analysis because CLBP status and opioid use are binary, categorical variables (i.e., a subject either experiences CLBP or does not). An example of the results obtained from Student t-tests analyses conducted on preliminary data collected with the IMU placed on the C7 of the spine during flexion left is depicted in Figure 5.9a. The Bonferroni correction will be applied in the statistical analyses to account for the multiple comparisons that will be conducted. Quantitative patient-reported outcomes (ODI, PROMIS, and IPAQ scores) will be correlated with spinal kinematics by running several regression analyses. Multiple linear regression models will be developed to predict PROs as functions of spinal kinematics and demographics. Model features will be selected using Stepwise Regression techniques (a hybrid of forward and backward feature selection). The number of features included in the final models will be determined by evaluating the adjusted R-squared of each model with different number of explanatory variables. A sample of the correlation between a single kinematic measurement and a PRO is depicted in Figure 5.9b.

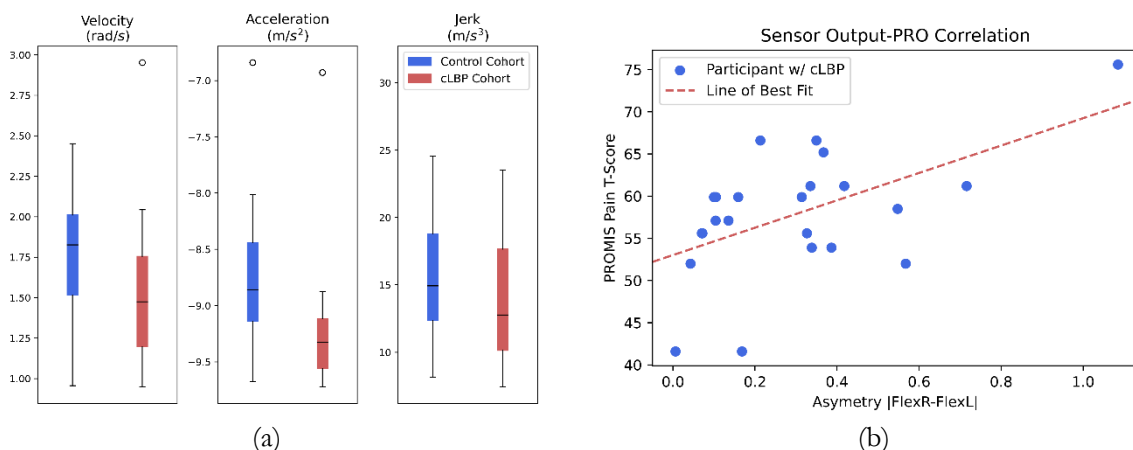


Figure 5.9 (a) An example of a comparison between the velocity, acceleration, and jerk between 16 control subjects (blue) and 28 subjects with CLBP (red) during Flexion Left collected from the IMU placed on the C7 (p-values of 0.26, 0.08, and 0.60 for velocity, acceleration, and jerk respectively) and (b) scatterplot of asymmetry of motion during flexion -estimated by the absolute value of the difference in the sensor readings during the Flexion Left and Flexion Right motions – and the PROMIS Pain T-score for participants with CLBP (blue dots) with the corresponding best fit line (red).

The IPAQ questionnaire categorizes persons' activity levels into one of three bins: low, medium, and high. This data format is well suited for F-statistic and ANOVA tests to investigate whether physical activity is correlated with spinal kinematics.

It is anticipated that the results of these analyses will provide clinicians and researchers with an understanding of how spinal kinematics can be used to interpret the different metrics of patient well-being, to what extent spinal kinematics correlate with PROs, and which features are most informative in assessing a subject's condition.

5.4.2. Phenotype Identification and Interpretation

The primary objective of this research endeavor is to identify and analyze movement phenotypes of spinal motion. Different etiologies of acute cases of low back pain are often associated with specific changes in spinal motion and specific treatment paradigms exist [85-92, 212]. It is therefore reasonable to suppose that patients with CLBP who exhibit similar abnormalities in spinal motion respond similarly to a certain treatment [96]. Objectively identifying and analyzing these motion patterns may lead to more personalized treatment paradigms and improved outcomes for patients suffering from CLBP [213]. Phenotype identification will be accomplished via an unsupervised clustering analysis. The approach of this endeavor involves three steps:

1. Cluster participants (from both the symptomatic and asymptomatic cohort) according to spinal motion characteristics observed during the standard exercise routine and demographics by their respective phenotypes.
2. Rank the features of each cluster to determine the features most useful for phenotype segmentation, identify the predominant characteristic(s) of each cluster / phenotype, and quantify the difference of dominant features between clusters.
3. Analyze the relationship between phenotype cluster and patient-report outcomes using one-way analysis of variance (ANOVA) statistical tests.

5.4.2.1 Phenotype Identification

The clustering analysis entails selecting which features ought to be included in determining phenotypes, choosing an appropriate algorithm for grouping participants with similar features together, and determining the optimal number of clusters that will be conveyed to clinicians and patients.

Features of Interest

Several features will be included in the clustering analysis to identify phenotypes among subjects with CLBP; they are:

- Spinal kinematics collected from the skin-mounted sensors. The kinematic measurements of spinal motion that most clearly differentiate between the motion of CLBP and asymptomatic subjects will be prioritized in the clustering analysis (see 5.4.1. Biomechanical Analysis).
- Subject demographics as collected from the questionnaires.
- Anatomical assessment of the lumbar spine as determined by a radiologist from MRI scans. Although MRI scans of the spine are insufficient on their own to provide adequate detail regarding a patient's condition to indicate the optimal treatment paradigm [149], evidence suggests that MRI images still provide valuable information (such as ailment severity [214], which has the potential for clinical application [215]) when considered in conjunction with additional metrics. The presence of specific anatomical anomalies will be included as binary variables (e.g., degenerated intervertebral disc in the lumbar spine – 0 if no, 1 if yes).

Each feature will be normalized to objectively compare its impact on the final phenotype identification. A principal component analysis will then be used to reduce the number of data dimensions and eliminate feature collinearity.

Clustering Algorithm

The objective of the phenotype identification is to group together datapoints (i.e., participants) that exhibit similar features. Clustering analyses are ideal for identifying predominant spinal-motion phenotypes because the algorithms will dissect data such that the variance between clusters is maximized while the variance within a cluster is minimized (i.e., the clusters are dissected along the natural segmentation in the data) [216]. Hierarchical clustering is well-suited for the phenotype-identification analysis due to its ability to cluster both quantitative features (such as spinal kinematics) and categorical features (such as demographics and MRI features) in the same dataset.

Hierarchical clustering will yield different results depending on the linkage type, which is used to quantify similarity / dissimilarity between data points (Figure 5.10, obtained from [217], depicts how different linkage types employed in clustering analyses cause different results for several hypothetical data set). Due to its robust nature, the Ward Linkage will be implemented in the phenotype analysis [218].

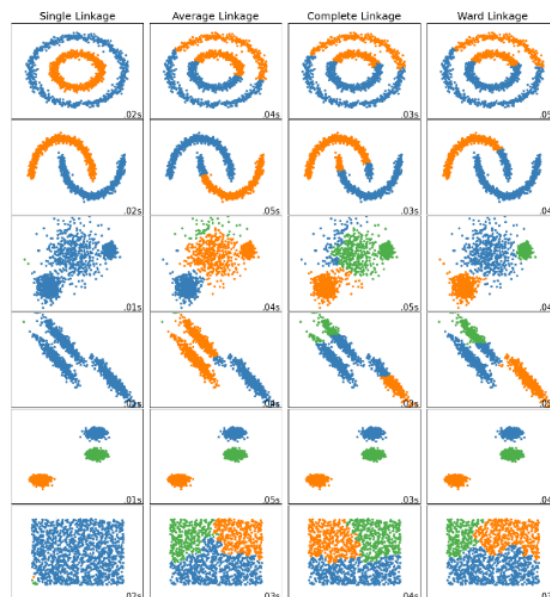


Figure 5.10 A depiction of how different linkage methods perform for hypothetical data sets, obtained from [217]. Single Linkage performs well on non-globular data, but performance is diminished by noisy data. Average Linkage and Complete Linkage perform well on data that exhibits clean separations between clusters, but the quality of the results is diminished if the separations are not as distinct. Ward Linkage is optimal when clustering noisy data and will be implemented in this endeavor [218].

Determining the desired number of clusters

One decision during the clustering process involves determining the desired number of clusters. An example of how the results of a clustering algorithm may vary according to the number of clusters into which a dataset is segmented is depicted by the dendrogram Figure 5.11 (generated from a hypothetical dataset). The height of the dendrogram tree demonstrates the dissimilarity score between pairs of observations. A higher

dendrogram cutoff score will result in fewer clusters with more observations per cluster. Lower dendrogram cutoff scores will result in more clusters with fewer observations per cluster.

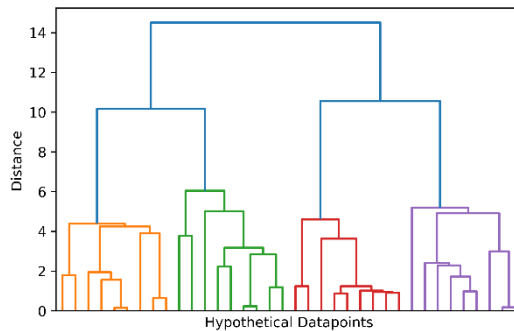


Figure 5.11 An example of a cluster dendrogram [219]. By using a cutoff distance score of 8, three clusters were extracted from the data, marked by orange, green, red, and purple. A cutoff distance score of >8 would have resulted in fewer clusters with more observations per cluster, and a cutoff distance score of <8 would have resulted in more clusters with fewer observations.

The objective to minimize the variance within clusters and maximize the variance between clusters can be quantified using the Calinski-Harabasz criterion [216]. Higher Calinski-Harabasz scores indicate better segmentation of the data. The Calinski-Harabasz score will be calculated for a wide range of potential targeted number of clusters, and the number of clusters that result with the highest score will be implemented in the final analysis. This will provide clinicians with the clearest distinction between participant phenotypes. A hypothetical dataset and the corresponding Calinski-Harabasz scores at a variable number of clusters is depicted in Figure 5.12.

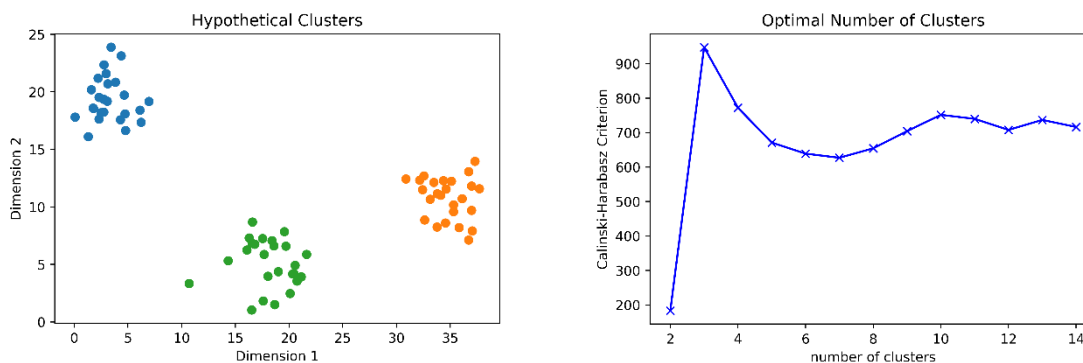


Figure 5.12 (a) The Hypothetical dataset is composed of data normally distributed around three centers and (b) the corresponding Calinski-Harabasz Criterion for 2 through 14 clusters. The Calinski-Harabasz score is the highest when the number of clusters is three, indicating three clusters provide the clearest segmentation between groups of datapoints.

5.4.2.2 Feature Ranking – Phenotype Description

While a principal component analysis of the original dataset will be used to remove the collinearity between features and reduce the number of dimensions in the clustering analysis, the resulting phenotypes will be described in terms of the original biomechanical features to preserve interpretability for clinicians and patients. The normalized original feature values will be averaged for each cluster. The difference between average feature values will be calculated for each pair of clusters, which will indicate which features had the largest effect in differentiating the phenotypes. This will enable us to rank feature importance for each cluster

and interpret the dominant subject characteristics (e.g., subjects from cluster A demonstrated limited motion during lateral bending exercises, while subjects from cluster B experience high levels of anxiety, etc.).

Additionally, this feature ranking will enable us to determine which features had the least impact on distinguishing between clusters. We can make future analyses more efficient by neglecting the features of little consequence in future studies.

5.4.2.3. Clinical Significance of Phenotypes

Once the phenotypes are distinguished, and the dominant features of each phenotype are determined, we will analyze the relationship between phenotypes and the PROs. It is our hypothesis that some phenotypes will be associated with more severe symptoms and lower quality of life, while other phenotypes will be associated with positive PROs scores and a higher quality of life. This hypothesis will be tested using one-way ANOVA tests to evaluate whether the PROs associated with the different phenotypes significantly differ one from another. As multiple PROs will be tested, the Bonferroni correction factor will be implemented to mitigate the risk of Type I error. An F-statistic with a p-value of less than 0.05 (after implementing the Bonferroni correction factor to account for multiple comparisons) will be considered statistically significant. An example of a preliminary phenotype analysis (conducted on data from the first 40 participants - 27 symptomatic and 13 control) and its corresponding implicated regarding Pain Intensity scores (on a scale of 0-10) from the participants in each phenotype is depicted in Figure 5.13.

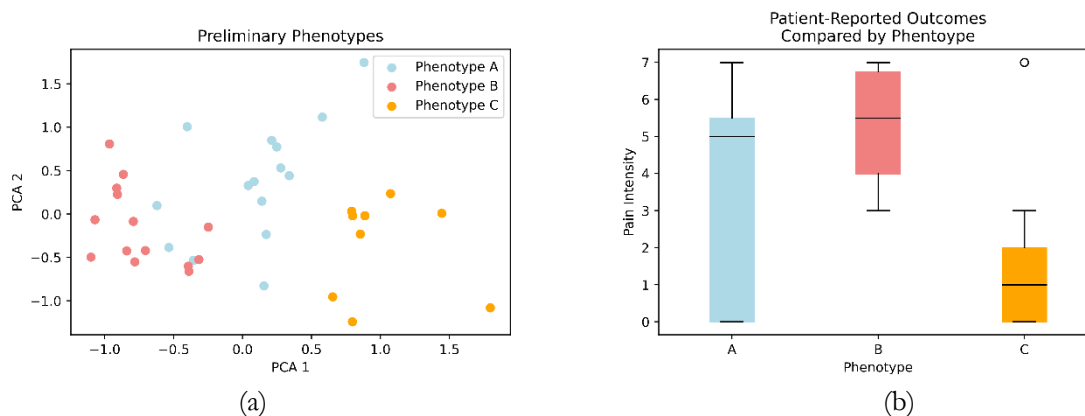


Figure 5.13 An example of the results of a phenotype identification analysis and its corresponding clinical interpretation from preliminary data. (a) Depicts the different phenotypes by color on the first two principal components of the motion and demographic data. Phenotype A was comprised of participants who exhibited significantly different velocities between their flexion right and flexion left motions (i.e., performing flexion towards one side was much faster than the other); Phenotype B was comprised of mostly participants with CLBP, high BMI scores, and who performed flexion right and flexion left with similar velocities; and Phenotype C was comprised of mostly asymptomatic patients with low BMI scores and a dominant side during lateral bending. (b) Depicts boxplots of the Pain Intensity scores for the participants, grouped by phenotype. A one-way ANOVA test calculated an F-statistic of 7.23 and a corresponding p-value of 0.002 comparing the Intensity scores between the phenotypes.

It is also our expectation that each phenotype will be dominantly comprised of either control or symptomatic participants (i.e., there will be little mixing of controls in any given phenotype). Exceptions to this supposition may indicate a participant is on the verge of transitioning between chronic low back pain and asymptomatic status (i.e., participants who experience CLBP but exhibit phenotypes typical of asymptomatic participants may indicate that they have managed their chronic pain well and thereby mitigated its severity). The PRO scores of participants with CLBP who exhibit “asymptomatic phenotypes” will be compared with the PRO scores of all other participants with CLBP using Student t-tests, applying a cutoff p-value of 0.05 before implementing the Bonferroni correction factor. Likewise, an asymptomatic participant who exhibits a phenotype typical of participants with CLBP may indicate that the asymptomatic individual is performing

suboptimal spinal motions and could benefit from preventative treatment. The PRO scores from these groups will also be compared using Student t-tests.

5.5. Discussion

Although many people suffer from CLBP, treatment efficacy is limited in part due to the difficulty of pinpointing the etiology of chronic and other types of non-specific LBP using the conventional methods of taking static images of the spine. A potential alternative method of assessing spinal health through an analysis of spinal motion and movement patterns. Previous studies have investigated the effects of CLBP on spinal motion and found significant differences between the motion of subjects who do and do not experience CLBP symptoms [46, 93, 210, 211]. Other studies have attempted to leverage this phenomenon for clinical application by tailoring treatments according to patient spinal motion patterns with promising results, but there are currently still insufficient data that warrants validation and widespread clinical implementation [96]. However, more quantitative analyses of spinal motion could lead to more objective classification methods that are robust to clinical subjectivity [48] and provide clinicians with the information needed to prescribe more personalized treatments and facilitated improved treatment outcomes [44].

In order to acquire the requisite objective and quantitative biomechanical insights relating to CLBP, this protocol manuscript presents (1) the development and validation of a spinal-motion monitoring device that is economical and practical for clinical and personal implementation – the SPINE Sense System – and (2) the methods that will be used to analyze the spinal kinematic data to provide clinicians and patients with valuable information in assessing and treating CLBP.

Spinal kinematics will be estimated via an array of high-deflection, inversely-piezoresistive strain gauges. These sensors were optimally placed on LoME of the lower back to extract the clearest and most reliable signal from the sensors during different motions. This design was validated by assessing the ability to interpret exercise type using skin-strain predictors with 90% accuracy. A model to predict spinal motions as a function of sensor output was developed using spinal motion data from an electromagnetic tracking system, adhered to a cadaver spine via bone pins. The model provided an estimate of the spinal kinematics along the sagittal plane with a root-mean squared error of less than 10% [194]. This device – the SPINE Sense System – has already been presented to prospective users among clinicians and CLBP patients, who rated the appliance as user-friendly [196]. As a result of the provided feedback from the study, future iterations of the SPINE Sense System will be produced in multiple sizes to produce a better fit for users. A corresponding phone application has been developed to provide an intuitive and efficient means of storing and transferring data collected from the sensor array.

Data collected from the SPINE Sense system device will be used to validate previous research findings and provide additional information by analyzing data from a broader range of single- and multi-planar spinal functional movements. Regression models will be developed to quantify the correlation between spinal kinematics and additional PROs, including opioid-use, anxiety, self-assessed disability, and activity level. Finally, an unsupervised machine learning clustering algorithm will be implemented to identify distinct spinal-motion phenotypes. Additional statistical tests will analyze the relationship between subject phenotype and PROs to provide additional information regarding the clinical significance of each phenotype cluster. The anticipated outcomes of this study will include (1) a set of identified movement-based and demographical features that are most important in the clustering of phenotypes, (2) the phenotype identification of each participant in the study, and (3) initial observations of the relationship between biomechanical response and PROs that may guide treatment response for patients with CLBP going forward. Future validation regarding the clinical significance of the diagnosed phenotypes may include treatment-based classification studies to evaluate which treatment paradigms are best suited for patients in each phenotype.

It is our hypothesis that this information regarding subject phenotypes and their corresponding descriptions will enable clinicians to select treatment paradigms individually tailored according to patient conditions. This in turn will improve treatment efficacy and the quality of life for the millions of patients suffering from CLBP worldwide.

CHAPTER 6 PHENOTYPE IDENTIFICATION AND POTENTIAL CLINICAL APPLICATION FOR TREATING CHRONIC LOW BACK PAIN

Spencer A. Baker¹, Tyler A. Hutchinson¹, Hailey E. Jones¹, Ulrike H. Mitchell², Anton E. Bowden¹, David T. Fullwood^{1*}

¹Department of Mechanical Engineering, Brigham Young University, Provo, UT

²Department Exercise Sciences, Brigham Young University, Provo, UT

*Correspondence to dfullwood@byu.edu

6.0 Abstract

Introduction: Chronic low back pain (CLBP) is a prevalent ailment that has many adverse effects on patients' quality of life. Significant time and resources have been spent attempting to alleviate these effects and improve quality of life. However, these interventions are largely hampered by the multifactorial nature of CLBP, which hinders clinicians' ability to identify a personalized and therefore possibly optimal treatment paradigm according to a patient's needs. This work provides the initial results of a promising technique – motion-based phenotyping – which has the potential to be clinically relevant for the evaluation, treatment, and progress assessment of people with CLBP.

Methods: Several features of motion and demographics were identified that have been shown to be associated with CLBP prevalence, severity, and general patient wellbeing. These features were used to develop a model that predicts patient-reported outcome (PRO) scores, which was trained and tested using 5-fold cross validation. The features were then used to cluster study participants into their respective phenotypes. One-way analysis of variance with a post hoc Holm correction factor followed by Student t-tests were conducted to evaluate the potential clinician implications of the phenotypes.

Results: Models were developed that capture 33-41% of the variance of physiological wellbeing metrics and 39-58% of the variance of psychological wellbeing metrics. Seven phenotypes of spinal motion were identified, which showed strong statistical significance in the context of PROs.

Discussion: Identifying motion-based phenotypes of patients with CLBP that are correlated with subjective and functional outcome measures could be a powerful first step to identifying patient-specific treatment paradigms that have the highest likelihood of success. Future work will be dedicated towards identifying the optimal treatment paradigm for these patients.

Acknowledgements: Research reported in this publication was supported by the NIH HEAL Initiative under award number NIAMS UH3AR076723. The content is solely the responsibility of the authors and does not necessarily represent the official views of the National Institutes of Health.

6.1. Introduction

Pain mitigation is one of the primary components of nearly every medical intervention [1]. One of the most common health ailments, which has even been deemed “the nemesis of medicine” [2], is low back pain (LBP). The lower back, as defined by a National Institute of Health Research Consortium, refers to “the space between the lower posterior margin of the rib cage and the horizontal gluteal fold” [3]. Multiple studies

have identified LBP as the leading cause of disability worldwide [16, 17], and it is estimated that up to 80% of the population will experience LBP at least once in their lifetime [10-12]. LBP also imposes serious economic consequences as well. Studies have estimated the direct medical costs of treating LBP ranges between \$17.7 and \$105.4 billion annually, with an additional \$22 billion lost indirectly through sick days and reduced productivity in patients [21].

When the source of LBP is readily identifiable, it is classified as being acute or pathology specific. However, up to 95% of LBP is classified as non-specific, meaning that there is no identifiable pathology associated with its cause [47, 48]. A particular type of non-specific LBP that causes patients, healthcare providers, and society in general much distress is chronic low-back pain (CLBP). A National Institute of Health Pain Consortium Research Task Force defined CLBP as “a back pain problem that has persisted at least three months and has resulted in pain on at least half the days in the past six months” [3]. This threshold of 3 months or 12 weeks has been widely used in past studies [22, 49-51], and is generally regarded as beyond the window of anticipated recovery. While most cases of acute LBP are resolved within that expected timeframe, there is a fraction that continues to have recurrent pain months and even years later that interfere with work and other activities [4, 8]. In addition to the persistent physiological impediments, CLBP also imposes significant social, physiological, and physiological challenges in a patient’s life [43]. Chronic LBP also entails a severe economic burden on society. Most of the economic resources associated with LBP are consumed by a minority of cases, usually in the form of long-term treatment and compensation benefits [14, 25-27].

Given its prevalence and serious consequences, CLBP has been the frequent topic of medical research and intervention. There is a plethora of treatments available to patients suffering from CLBP, but no single treatment has proven to be superior to the others for all patients [56]. Classifying sub-groups of patients suffering from CLBP and identifying their optimal treatment paradigm has been the goal of clinical researchers for many years in an effort to provide more effective patient treatments, improve patient outcomes and reduce financial costs [48]. However, CLBP is a highly multifactorial ailment, influenced by structural, psychological, social, genetic, and other factors [48]. Consequently, it is difficult to develop optimal treatment paradigms based solely on traditional assessment methods such as static images of the spine (e.g., MRI or CT scans) [48, 59].

An alternative method of assessing a patient’s case and consequently devising a personalized treatment plan is through a quantitative assessment of spinal kinematics. Biopsychosocial influences associated with CLBP affect the way that we move [44, 220]. Past studies have identified several motion characteristics that are associated with CLBP (such as lower ranges of motion, slower velocities, longer rise times, and smaller jerk levels [46, 93, 210, 211]) and that different pathologies of acute LBP that are linked with specific changes in movement [81, 93, 187]. However, most clinical assessments of spinal motion rely on qualitative assessments [191]. Past studies have found that incorporating spinal motion to inform treatment paradigms is only somewhat effective, and only when the clinicians are extensively trained to use a classification system [96]. Rather than rely on subjective observations, the use of an objective accurate, economic, and user-friendly motion-monitoring device is preferable. In addition, this could be employed in widespread clinical applications.

As part of the 2019 initiative by the National Institute of Health (NIH) to form the Back Consortium (BACPAC), several university programs have developed innovative devices to objectively monitor spinal motion, which will be used to inform clinicians who treat patients with CLBP [44, 57]. At Brigham Young University, the Applied Biomechanics Lab has developed an inexpensive, wearable array of nanocomposite sensors that measure the skin strain field of the lumbar spine and derive segmental spine kinematics. This device is known as the SPInal Nanosensor Environment (SPINE Sense System). Past reports detail the development of the SPINE Sense System [145], its validation [221], and clinical usability [196].

The objective of this research is to

1. Reaffirm and further analyze the relationship between motion characteristics and demographics with different aspects of well-being.
2. Identify and interpret the dominant spinal-motion phenotypes (i.e., dominant motion patterns) exhibited by participants, using data collected from the SPINE Sense System and questionnaires.
3. Demonstrate the potential clinical significance of the phenotypes.

Data was collected from two cohorts of subjects – one cohort that experiences CLBP symptoms and another cohort that is CLBP asymptomatic. This will enable the identification of phenotypes representative of individuals with spines in good health and contrast them with phenotypes of individuals who are suffering from CLBP.

The results from this work will lay the foundation for future research that will conduct randomized experiments to identify the optimal treatment paradigm for patients according to their phenotypes (see Figure 6.1). Different etiologies of acute LBP are often associated with specific changes in spinal motion that are indicative of the optimal treatment paradigm [85-92, 212]. It is therefore anticipated that the findings from this and subsequent studies will result in a precision medicine approach to treating patients with CLBP. This in turn would improve treatment outcomes, expedite recovery, and reduce medical costs worldwide [44, 145].

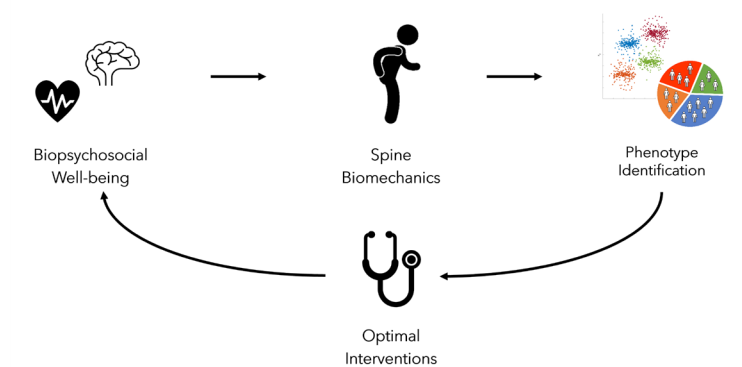


Figure 6.1 Overview of the NIH BACPAC initiative. An individual's biopsychosocial well-being influences spinal biomechanics, which can be objectively monitored using the SPINE Sense System. The objective of this work is to analyze the data from the SPINE Sense System and other relevant factors to identify phenotypes of spinal motion, which in future work will be conveyed to clinicians, who can then identify the optimal treatment paradigm for patients according to their phenotype. This can then be implemented on a widescale to reliably apply treatments best suited to patients' needs, improving treatment outcomes and saving medical costs worldwide.

6.2. Methods

6.2.1. Data Collection

The protocol for conducting human-subject tests was described previously in [145]. A summary of the methodology used in this study is provided here for reference.

Two cohorts of participants were recruited for this study – individuals who report having experienced CLBP (cases) and CLBP asymptomatic (control) individuals. Both cohorts were 35-65 years of age (which is the age range of the highest prevalence of CLBP [52]). Part of the test procedures included an MRI scan – hence the exclusion criteria included metal or electrical implants, claustrophobia, and possible pregnancy. Furthermore, each subject had to be capable of assuming a vertical position without an assistive device. Individuals who had undergone hip or knee surgery were excluded from this study.

The control group was recruited via flyers to the local community. Due to the prevalence of LBP and its wide range of severities, controls, individuals with CLBP, and individuals with acute LBP are very heterogeneous

populations and at times difficult to differentiate [44]. Past studies have recruited only individuals with well-documented cases of LBP to mitigate this issue [46]. In this study, CLBP asymptomatic individuals with diagnosed disorders known to influence motion – including known scoliosis or history of treatment for lumbar spine pain – were excluded to avoid conflating effects between CLBP and other ailments.

The CLBP symptomatic cohort was recruited from individuals who were already scheduled for physical therapy for complaints of CLBP. The symptoms had to be primarily axial (as opposed to radicular, radiating into one leg), and persistent for at least three months prior to the study.

6.2.1.1. Motion Testing

After being screened for eligibility, participants were fitted with the SPINE Sense System adhered to their lower back (see Figure 6.2).



Figure 6.2 Depiction of (a) the SPINE Sense System adhered to a subject’s back and (b) the SPINE Sense System collecting data during motion.

With the SPINE Sense System in place, the participants were directed through a series of single-planar motions (as have been used in a variety of past studies to investigation the motion of individuals with CLBP [150]) and multi-planar motions (which is more representative of daily tasks), each repeated six times. The motions included in this test are depicted in Figure 6.3. See also [145] for full details regarding the motion-collection protocol.

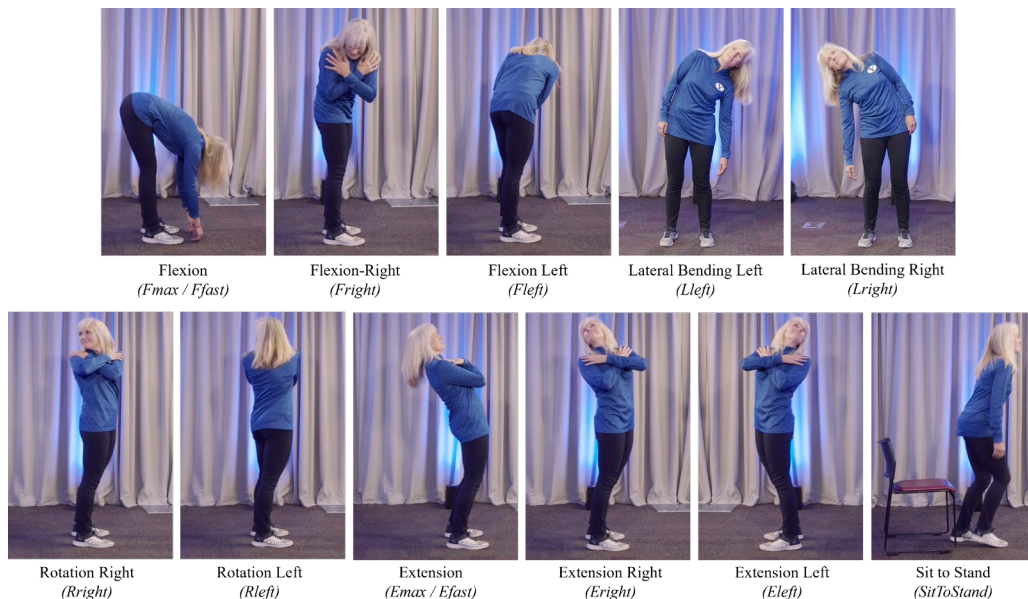


Figure 6.3. Depiction of the different single- and multi-planar motions included in this research with the full motion name and abbreviated motion name listed below each figure.

The high deflections strain gauges respond to skin stretch during motions, and the outputs are recorded by the SPINE Sense System as a proxy for spinal kinematics. The SPINE Sense System outputs were calibrated using a knee-touch exercise [145]. The calibrated outputs were then processed using a model that converts strain gauge outputs to estimations of motion [144]. The following motion features were estimated from the data.

- Range of motion (“delta”): The maximum range of motion performed during a motion.
- Velocity of motion (“dot”): The velocity of motion.
- Duration of motion (“interval”): The time required to achieve the max range of motion.
- The spread of time ratios (“spread”): The ratio of the time to complete a preliminary repetition to the final repetition of the same motion. E.g., a value > 1 indicates the participant took longer to complete the final repetition compared to previous repetitions.
- Asymmetry (“asym”): The absolute value of the difference between the left and right side of the body during single-planar motions (for both range of motion and velocity). This feature corresponds to exercises performed along a single plane: namely Flexion, Flexion Fast, Extension, and Extension Fast.
- Twist (“twist”): The absolute value of the difference between the left and right side of the body, in terms of range and velocity, between exercises performed on either side of the sagittal plane. Relevant exercises for this feature include Flexion left-right, Extension left-right, and Lateral bending left-right.

Each motion is performed six times, the first being regarded as a practice repetition. The median value of the 2nd-6th repetitions was included in the subsequent analyses. The eccentric motion was the primary consideration for each feature. Each variable is referred to by both the exercise name and the feature being monitored – e.g., the range of motion during Flexion Max is referred to as “Fmax_delta”.

6.2.1.2. Demographics

A series of studies have found that certain demographics, lifestyle, occupational, and psychological factors influence the prevalence and severity of LBP [6, 28, 33, 43], which need to be accounted for when developing classification techniques to identify the optimal treatments for sub-groups of patients with CLBP [96]. Some of the more commonly identified risk factors from past studies have been included in this work and are described below.

Age: Past studies have observed that the prevalence of LBP increases with age to approximately 55 years, and CLBP is the most prevalent among individuals 35-65 years of age CLBP [52]. Age was therefore included as a quantitative variable.

Socioeconomics: A plethora of studies have identified work-related factors to increase the risk of LBP and CLBP, especially for blue-collared workers who are exposed to heavy loads and prolonged vibrations (such as experience during driving) [2, 14, 15, 30-32]. Furthermore, past studies have found that populations from a higher socioeconomic background (i.e., advanced levels of education, white-collar workers, higher job rank, increased salaries) have a lower prevalence of CLBP [9, 33]. Both income and education were included in the study as ordinal variables.

- Income (in USD / year): 1=<10,000, 2=10-25,000, 3=25-35,000, 4=35-50,000, 5=50-75,000, 6=75-100,000, 7=100-150,000, 8=150-200,000, 9=200,000+
- Education (in terms of degree completed): 1=<HS, 2=some HS, 3=HS, 4=Associates, 5=College, 6=Postgraduate.

Physical Fitness / Activity: It has long been observed that unhealthy lifestyles and high BMI score are associated with LBP prevalence, severity, and medical treatment – even when accounting for potential

confounding factors [33, 38]. There is also a plethora of evidence that physical activity has the potential to reduce pain [14, 43], improve functionality [43, 68, 69], and mitigate the risk of LBP occurrence / recurrence [4, 14, 20, 43]. The following features were included to capture these aspects of health.

- Body mass index (BMI): BMI is a commonly used indicator of body type and used to identify healthy and unhealthy ranges of weights according to an individual's height [33].
- Short Form International Physical Activity Questionnaire (IPAQ): Self-assessed physical activity in the week prior to subject participation in the study was estimated in terms of Metabolic Equivalent Task (MET) minutes per week using the IPAQ Questionnaire. Previous studies have compared IPAQ scores to objective metrics of physical activity and found it to be a moderately reliable for estimating vigorous physical activity [99].

Psychological Wellbeing: Many studies have investigated the relationship between psychosocial and physiological wellbeing. Patients with LBP tend to have weaker social networks [33], and low social support in the workplace has been identified as a factor for developing LBP [43]. Multiple studies have hypothesized that higher levels of fear-avoidance are associated with decreases in functional performance [43-45]. This is an especially important factor to consider when evaluating CLBP, which some studies describe as more of a psychosocial dysfunction than even a physiological impairment [4]. Psychosocial influences were considered in the subsequent analyses using the following metrics.

- Pain Catastrophizing Scale 6 (PCS-6): Pain catastrophizing is “an exaggerated negative orientation towards actual or anticipated pain experiences”, which past studies have found to be associated with higher pain intensities [163]. The PCS-6 is designed to capture three psychological components of catastrophizing: helplessness, rumination, and magnification [164].
- General Anxiety Disorder 2 (GAD-2): The GAD-2 questionnaire is used to identify General Anxiety Disorder (i.e., depression of mood over a two-week period), which has exhibited acceptable accuracy in past studies [162].
- Relationship: Participant marital status was included as a binary feature.

Smoking: There is an overwhelming consensus that smoking is associated with a higher risk of LBP [30, 33, 37], possibly due to stresses caused by smoking-induced chronic cough [30] and / or vasoconstriction (impaired blood supply) to intervertebral discs [30, 33]. Smoking was included as an ordinal feature (0=non-smoker, 1=<monthly, 2=monthly, 3=weekly, 4=daily).

Opioids: Opioid use is an extremely common method of treating the symptoms associated with CLBP. However, the current consensus on the efficacy of opioids is under scrutiny and additional studies are needed to evaluate their benefits and long-term effects [60]. There are also several potential adverse side-effects related to opioid use that can impact an individual's psychological and physiological health, such as hyperalgesia, hypogonadism, constipation, nausea, sedation, increased risk of falls and fractures, depression, sexual dysfunction, and potentially (and ironically) increased sensitivity to pain [58, 62]. Participants were therefore asked to report whether they were currently using prescribed opioids, which was included in the study as a binary factor (0=no opioid use, 1=opioid use).

Sex: Sex has been identified in past studies as a potential feature that impacts LBP severity and prevalence [2, 6, 17, 33]. Some studies have postulated that sex has direct biopsychological implications that influence LBP (e.g., osteoporosis, menstruation, pregnancy, smoking, BMI) [30], while others believe that sex plays a more indirect role through psychosocial influences [6]. To account for the potential direct and indirect influences, sex was included in subsequent analyses as a binary variable (0=female, 1=male).

Within the week prior to the motion testing and collecting MRI spinal scans, subjects were asked to fill out a survey reporting these demographics, which were included in subsequent analyses as binary, categorical, and continuous variables.

6.2.1.3. Patient-Reported Outcomes

The different aspects of an individual's biopsychosocial well-being can be quantified using patient-reported outcomes (PROs). PROs are being implemented by healthcare providers with increasing frequency to inform clinical decisions [97]. Substantial research has been conducted that evaluates the average PROs among patients suffering from different ailments [105-107] and analyzes the change of PROs prior to and following intervention [108-114]. The PROs measured in this study include those collected in the Back Pain Consortium Research Program [159] and additional metrics. A brief description of each PRO is as follows:

Pain Intensity: Low-back pain intensity was measured using a numeric rating scale from 0-10 (0 representing 'no pain' and 10 representing the most severe pain possible) in the previous week. Pain mitigation is one of the primary components of nearly every medical intervention [1]; and low-back pain is also one of the most frequent causes for hospitalizations, physician visits, and medical consultation [21, 104]. It is a vital metric to consider when assessing patient well-being.

Oswestry-Disability Index (ODI): Spine-related disability was measured using the widely used ODI metric [98]. The ODI metric has been thoroughly vetted and is frequently used as the gold standard for quantifying disability related to LBP [118, 160], and has shown strong experimental reliability when evaluating patients with chronic pain [104].

Patient-reported outcomes measurement information systems (PROMIS) metrics: PROMIS scores are "a set of person-centered measures that evaluates and monitors physical, mental, and social health in adults and children" [101]. Past studies have evaluated PROMIS metrics and concluded them to be "efficient, flexible, and precise" [97]. The short-form PROMIS metrics implemented in this research included the PROMIS Pain Interference 4a, PROMIS Physical Function 6b, PROMIS Sleep Disturbance 6a, PROMIS 4-item Depression, and PROMIS 4-item Anxiety.

6.2.2. Data Analysis

Using the data described above – subject motion as measured by the SPINE Sense System and the demographics and PROs collected via questionnaires – the following analyses were performed.

6.2.2.1. Features that Relate to Patient Reported Outcomes

For this study, the features of interest include the motion characteristics and the subject demographics described previously. Substantial evidence indicates that there exists a relationship between different motion and demographics data with subject well-being as quantified by PROs [6, 28, 33, 43]. The first analysis conducted was to quantify the strength of the correlation between each feature of interest and PRO for patients with CLBP. This was calculated using Pearson's correlation coefficient (r) and the Cohen evaluation thresholds: $|r|=0.10-0.30$ is considered small correlation strength, $|r|=0.31-0.50$ is considered moderate correlation, and $|r|>0.50$ is considered large correlation strength [165, 169]. This analysis was conducted to substantiate past findings and support the logic for using these features to identify phenotypes among patients to be considered by clinicians when treating patients who suffer from CLBP.

The second analysis is to utilize all the features of interest (all the demographics and motion data collected) to predict each PRO. A gradient boosted decision tree machine learning algorithm – Python's *XGBRegressor* – will be employed, which is a very versatile algorithm that performs well with nonlinear data. Models were trained and evaluated using a five-fold cross validation. A Shapley Additive Explanation (SHAP) chart was generated to depict the specific relationship between features and model outcomes.

6.2.2.2. Phenotype Identification

The primary objective of this investigation is to identify dominant phenotypes of motion and assign participants to their respective phenotypes [145]. This task is well-suited for unsupervised machine learning algorithms. These algorithms quantify the difference between each datapoint (in this case, each study participant) and identify clusters (sub-groups of the original dataset) that minimize variance within clusters and maximize the variance between clusters [216]. The analysis defines sub-groups of the original dataset that exhibit similarities across all the motion and demographic features considered – namely, the phenotypes of interest.

Data processing: Prior to the clustering analysis, outliers ($|z_{\text{score}}| > 3$) were filtered from the IPAQ scores (which past studies have shown is prone to biases and overestimations [165]) and motion metrics. This was done to prevent the results from being skewed by unrealistic anomalies [167]. Missing values in the dataset were replaced by the average feature values. Each feature was then scaled between 0-1 to give all features of interest an equal weight in the analysis. Finally, a principal component analysis of the filtered, scaled data will be performed to reduce the dimensionality and eliminate feature collinearity. The number of principal components (n) will be selected by including the first n components (ordered from largest to smallest in eigenvalue rank) that captures 95% of the variance from the original dataset.

Determining the optimal number of clusters: The first step to the clustering analysis is to define how many clusters to parse the dataset into. It was important to select an appropriate number of clusters that is practical for clinical use and provides clear segmentation between the clusters. A range of 4-11 potential clusters were evaluated. The Silhouette criterion, which quantifies how well-defined cluster segmentation is, was used to select the optimal number of clusters from this range.

Selecting the clustering algorithm and linkage method: The subsequent clustering analysis will be performed using a hierarchical clustering, which is well-suited for this application due to its ability to incorporate both quantitative features (such as spinal kinematics) and categorical features (such as demographics). Python's *AgglomerativeClustering* algorithm was used in this endeavor. The results of the clustering analyses also depend on the linkage type, which is used to quantify the similarity / dissimilarity between data points. Due to its robust nature against noise, the Ward Linkage was implemented [218].

Phenotype interpretation: Once the clustering analysis is complete, each phenotype-cluster will be described in terms of which features most differentiated it from the other clusters in terms of the original, scaled features. This will provide both an intuitive explanation of what each phenotype identification entails and will identify which features are most important in detecting dominant spinal motion patterns.

6.2.2.3. Evaluating the Potential Clinical Implications of Phenotypes

It is expected that patients who exhibit similar phenotypes will also respond in a like-manner to different intervention techniques. Future work will investigate which treatment paradigm is most effective for patients suffering from CLBP according to their phenotype. Additionally, the potential clinical implications of these phenotypes were investigated by analyzing the relationship between phenotypes and the PROs of interest. This was done using one-way analysis of variance (ANOVA) tests to evaluate whether the PROs associated with the different phenotypes significantly differ from one another. An F-statistic with a p value < 0.05 is considered significant, after applying a post-hoc Holm correction factor. If the ANOVA test showed statistical significance, Student t tests were performed on each pairwise comparisons between the phenotypes to evaluate for which phenotypes differed statistically between each other for each PRO of interest, again using an alpha of 0.05 after applying a post-hoc Holm correction factor.

6.3. Results

6.3.1. Participants

A total of 217 participants were included in this study – 126 who reported experiencing CLBP and 91 who were CLBP asymptomatic. A summary of the demographics for the two cohorts are described in Table 6.1.

Table 6.1 Summar of the demographics of the two cohorts of interest - those who were CLBP asymptomatic (controls) and those who reported having experienced CLBP symptoms (cases).

Demographic	Controls	Cases
Age (Mean [stdev])	47.32 [7.80]	48.82 [8.89]
Income (USD / year)		
<10,000	1	2
10,000-24,999	2	1
25,000-34,999	2	7
35,000-49,999	9	13
50,000-74,999	15	23
75,000-99,999	10	17
100,000-149,999	31	31
150,000-199,999	13	18
>200	8	14
Education (degree)		
No High School	0	2
Some High School	0	5
High School	7	20
Associate's	12	17
Baccalaureate	33	45
Postgraduate	39	37
BMI (kg/m ²)	27.03 [4.78]	28.32 [6.52]
IPAQ MET (Mean [stdev])	6271 [9030]	5839 [9197]
PCS-6 (Mean [stdev])	5.68 [4.48]	9.74 [5.64]
GAD (Mean [stdev])	0.68 [1.04]	1.61 [1.73]
Not married / married	10 / 81	19 / 107
No Opioid Use / Opioid Use / No Answer	91 / 0 / 0	11 / 114 / 1
Female / Male	42 / 49	62 / 64

6.3.2. PRO Correlations

6.3.2.1. Features that correlate with PROs

Moderate to strong correlations ($r > 0.3$) were observed between several of the demographic features tested in this study demonstrated with the PROs of interest (see Figure 6.4a and b). Some of the more notable trends observed are as follows:

- Small correlations were observed between participant BMI with the different metrics of interest, the strongest being the relationship between BMI and PROMIS Physical Function T (reverse), indicating high BMI is associated with physical dysfunction.
- Negative correlations were observed between the socioeconomic features (Income and Education) with the PROs, indicating that higher education and income are associated with better health.
- Positive correlations were observed between opioid use and the PROs.
- Being in a marital relationship was associated with better PROs metrics. The strongest correlations observed were negative relationships with pain interference and depression.
- Small to moderate correlation strength was observed between IPAQ MET Minutes / Week (IPAQ #) was with most of the PROs. These correlations were negative, reinforcing the finding that physical activity (as self-reported) is associated with better health.
- Strong correlations were observed between metrics that evaluate pain catastrophizing and general anxiety with the PROs of interest, especially the PROMIS Anxiety and Depression scores.

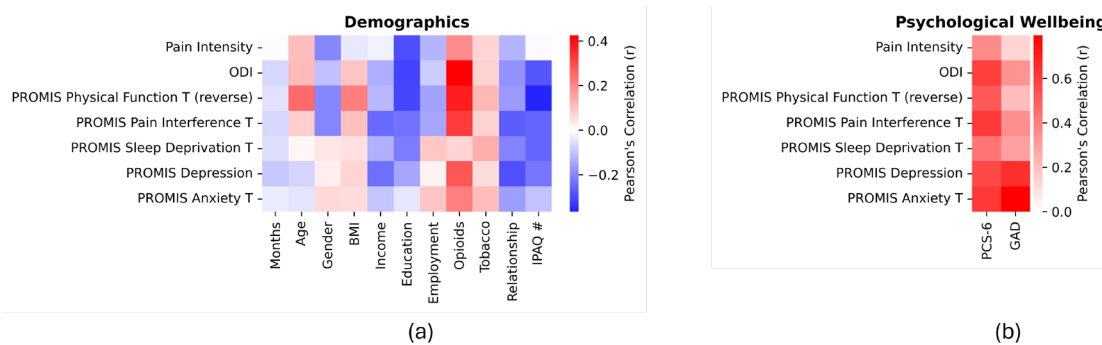


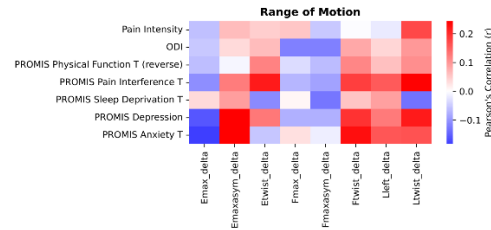
Figure 6.4 Summary of the Pearson's correlation strength (r) between (a) demographics with PROs and (b) metrics of Psychological Wellbeing with PROs. Again, the reverse of the PROMIS Physical Function T score is depicted above to provide consistent interpretation of the visualization (higher scores are indicative of worse participant health in each area).

Small to moderate correlations ($|r|$ ranging 0.1-0.35) were observed between several of the motion characteristics with the PROs of interest (see Figure 6.5). Specific observations include the following.

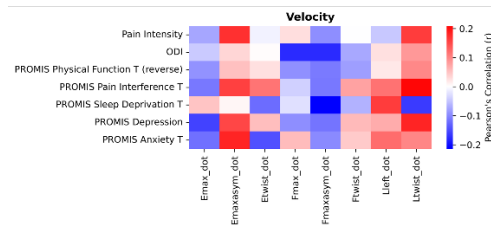
- Range of motion (ROM): Higher ranges of motion (ROM) during extension are generally negatively correlated with PRO scores, indicating that individuals with high ROM during extension have better health in the areas of interest. However, higher asymmetry of ROM during extension is positively correlated with PRO scores, indicating that asymmetric extension is indicative of worse outcomes. Asymmetric motions during multiplanar motions (Flexion Left-Right, Lateral Bending Left-Right) were also positively correlated with the PRO scores. Other relationships were too weak or varied to draw conclusions.
- Velocity of motion: Similar to ROM, negative correlations between Extension velocity with PROs were observed, but positive correlations between extension asymmetric velocity with the PROs. Asymmetry during lateral bending is also positively correlated with the PROs. However, negative

correlations between Flexion asymmetry and PROs, indicating that having a faster side during flexion is associated with better health.

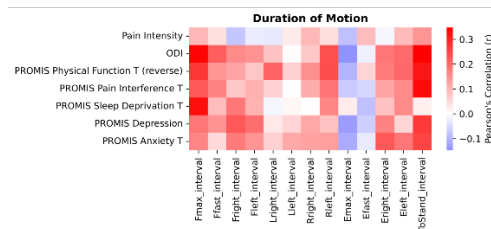
- Duration of interval: Unsurprisingly, longer times to complete an exercise were (generally) positively correlated with different PROs. The one notable exception was Emax, where longer duration times were weakly correlated with better health outcomes.
- Spread of interval: The strongest correlations between the Spread of Intervals with PROs were observed for the SitToStand motion. The Spread was weakly negatively correlated with most of the PROs of interest, indicating that subjects who took the same amount of time (or less) to complete the final repetitions as the first generally had better health.



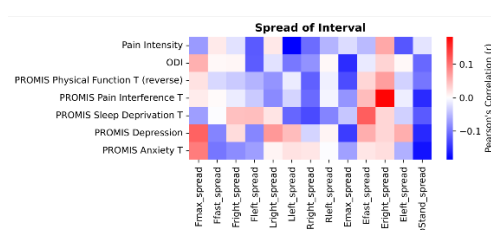
(a)



(b)



(c)



(d)

Figure 6.5 Summary of the Pearson's correlation strength (r) observed between the motion features collected in this study and the PROs of interest for patients suffering from CLBP. Shades of red indicate positive correlations and shades of blue indicate negative correlations. Note: The reverse of PROMIS Physical Function T (i.e., $100 - \text{PROMIS Physical Function T}$) is depicted above for visualization purposes (lower PRO scores for each metric depicted are indicative of better wellbeing).

6.3.2.2. Modeling PROs

The accuracies of the *XGBRegressor* machine learning model predicting each PRO of interest are listed in Table 6.2.

Table 6.2 A summary of the model accuracies (in terms of Pearson's correlation squared) for modeling each PRO of interest.

PRO	r^2
Pain Intensity	0.351
ODI	0.412
PROMIS Physical Function T	0.332
PROMIS Pain Interference T	0.388
PROMIS Sleep Deprivation T	0.091
PROMIS Depression T	0.396
PROMIS Anxiety T	0.575

The model did moderately well (r^2 ranging from 0.33 to 0.41) at predicting PROs that relate to physiological wellbeing (Pain Intensity, ODI, PROMIS Physical Function T, and PROMIS Pain Interference T). The model performance for predicting PROs related to psychological wellbeing (PROMIS Depression T, PROMIS Anxiety T) was also moderate (r^2 0.40 – 0.58). However, the model performed poorly predicting PROMIS Sleep Deprivation ($r^2 < 0.10$). Overall, it was observed that motion features and demographics can be used to approximate subject wellbeing regarding metrics physiological function (Pain Intensity, ODI, PROMIS Physical Function T, and PROMIS Pain Interference T) as well as psychological distress (PROMIS Depression T, PROMIS Anxiety T), but though they exhibit little association with sleep deprivation.

SHAP values were generated to quantify the effect of each feature on the resulting outcome. An example of the how different features affect two specific predictions are depicted in Figure 6.6.

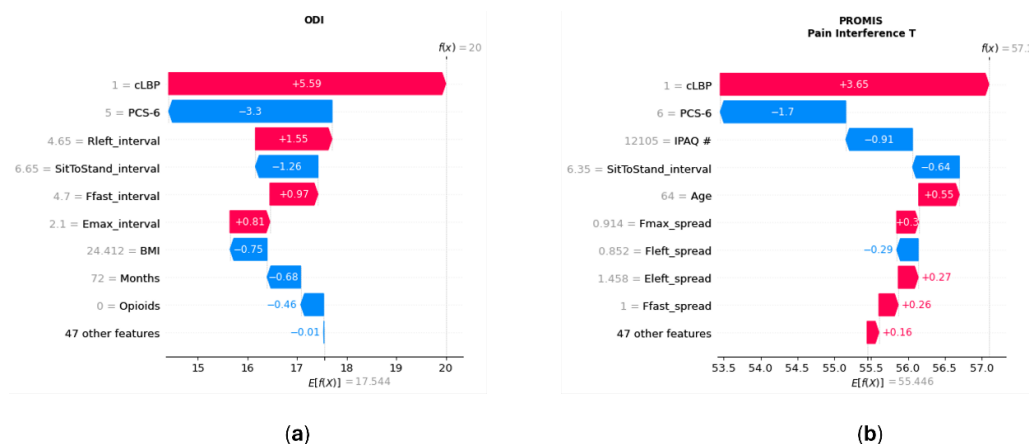


Figure 6.6 SHAP waterfall plots, depicting the effect of different features on two specific instances: (a) the ODI of a subject and (b) the PROMIS Pain Interference T of a different subject. The default value prediction (the average of all observations) is represented at the bottom of the SHAP waterfall plots (e.g., 17.5 for ODI). The values of key features are presented on the left, and the effect on the prediction are depicted by the colors and length of the horizontal bars. The net prediction for the instance (i.e., for the subject of interest) is represented by $f(x)$ at the top of the waterfall plot.

SHAP scatterplots were used to depict the general effects of each feature across all instances. Figure 6.7 depicts the SHAP values for the SitToStand_interval motion feature and the IPAQ MET Minutes / Week demographic feature on different PROs of interest.

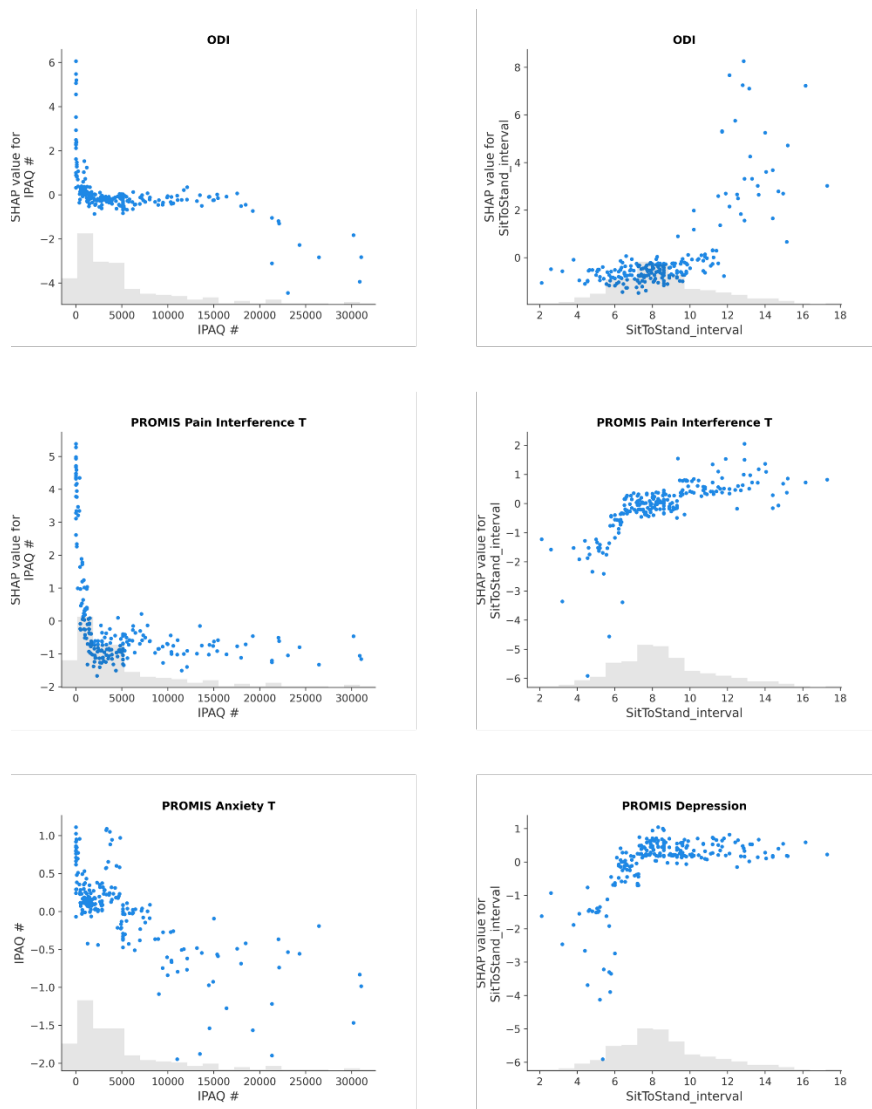


Figure 6.7 SHAP plots depicting the relationship of IPAQ Met Minutes / Week (left) and the SitToStand_interval (right) for different PROs of interest. The PRO of interest is noted by the subplot title. Notice that higher IPAQ MET Minutes / Week are associated with better ODI, PROMIS Pain Interference, and PROMIS Anxiety scores, and that longer SitToStand_interval durations are associated with higher ODI, PROMIS Pain Interference T, and PROMIS Depression T scores.

6.3.3. Phenotype Analysis

6.3.3.1. Phenotype Identification

After outliers in the dataset were removed, a principal component analysis then revealed that the first 39 principal components captured 95% of the variance demonstrated in the original 56 features. Those 39 principal components were then used in the subsequent clustering analysis. The Silhouette Criterion scores of the dataset were calculated for a range of potential number of clusters (see Figure 6.8). It was observed that the best segmentation of the subjects was achieved when they were assigned to seven phenotype-clusters.

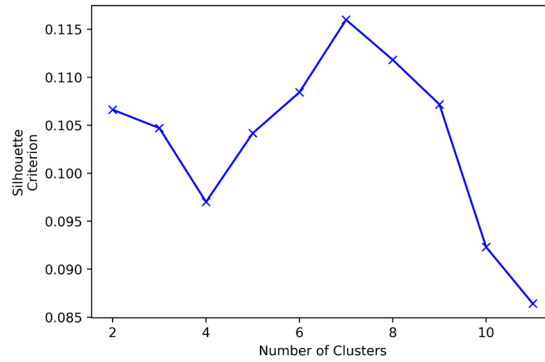


Figure 6.8 The Silhouette Criterion score for a range of clusters from 2-12. It was observed that at a separation of seven clusters, the Silhouette Criterion score was the greatest, indicating the best segmentation of clusters was achieved when the subjects were divided into seven phenotype-clusters.

The study participants were then clustered into different phenotypes. The phenotypes were named according to the features that had the most impact in differentiating between the clusters. The phenotypes identified in the analysis were (A) control females with large flexion spread; (B) control males with consistent flexion motions; (C) case males with large Rright spread; (D) elder case females; (E) younger females with quick, consistent motions; (F) single case females with short Ffast durations; (G) cases with longer motion durations and prescription medications. A depiction of the phenotypes on the first two principal components is shown in Figure 6.9. A summary of the average values for the key features for each phenotype are described in Table 6.3.

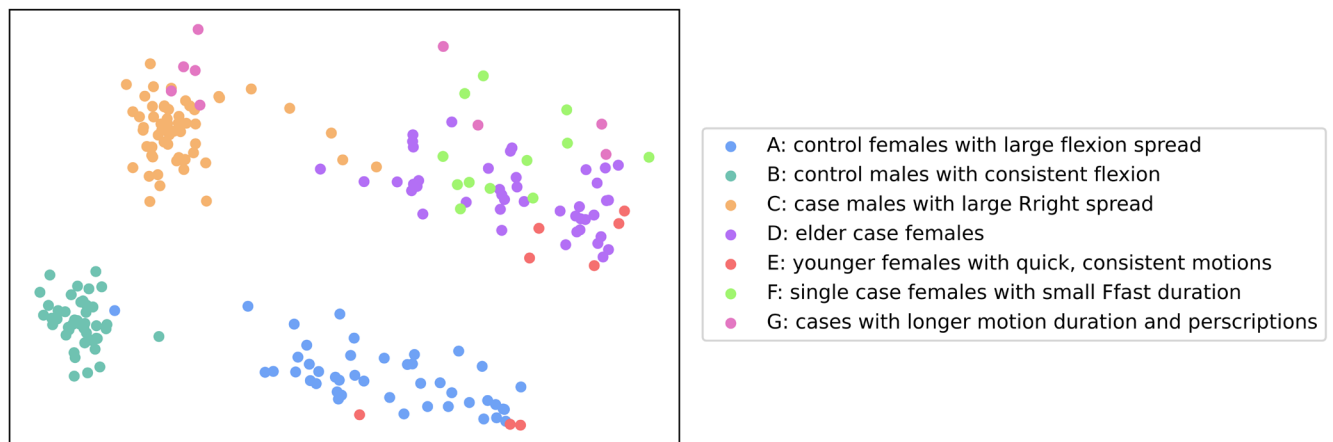


Figure 6.9 Scatterplot of the study participants on the first two principal components of the data, color-coded by phenotype.

Table 6.3 A summary of the average values for the key features for each phenotype, in terms of their unscaled values.

Phenotype	Distinguishing Features	Feature Averages
A	CLBP	0.00
	Sex	0.11
	Fright_Spread	1.21
B	CLBP	0.00
	Sex	1.00
	Fleft_spread	0.97
C	CLBP	1.00
	Sex	1.00
	Rright_spread	1.38
D	CLBP	1.00
	Sex	0.05
	Age	52.51
	Sex	0.00
E	Age	44.4
	Employment	0.50
	Ltwist_delta	1.24
	Lright_interval	2.34
	Ftwist_dot	0.43
	Ftwist_delta	0.80
F	CLBP	1.00
	Sex	0.00
	Relationship	0.00
	Eleft_spread	0.85
G	Ffast_interval	1.29
	Opioids	1.00
	SitToStand_Interval	11.57
	Rright_interfal	4.07
	Fright_interval	3.96
	Eright_interval	4.47
	Emax_interval	0.67
Eleft_interval	4.05	

6.3.3.2. Phenotype Significance

The ANOVA tests revealed that there were statistically significant differences between the phenotypes for each of the PROs of interest (see Table 6.4). Once the ANOVA tests established statistically significant differences between the phenotypes for each PRO, Student t tests were conducted between each pair of phenotypes, and post-hoc Holm correction factors were applied. Phenotypes that exhibited no statistically significant differences in the t tests were marked with a common underline underneath their corresponding boxplots (see Figure 6.10).

Table 6.4 Summary of the resultant F-statistics, p-values, and adjusted p-values (corrected for multiple comparisons use the Holm post-hoc test)

PRO	F-statistic	p-value	adjusted p-value
Intensity	40.38	1.71E-32	1.19E-31
PROMIS Pain Interference T	33.68	2.51E-28	1.51E-27
ODI	32.25	2.59E-27	1.30E-26
PROMIS Physical Function T	31.93	3.63E-27	1.45E-26
PROMIS Sleep Deprivation T	11.65	2.98E-11	8.93E-11
PROMIS Depression T	11.15	8.54E-11	1.71E-10
PROMIS Anxiety T	5.25	4.66E-05	4.66E-05

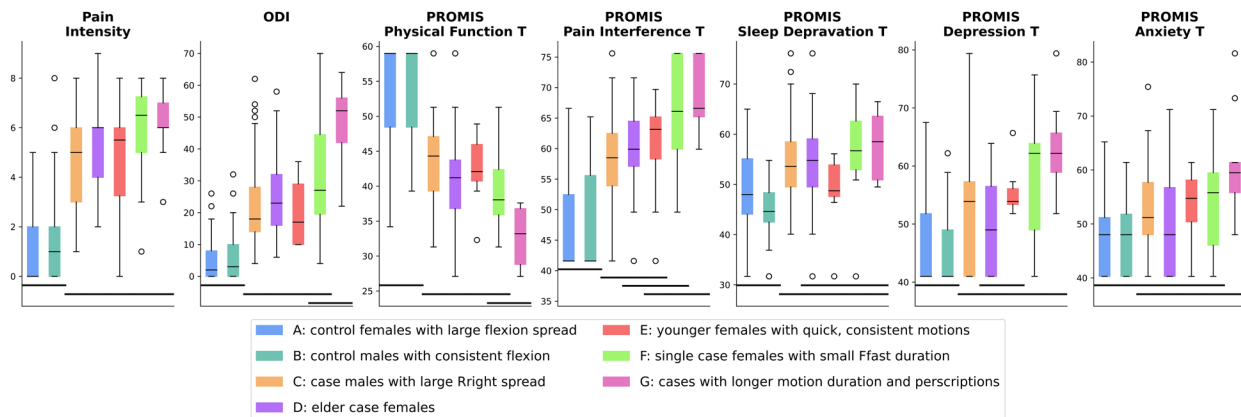


Figure 6.10 Summary of the comparisons between phenotypes for each PRO of interest. Each ANOVA test revealed that there were statistically significant differences between the phenotypes. Student t tests were then conducted to evaluate which phenotypes differed. Phenotypes that showed no statistically significant differences for a particular metric were indicated by underling the two or more boxplots.

The following statistically significant observations were noted in the pairwise comparisons.

Pain Intensity: The phenotypes comprised primarily of controls (A and B) differed from all other phenotypes, which were comprised of either primarily of cases or were a mix of cases and controls (C-G).

ODI: Again, there were no statistical differences between phenotypes A and B. Cases with longer motion duration and perscriptions (G) differed from case males with large Rright spread (C), elder case females (D), and younger females with quick, consistent motions (E). Single case females with small Ffast durations (F) differed from the control phenotypes but overlapped with both the G phenotype and the C-E case phenotypes.

PROMIS Physical Function T: The control phenotypes (A and B) had higher physical function scores than the case phenotypes (C-G). Again, the case phenotypes C-E had higher function scores than cases with longer motion duration and perscriptions (G), and single case females with small Ffast durations (F) overlapped with all other case phenotypes.

PROMIS Pain Interference T: The control phenotypes (A-B) differed from the case and mixed phenotypes (C-G). Case males with a large Rright spread (C) differed from single females with small Ffast durations (F) and cases with longer motion and prescriptions (G). Cases with longer motion durations and prescriptions (G) also differed from elder case females (D). Younger females with quick, consistent motions overlapped (E) overlapped with all other case and mixed phenotypes.

PROMIS Sleep Deprivation T: The only case phenotype that differed from the control phenotypes (A-B) were case males with large Rright spread (C). However, no statistically significant differences were observed between the case phenotypes (C-G) regarding sleep deprivation.

PROMIS Depression T: There were three case phenotypes that had higher depression scores than the control phenotypes (A-B), namely case males with large Rright spread (C), single case females with small Ffast duration (F), and cases with longer motion duration and prescriptions (G). However, no differences were observed between the case phenotypes.

PROMIS Anxiety T: The only case phenotype that differed from the control phenotypes (A-B) in terms of anxiety were cases with longer motion durations and prescriptions (G), who exhibited higher anxiety scores. However, no statistically significant differences were observed between any of the case and mixed phenotypes (C-G).

6.4. Discussion

Past studies have reported relationships between CLBP severity and prevalence with subject demographics [6, 28, 33, 43]. In this study, small to moderate correlation strengths ($|r|$ ranging from 0.10-0.50) were observed between several demographics with the PROs of interest. Some of the most prominent trends observed were that higher education and income levels were associated with lower anxiety, pain, and disability. Being in a marital relationship was associated with better health scores, as was having an active lifestyle. These findings are consistent with past studies [9, 14, 33, 43, 68, 69]. However, the strongest correlation with the PROs of interest were exhibited by the demographics that quantify psychological distress, namely the PCS-6 and GAD responses, which quantify negative orientation towards pain [163] and general anxiety [162], respectively. The Pearson's correlation (r) between these metrics with pain intensity, disability, physical dysfunction, and pain interference scores ranged 0.13-0.60. They also demonstrated moderate correlations with sleep deprivation (r 0.29-0.43), and strong correlation with the PROMIS Anxiety and Depression scores (r ranging 0.57-0.80). This is hardly surprising given the current consensus that CLBP is a highly psychological ailment [4, 43-45].

Past studies have also noted relationships between human motion with different metrics of wellbeing [44, 46, 93, 210, 211, 220]. In this study, correlations between motion metrics and PROs were also observed, though to a lesser extent than the correlations between PROs with demographics. It was noted that having a higher range of motion and velocity during extension exercises were associated with better PROs in almost every category. Asymmetry during extension, on the other hand, tended to be associated with worse health metrics. Asymmetry during lateral bending was also associated with worse PROs. It was surprising, however, to note that asymmetry during flexion demonstrated did not follow this trend. Longer times to complete a motion were generally associated with worse PROs, especially the Sit to Stand test. It was also noted that shorter spread of durations (i.e., taking less time to complete the final repetition of a motion compared to the first repetition) was also associated with better PROs.

Overall, these features can be used to train a model to predict different metrics of physiological and psychological wellbeing. The model was unable to predict Sleep Deprivation with significant accuracy. However, the model was able to capture 33-41% of the variance of different metrics of psychological wellbeing (e.g., Pain Intensity, ODI, PROMIS Physical Function T, and PROMIS Pain Interference T), and 39-58% of the variance of different psychological metrics (PROMIS Depression T and PROMIS Anxiety T).

The SHAP values of the model also revealed the nature of the relationship between different demographic and motion metrics. Several nonlinearities were observed. Often, distinct thresholds were observed at which noticeable differences in PROs occurred (such as the sudden drop in PROMIS Pain Interference T once the IPAQ MET scores reached above 2000).

The driving motivation for this research was to assist in developing a precision medicine algorithm for treating patients suffering from CLBP. No single treatment for assisting patients with CLBP has proven to be superior to all others. It has been hypothesized that treatment outcomes could be vastly improved by linking patients to their optimal treatment paradigm [44]. Past efforts in this endeavor have been hampered by the highly heterogeneous spectrum of CLBP severities, the multifactorial nature of CLBP [96], and the lack of objective motion monitoring techniques [96]. This study provides a vital step towards developing this precision medicine technique by accounting for a variety of subject demographics as well as a quantitative and user friendly means of monitoring spinal motion [145]. It was demonstrated in this work that by phenotyping individuals according to their motion patterns and demographic characteristics, statistically significant differences in PROs are revealed between these phenotypes. An analysis of these phenotypes revealed that although there is a wide spectrum of CLBP severities, sub-groups among patients can be identified that exhibit significantly worse scores (such as individuals who are taking opioid prescriptions and require longer time to perform a task). Furthermore, a phenotype of spinal motion was identified that is comprised of both cases and controls. Control individuals who exhibit this phenotype may benefit from preventative treatment.

The statistically significant differences in the PROs between phenotypes is a promising indicator that the phenotypes also will have relevance for clinicians. The results from this study can be conveyed to clinicians and patients as a next step towards developing a precision medicine algorithm, along with the SPINE Sense System and a means of classifying future participants to their respective phenotype. This will facilitate studies in which patients suffering from CLBP will undergo randomized treatment experiments to identify what is the optimal method for assisting patients in each phenotype. Additionally, the interpretation of each phenotype may provide clinicians with an additional understanding of which elements of the biopsychosocial triad are the primary causative elements in the patient's pain, and thus the primary targets for clinical intervention.

CHAPTER 7 DISCUSSIONS

This dissertation presents research conducted to monitor and analyze spinal motion with the intent of identifying sub-groups of individuals who exhibit similar motion patterns and demographic characteristics – i.e., phenotypes. Preliminary chapters in this work presented work done with high deflection strain gauges, motivated by the purpose of monitoring spinal motion. Later chapters investigate different metrics of subject wellbeing, as well as the methods used to identify phenotypes of motion, the results obtained, and the potential clinical application of these phenotypes.

7.1. High Deflection Strain Gauge Modeling

In Chapter 2, a model is presented that converts strain to resistance, as well as interprets strain as a function of resistance. This model accounts for the nonlinearities in the electrical response and time-based transient phenomena exhibited by the high deflection strain gauges. The model is comprised of two components: the first is a spline fit curve that captures the relationship between quasistatic strain and resistance, and the second is a dynamic model that predicts transient resistance spikes and their subsequent exponential decay as a function of the stress relaxation time coefficient. The two model components are superimposed to interpret sensor output under a wide range of applications.

The model was tested on the Instron tensile tester, programmed to imitate biomechanical strains. The model achieved a MAE of 1.6% strain when used to interpret static strains. The model prediction of sensor output of dynamic strain applications captured the general trends of the viscoelastic resistance behavior and achieved high accuracy at low to intermediate strain rates – MAE values of 5.00Ω , 4.03Ω , and 8.59Ω at elongation rates of 0.05 mm/s, 0.50 mm/s, and 5.0 mm/s, respectively. The model interpretation of dynamic strains was able to estimate strain magnitude with an MAE of 1.4% strain and strain rate with an MAE of 0.036 mm/s.

7.2. Mitigating Viscoplastic Deformation with Multilayered Architecture

During the model developed described above, it was noted that the sensor performance and strain range was limited due to viscoelastic and viscoplastic deformation of the sensors. While the base material of the sensors, silicone, is highly elastic, the conductive nanoparticles in the silicone matrix induce stress concentrations. The resulting effects on the electrical signals are difficult to simulate and interpret in terms of accurate strain values [144]. In the application of repeated stress and relaxation, the viscoplastic creep influences become more pronounced on the sensor output.

Understanding that the sensor electrical signal is highly intertwined with the material properties, a multi-layered silicone architecture was developed to encase the nanocomposite strain gauges as described in Chapter 3. It was observed that the multi-layered architecture mitigated internal stresses at high strains and made the strain gauges less prone to buckling during cyclic strains. One of the key improvements in the sensor performance as a result of this change was an increase of signal monotonicity (i.e., that the resistances changes only in one direction – either increasing or decreasing – with additional strain) [146]. The monotonic region was approximately 18-50% strain for the single-layered sensors and approximately 5-50% for the multi-layered sensors. Furthermore, the multilayered architecture reduced the quasi-static electrical signal drift by as much as 74% during cyclic application.

7.3. Relationship between PROs and Moderating Effects of CLBP

The objective of the strain gauge characterization and optimization for this application was to be used in subject motion testing. In addition to the motion tests, study participants were asked to fill out questionnaires regarding their quality of life in different areas. These questionnaires provide quantitative metrics, known as patient-reported outcomes (PROs). There were seven patient-reported outcomes included in this study: Pain

Intensity, Oswestry Disability Index (ODI), PROMIS Physical Function, PROMIS Pain Interference, PROMIS Sleep Deprivation, PROMIS Anxiety, and PROMIS Depression. Chapter 4 describes several analyzes conducted to understand the effects of CLBP on these metrics and their relationship to one another.

From an exploratory factor analysis, these PROs appear to be summarized by four generalized dimensions of well-being represented: Pain and Physical Limitations, Psychological Distress, Physical Activity, and Sleep Deprivation. Individuals who suffer from CLBP reported a significantly lower quality of life in metrics that quantify Pain and Physical Limitations (Pain Intensity, ODI, PROMIS Pain Interference, and PROMIS Physical Function), Psychological Distress (PROMIS Depression and PROMIS Anxiety), and PROMIS Sleep Deprivation.

Moderate to strong relationships were observed between the different PROs, indicating that the different components of wellbeing are highly related to each other. Furthermore, the presence of CLBP is a statistically significant moderating factor in the relationship between the PROMIS Metrics with physiological wellbeing (Pain Interference and ODI). This provides an important context for interpreting PROMIS and legacy PROs in future clinical investigations. This in turn may enable clinicians to more effectively monitor patient progress compared to the baseline of asymptomatic subjects, make more quantitative assessments of patients, and perhaps eventually contribute to the objective selection of treatment paradigms according to patient needs [44].

7.4. Phenotype Identification and Analysis

The primary purpose of this research endeavor was to identify phenotypes of spinal motion and demographics. In this analysis, skin stretch on the lower back served as a proxy for spinal kinematics. High deflection strain gauges were placed on the lines of maximum extension during different spinal motions. The array of the sensors, along with the corresponding wiring and PCB is known as the SPInal Nanosensor Environment (SPINE Sense System). Chapter 5 describes the development of the SPINE Sense System, the subject testing protocol, and anticipated data analysis methodology. Chapter 6 details the results from the final analysis.

The first analysis evaluated the strength of the correlation between individual features (namely motion patterns and subject demographics) with the PROs of interest. Small to moderate Pearson's correlation strengths ($|r|$ ranging from 0.10-0.50) were observed between several demographics with the PROs of interest. Some of the most prominent correlations were that higher education and income levels were associated with lower anxiety, pain, and disability. Being in a marital relationship was associated with better health scores, as was having an active lifestyle. These findings are consistent with past studies [9, 14, 33, 43, 68, 69]. The strongest correlation with the PROs of interest were exhibited by the demographics that quantify psychological distress, namely the PCS-6 and GAD responses, which quantify negative orientation towards pain [163] and general anxiety [162], respectively. The Pearson's correlation (r) between these metrics with pain intensity, disability, physical dysfunction, and pain interference scores ranged 0.13-0.60. They also demonstrated moderate correlations with sleep deprivation (r 0.29-0.43), and strong correlation with the PROMIS Anxiety and Depression scores (r ranging 0.57-0.80). This is hardly surprising given the current consensus that CLBP is a highly psychological ailment [4, 43-45].

Correlations between motion metrics and PROs were also observed, though to a lesser extent than the correlations between PROs with demographics. It was noted that having a higher range of motion and velocity during extension exercises were associated with better PROs in almost every category. Asymmetry during extension, on the other hand, tended to be associated with worse health metrics. Asymmetry during lateral bending was also associated with worse PROs. It was surprising, however, to note that asymmetry during flexion demonstrated did not follow this trend. Longer times to complete a motion were generally

associated with worse PROs, especially the Sit to Stand test. It was also noted that shorter spread of durations (i.e., taking less time to complete the final repetition of a motion compared to the first repetition) was also associated with better PROs.

These input features were combined to train a model to predict different metrics of physiological and psychological wellbeing. The model was unable to predict Sleep Deprivation with significant accuracy. However, the model was able to capture 33-41% of the variance of different metrics of psychological wellbeing (e.g., Pain Intensity, ODI, PROMIS Physical Function T, and PROMIS Pain Interference T), and 39-58% of the variance of different psychological metrics (PROMIS Depression T and PROMIS Anxiety T).

The input features were also used to cluster subjects who exhibited similar motion patterns and demographics. Seven phenotype clusters were identified in this analysis: (A) control females with large flexion spread; (B) control males with consistent flexion motions; (C) case males with large Rright spread; (D) elder case females; (E) younger females with quick, consistent motions; (F) single case females with short Ffast durations; (G) cases with longer motion durations and prescription medications. Statistically significant differences were observed between the control phenotypes (A-B) and the case and mixed phenotypes (C-G). Phenotype G generally exhibited the most severe symptoms, even exhibiting statistically significant differences from other case phenotypes regarding ODI and PROMIS Physical Function T.

These results provide a vital step towards developing this precision medicine technique by accounting for a variety of subject demographics as well as a quantitative and user friendly means of monitoring spinal motion [145]. The statistically significant differences in the PROs between phenotypes is a promising indicator that the phenotypes also will have relevance for clinicians. This will facilitate studies in which patients suffering from CLBP will undergo randomized treatment experiments to identify what is the optimal method for assisting patients in each phenotype. In addition to identifying sub-populations among cases and controls, Phenotype E was comprised of both cases and controls, it is possible that the controls in this phenotype could benefit from preventative treatment.

7.5. Future Work

The results from this work, in addition to their innate contributions to the fields of engineering and medicine, will also facilitate future research.

Clinical Application of Phenotypes: The follow-up from the BACPAC study will be the Biomarkers for Evaluating Spine Treatments Trial (BEST) program. The BEST study will be a multi-site, multiple assignment randomized trial to evaluate four potential interventions: acceptance and commitment therapy, duloxetine, evidence-based exercise and manual therapy, and enhanced self-care. It is our hypothesis that this information regarding subject phenotypes and their corresponding descriptions will enable clinicians to select treatment paradigms individually tailored according to patient conditions. This in turn will improve treatment efficacy, improve the quality of life for the millions of patients suffering from CLBP worldwide, and save millions of dollars in medical resources worldwide every year.

Sensor Characterization and Optimization: Additional characteristics the HDSG can be altered to optimized performance, such as the cross-sectional area and the concentration of nanoparticles in the silicone matrix. Preliminary work has already demonstrated that altering these aspects of the sensors has the potential to further enhance the quality and performance of the sensors. These optimized HDSGs will have immense impact in the field of biomechanics, soft robotics, human-machine interfaces, and more fields [125].

Evaluating sex as a moderating factor in relationships between PROs: Further investigation, using the methods described in Chapter 4, can be used to determine whether other moderating factors influence the relationship between PROs. Potential moderating factors include sex (male or female) and the presence of other ailments other than CLBP.

REFERENCES

- [1] C. Bombardier, "Outcome Assessments in the Evaluation of Treatment of Spinal Disorders: Summary and General Recommendations," *Spine*, vol. 25, no. 24, pp. 3100-3103, 2000. [Online]. Available: https://journals.lww.com/spinejournal/Fulltext/2000/12150/Outcome_Assessments_in_the_Evaluation_of_Treatment.3.aspx.
- [2] H. Riihimäki, "Low-back pain, its origin and risk indicators," *Scandinavian journal of work, environment & health*, pp. 81-90, 1991.
- [3] R. A. Deyo *et al.*, "Report of the NIH Task Force on Research Standards for Chronic Low Back Pain," *The Journal of Pain*, vol. 15, no. 6, pp. 569-585, 2014/06/01/ 2014, doi: <https://doi.org/10.1016/j.jpain.2014.03.005>.
- [4] G. B. J. Andersson, "Epidemiological features of chronic low-back pain," *The Lancet*, vol. 354, no. 9178, pp. 581-585, 1999/08/14/ 1999, doi: [https://doi.org/10.1016/S0140-6736\(99\)01312-4](https://doi.org/10.1016/S0140-6736(99)01312-4).
- [5] A. Praemer, S. Furner, and D. P. Rice, *Musculoskeletal conditions in the United States*. American Academy of Orthopaedic Surgeons Rosemont, IL, 1999.
- [6] D. Hoy *et al.*, "A systematic review of the global prevalence of low back pain," *Arthritis & Rheumatism*, vol. 64, no. 6, pp. 2028-2037, 2012/06/01 2012, doi: <https://doi.org/10.1002/art.34347>.
- [7] B. F. Walker, "The Prevalence of Low Back Pain: A Systematic Review of the Literature from 1966 to 1998," *Clinical Spine Surgery*, vol. 13, no. 3, pp. 205-217, 2000. [Online]. Available: https://journals.lww.com/jspinaldisorders/fulltext/2000/06000/the_prevalence_of_low_back_pain_a_systematic.3.aspx.
- [8] J. A. Ricci, W. F. Stewart, E. Chee, C. Leotta, K. Foley, and M. C. Hochberg, "Back pain exacerbations and lost productive time costs in United States workers," *Spine*, vol. 31, no. 26, pp. 3052-3060, 2006.
- [9] R. A. Deyo, S. K. Mirza, and B. I. Martin, "Back Pain Prevalence and Visit Rates: Estimates From U.S. National Surveys, 2002," *Spine*, vol. 31, no. 23, pp. 2724-2727, 2006, doi: 10.1097/01.brs.0000244618.06877.cd.
- [10] D. I. Rubin, "Epidemiology and Risk Factors for Spine Pain," *Neurologic Clinics*, vol. 25, no. 2, pp. 353-371, 2007/05/01/ 2007, doi: <https://doi.org/10.1016/j.ncl.2007.01.004>.
- [11] F. Biering-Sørensen, "A prospective study of low back pain in a general population. I. Occurrence, recurrence and aetiology," *Journal of Rehabilitation Medicine*, vol. 15, no. 2, pp. 71-79, 1983.
- [12] H.-O. Svenson, G. B. J. Andersson, S. Johansson, C. Wilhemsson, and A. Vedin, "A Retrospective Study of Low-Back Pain in 38- to 64-Year-Old Women: Frequency of Occurrence and Impact on Medical Services," *Spine*, vol. 13, no. 5, pp. 548-552, 1988. [Online]. Available: https://journals.lww.com/spinejournal/fulltext/1988/05000/a_retrospective_study_of_low_back_pain_in_38_to.19.aspx.
- [13] E. L. Hurwitz, K. Randhawa, H. Yu, P. Côté, and S. Haldeman, "The Global Spine Care Initiative: a summary of the global burden of low back and neck pain studies," *European Spine Journal*, vol. 27, no. 6, pp. 796-801, 2018/09/01 2018, doi: 10.1007/s00586-017-5432-9.
- [14] J. T. Robertson, "The rape of the spine," *Surgical Neurology*, vol. 39, no. 1, pp. 5-12, 1993/01/01/ 1993, doi: [https://doi.org/10.1016/0090-3019\(93\)90102-7](https://doi.org/10.1016/0090-3019(93)90102-7).
- [15] M. L. Skovron, "Epidemiology of low back pain," *Baillière's Clinical Rheumatology*, vol. 6, no. 3, pp. 559-573, 1992/10/01/ 1992, doi: [https://doi.org/10.1016/S0950-3579\(05\)80127-X](https://doi.org/10.1016/S0950-3579(05)80127-X).
- [16] V. Feigin, "Global, regional, and National Incidence, prevalence, and years lived with disability for 310 acute and chronic diseases and injuries, 1990-2015: a systematic analysis for the global burden of disease study 2015," *The Lancet*, vol. 388, no. 10053, pp. 1545-1602, 2016.
- [17] D. Hoy *et al.*, "The global burden of low back pain: estimates from the Global Burden of Disease 2010 study," *Annals of the Rheumatic Diseases*, vol. 73, no. 6, pp. 968-974, 2014, doi: 10.1136/annrheumdis-2013-204428.

- [18] V. M. Taylor, R. A. Deyo, D. C. Cherkin, and W. Kreuter, "Low Back Pain Hospitalization: Recent United States Trends and Regional Variations," *Spine*, vol. 19, no. 11, pp. 1207-1212, 1994. [Online]. Available: https://journals.lww.com/spinejournal/fulltext/1994/05310/low_back_pain_hospitalization_recent_united.2.aspx.
- [19] A. L. Nachemson, "The Lumbar Spine An Orthopaedic Challenge," *Spine*, vol. 1, no. 1, 1976. [Online]. Available: https://journals.lww.com/spinejournal/fulltext/1976/03000/the_lumbar_spine_an_orthopaedic_challenge.9.aspx.
- [20] C. f. D. Control and Prevention, "Prevalence of disabilities and associated health conditions among adults--United States, 1999," *MMWR. Morbidity and mortality weekly report*, vol. 50, no. 7, pp. 120-125, 2001.
- [21] A. Parthan, C. J. Evans, and K. Le, "Chronic low back pain: epidemiology, economic burden and patient-reported outcomes in the USA," *Expert Rev Pharmacoecon Outcomes Res*, vol. 6, no. 3, pp. 359-69, Jun 2006, doi: 10.1586/14737167.6.3.359.
- [22] R. Chou, "Low back pain (chronic)," *American family physician*, vol. 84, no. 4, pp. 437-438, 2011.
- [23] F. Tubach, A. Leclerc, M.-F. Landre, and F. Pietri-Taleb, "Risk factors for sick leave due to low back pain: a prospective study," *Journal of Occupational and Environmental Medicine*, pp. 451-458, 2002.
- [24] W. F. Stewart, J. A. Ricci, E. Chee, D. Morganstein, and R. Lipton, "Lost Productive Time and Cost Due to Common Pain Conditions in the US Workforce," *JAMA*, vol. 290, no. 18, pp. 2443-2454, 2003, doi: 10.1001/jama.290.18.2443.
- [25] B. S. Webster and S. H. Snook, "The Cost of Compensable Low Back Pain," *Journal of Occupational Medicine*, vol. 32, no. 1, pp. 13-15, 1990. [Online]. Available: <http://www.jstor.org/stable/45008033>.
- [26] M. Rossignol, S. Suissa, and L. Abenhaim, "Working disability due to occupational back pain: three-year follow-up of 2,300 compensated workers in Quebec," *Journal of occupational medicine*, pp. 502-505, 1988.
- [27] J. W. Frymoyer and W. L. Cats-Baril, "An Overview of the Incidences and Costs of Low Back Pain," *Orthopedic Clinics of North America*, vol. 22, no. 2, pp. 263-271, 1991/04/01/ 1991, doi: [https://doi.org/10.1016/S0030-5898\(20\)31652-7](https://doi.org/10.1016/S0030-5898(20)31652-7).
- [28] D. Hoy, P. Brooks, F. Blyth, and R. Buchbinder, "The Epidemiology of low back pain," *Best Practice & Research Clinical Rheumatology*, vol. 24, no. 6, pp. 769-781, 2010/12/01/ 2010, doi: <https://doi.org/10.1016/j.berh.2010.10.002>.
- [29] C. E. Dionne, K. M. Dunn, and P. R. Croft, "Does back pain prevalence really decrease with increasing age? A systematic review," *Age and Ageing*, vol. 35, no. 3, pp. 229-234, 2006, doi: 10.1093/ageing/afj055.
- [30] J. W. FRYMOYER, M. H. POPE, M. C. COSTANZA, J. C. ROSEN, J. E. GOGGIN, and D. G. WILDER, "Epidemiologic Studies of Low-Back Pain," *Spine*, vol. 5, no. 5, pp. 419-423, 1980. [Online]. Available: https://journals.lww.com/spinejournal/fulltext/1980/09000/epidemiologic_studies_of_low_back_pain.5.aspx.
- [31] M. Heliövaara, "Occupation and risk of herniated lumbar intervertebral disc or sciatica leading to hospitalization," *Journal of Chronic Diseases*, vol. 40, no. 3, pp. 259-264, 1987/01/01/ 1987, doi: [https://doi.org/10.1016/0021-9681\(87\)90162-7](https://doi.org/10.1016/0021-9681(87)90162-7).
- [32] P. Leino, J. Hasan, and S.-L. Karppi, "Occupational class, physical workload, and musculoskeletal morbidity in the engineering industry," *British journal of industrial medicine*, vol. 45, no. 10, p. 672, 1988.
- [33] S. Schneider, D. Randoll, and M. Buchner, "Why Do Women Have Back Pain More Than Men?: A Representative Prevalence Study in the Federal Republic of Germany," *The Clinical Journal of Pain*, vol. 22, no. 8, pp. 738-747, 2006, doi: 10.1097/01.ajp.0000210920.03289.93.
- [34] R. van Abbema *et al.*, "Factors Associated with Functional Capacity Test Results in Patients With Non-Specific Chronic Low Back Pain: A Systematic Review," *Journal of Occupational Rehabilitation*, vol. 21, no. 4, pp. 455-473, 2011/12/01 2011, doi: 10.1007/s10926-011-9306-4.

- [35] G. Christe, G. Crombez, S. Edd, E. Opsommer, B. M. Jolles, and J. Favre, "Relationship between psychological factors and spinal motor behaviour in low back pain: a systematic review and meta-analysis," *PAIN*, vol. 162, no. 3, 2021. [Online]. Available: https://journals.lww.com/pain/fulltext/2021/03000/relationship_between_psychological_factors_and_3.aspx.
- [36] C. Leboeuf-Yde, "Alcohol and low-back pain: A systematic literature review," *Journal of Manipulative and Physiological Therapeutics*, vol. 23, no. 5, pp. 343-346, 2000/06/01/ 2000, doi: <https://doi.org/10.1067/mmt.2000.106866>.
- [37] Z. Lv, J. Cui, and J. Zhang, "Smoking, alcohol and coffee consumption and risk of low back pain: a Mendelian randomization study," *European Spine Journal*, vol. 31, no. 11, pp. 2913-2919, 2022.
- [38] R. Shiri, J. Karppinen, P. Leino-Arjas, S. Solovieva, and E. Viikari-Juntura, "The Association Between Obesity and Low Back Pain: A Meta-Analysis," *American Journal of Epidemiology*, vol. 171, no. 2, pp. 135-154, 2009, doi: 10.1093/aje/kwp356.
- [39] M. Szumilas, "Explaining odds ratios," *Journal of the Canadian academy of child and adolescent psychiatry*, vol. 19, no. 3, p. 227, 2010.
- [40] F. Fatoye, T. Gebrye, and I. Odeyemi, "Real-world incidence and prevalence of low back pain using routinely collected data," *Rheumatology International*, vol. 39, no. 4, pp. 619-626, 2019/04/01 2019, doi: 10.1007/s00296-019-04273-0.
- [41] K. C. Kamal *et al.*, "Managing low back pain in primary care," *Current Health Sciences Journal*, vol. 46, no. 4, p. 396, 2020.
- [42] I. Heuch, I. Heuch, K. Hagen, and J.-A. Zwart, "Body Mass Index as a Risk Factor for Developing Chronic Low Back Pain: A Follow-up in the Nord-Trøndelag Health Study," *Spine*, vol. 38, no. 2, pp. 133-139, 2013, doi: 10.1097/BRS.0b013e3182647af2.
- [43] J. Rainville, C. Hartigan, E. Martinez, J. Limke, C. Jouve, and M. Finno, "Exercise as a treatment for chronic low back pain," *The Spine Journal*, vol. 4, no. 1, pp. 106-115, 2004/01/02/ 2004, doi: [https://doi.org/10.1016/S1529-9430\(03\)00174-8](https://doi.org/10.1016/S1529-9430(03)00174-8).
- [44] D. Adam Quirk *et al.*, "Biomechanical Phenotyping of Chronic Low Back Pain: Protocol for BACPAC," *Pain Medicine*, 2022, doi: 10.1093/pm/pnac163.
- [45] M. Pflingsten *et al.*, "Fear-Avoidance Behavior and Anticipation of Pain in Patients With Chronic Low Back Pain: A Randomized Controlled Study," *Pain Medicine*, vol. 2, no. 4, pp. 259-266, 2001, doi: 10.1046/j.1526-4637.2001.01044.x.
- [46] W. S. Marras *et al.*, "The Classification of Anatomic- and Symptom-based Low Back Disorders Using Motion Measure Models," *Spine*, vol. 20, no. 23, pp. 2531-2546, 1995. [Online]. Available: https://journals.lww.com/spinejournal/Fulltext/1995/12000/The_Classification_of_Anatomic_and_Symptom_based.13.aspx.
- [47] L. D. Bardin, P. King, and C. G. Maher, "Diagnostic triage for low back pain: a practical approach for primary care," *Medical Journal of Australia*, vol. 206, no. 6, pp. 268-273, 2017, doi: <https://doi.org/10.5694/mja16.00828>.
- [48] S. D. Tagliaferri *et al.*, "Chronic back pain sub-grouped via psychosocial, brain and physical factors using machine learning," *Sci Rep*, vol. 12, no. 1, p. 15194, Sep 7 2022, doi: 10.1038/s41598-022-19542-5.
- [49] C. Cedraschi, J. Robert, D. Goerg, E. Perrin, W. Fischer, and T. Vischer, "Is chronic non-specific low back pain chronic? Definitions of a problem and problems of a definition," *British journal of general practice*, vol. 49, no. 442, pp. 358-362, 1999.
- [50] D. G. Borenstein, "CHRONIC LOW BACK PAIN," *Rheumatic Disease Clinics of North America*, vol. 22, no. 3, pp. 439-456, 1996/08/01/ 1996, doi: [https://doi.org/10.1016/S0889-857X\(05\)70281-7](https://doi.org/10.1016/S0889-857X(05)70281-7).
- [51] J. Fairbank *et al.*, "The Role of Classification of Chronic Low Back Pain," *Spine*, vol. 36, pp. S19-S42, 2011, doi: 10.1097/BRS.0b013e31822ef72c.
- [52] J. K. Freburger *et al.*, "The Rising Prevalence of Chronic Low Back Pain," *Archives of Internal Medicine*, vol. 169, no. 3, pp. 251-258, 2009, doi: 10.1001/archinternmed.2008.543.
- [53] A. Becker *et al.*, "Low Back Pain in Primary Care: Costs of Care and Prediction of Future Health Care Utilization," *Spine*, vol. 35, no. 18, pp. 1714-1720, 2010, doi: 10.1097/BRS.0b013e3181cd656f.

- [54] J. Hong, C. Reed, D. Novick, and M. Happich, "Costs Associated With Treatment of Chronic Low Back Pain: An Analysis of the UK General Practice Research Database," *Spine*, vol. 38, no. 1, pp. 75-82, 2013, doi: 10.1097/BRS.0b013e318276450f.
- [55] P. B. Polatin, R. K. Kennedy, R. J. Gatchel, E. Lillo, and T. G. Mayer, "Psychiatric illness and chronic low-back pain: the mind and the spine—which goes first?," *Spine*, vol. 18, no. 1, pp. 66-71, 1993.
- [56] B. M. Wand and N. E. O'Connell, "Chronic non-specific low back pain—sub-groups or a single mechanism?," *BMC musculoskeletal disorders*, vol. 9, pp. 1-15, 2008.
- [57] M. C. Mauck *et al.*, "The Back Pain Consortium (BACPAC) Research Program: Structure, Research Priorities, and Methods," *Pain Medicine*, 2023, doi: 10.1093/pm/pnac202.
- [58] R. A. Deyo, S. K. Mirza, J. A. Turner, and B. I. Martin, "Overtreating chronic back pain: time to back off?," *The Journal of the American Board of Family Medicine*, vol. 22, no. 1, pp. 62-68, 2009.
- [59] B. W. Koes, M. W. van Tulder, and S. Thomas, "Diagnosis and treatment of low back pain," *BMJ*, vol. 332, no. 7555, p. 1430, 2006, doi: 10.1136/bmj.332.7555.1430.
- [60] A. Deshpande, A. D. Furlan, A. Mailis-Gagnon, S. Atlas, and D. Turk, "Opioids for chronic low-back pain," *Cochrane Database of Systematic Reviews*, no. 3, 2007, doi: 10.1002/14651858.CD004959.pub3.
- [61] J. Eriksen, P. Sjøgren, E. Bruera, O. Ekholm, and N. K. Rasmussen, "Critical issues on opioids in chronic non-cancer pain: An epidemiological study," *Pain*, vol. 125, no. 1, pp. 172-179, 2006/11/01/ 2006, doi: <https://doi.org/10.1016/j.pain.2006.06.009>.
- [62] R. A. Deyo, M. V. Korff, and D. Duhrkoop, "Opioids for low back pain," *BMJ : British Medical Journal*, vol. 350, p. g6380, 2015, doi: 10.1136/bmj.g6380.
- [63] R. B. Keller, S. J. Atlas, D. N. Soule, D. E. Singer, and R. A. Deyo, "Relationship Between Rates and Outcomes of Operative Treatment for Lumbar Disc Herniation and Spinal Stenosis," *JBJS*, vol. 81, no. 6, 1999. [Online]. Available: https://journals.lww.com/jbjsjournal/fulltext/1999/06000/relationship_between_rates_and_outcomes_of.2.aspx.
- [64] J. N. Abramovitz and S. R. Neff, "Lumbar disc surgery: results of the Prospective Lumbar Discectomy Study of the Joint Section on Disorders of the Spine and Peripheral Nerves of the American Association of Neurological Surgeons and the Congress of Neurological Surgeons," (in eng), *Neurosurgery*, vol. 29, no. 2, pp. 301-7; discussion 307-8, 1991/08// 1991, doi: 10.1097/00006123-199108000-00027.
- [65] H. Weber, "Lumbar Disc Herniation: A Controlled, Prospective Study with Ten Years of Observation," *Spine*, vol. 8, no. 2, 1983. [Online]. Available: https://journals.lww.com/spinejournal/fulltext/1983/03000/lumbar_disc_herniation_a_controlled_prospective.3.aspx.
- [66] A. Searle, M. Spink, A. Ho, and V. Chuter, "Exercise interventions for the treatment of chronic low back pain: a systematic review and meta-analysis of randomised controlled trials," *Clinical Rehabilitation*, vol. 29, no. 12, pp. 1155-1167, 2015, doi: 10.1177/0269215515570379.
- [67] I. Cohen and J. Rainville, "Aggressive Exercise as Treatment for Chronic Low Back Pain," *Sports Medicine*, vol. 32, no. 1, pp. 75-82, 2002/01/01 2002, doi: 10.2165/00007256-200232010-00004.
- [68] Y. Liu, Y. Wang, K. Dong, and G. Kuan, "Interventions of Exercise Therapy for Chronic Non-Specific Low Back Pain: A Comprehensive Systematic Review and Comparative Study of Effects," 2024.
- [69] A. Daneshjoo, H. Yazdani Esfahaninejad, and S. Roghanian, "The effect of yoga exercises on body posture, fatigue intensity, pain and trunk kinematics of girls with erectile dysfunction," *Journal of Sports Physiology and Athletic Conditioning*, vol. 10, no. 10, p. 1.
- [70] S. D. Liddle, G. D. Baxter, and J. H. Gracey, "Exercise and chronic low back pain: what works?," *Pain*, vol. 107, no. 1, pp. 176-190, 2004/01/01/ 2004, doi: <https://doi.org/10.1016/j.pain.2003.10.017>.
- [71] A. Nachemson, "Back Pain: Delimiting the Problem in the Next Millennium," *International Journal of Law and Psychiatry*, vol. 22, no. 5, pp. 473-490, 1999/09/01/ 1999, doi: [https://doi.org/10.1016/S0160-2527\(99\)00022-9](https://doi.org/10.1016/S0160-2527(99)00022-9).

- [72] J. Barth *et al.*, "Biometric and mobile gait analysis for early diagnosis and therapy monitoring in Parkinson's disease," in *2011 annual international conference of the IEEE engineering in medicine and biology society*, 2011: IEEE, pp. 868-871.
- [73] G. Allali, F. Assal, R. W. Kressig, V. Dubost, F. R. Herrmann, and O. Beauchet, "Impact of impaired executive function on gait stability," *Dementia and geriatric cognitive disorders*, vol. 26, no. 4, pp. 364-369, 2008.
- [74] Y. Cedervall, K. Halvorsen, and A. C. Åberg, "A longitudinal study of gait function and characteristics of gait disturbance in individuals with Alzheimer's disease," *Gait & posture*, vol. 39, no. 4, pp. 1022-1027, 2014.
- [75] L. Wallard, G. Dietrich, Y. Kerlirzin, and J. Bredin, "Balance control in gait children with cerebral palsy," *Gait & Posture*, vol. 40, no. 1, pp. 43-47, 2014/05/01/ 2014, doi: <https://doi.org/10.1016/j.gaitpost.2014.02.009>.
- [76] M. Montero-Odasso, C. Annweiler, V. Hachinski, A. Islam, N. Toma, and A. Vasudev, "Vascular burden predicts gait, mood, and executive function disturbances in older adults with mild cognitive impairment: results from the gait and brain study," *Journal of the American Geriatrics Society*, vol. 60, no. 10, pp. 1988-90, Oct 2012, doi: 10.1111/j.1532-5415.2012.04180.x.
- [77] D. R. Howell, L. R. Osternig, and L.-S. Chou, "Adolescents Demonstrate Greater Gait Balance Control Deficits After Concussion Than Young Adults," *The American Journal of Sports Medicine*, vol. 43, no. 3, pp. 625-632, 2015/03/01 2014, doi: 10.1177/0363546514560994.
- [78] M. Arazpour, S. R. Mehrpour, M. A. Bani, S. W. Hutchins, M. Bahramizadeh, and M. Rahgozar, "Comparison of gait between healthy participants and persons with spinal cord injury when using a powered gait orthosis-a pilot study," *Spinal Cord*, vol. 52, no. 1, pp. 44-8, Jan 2014, doi: 10.1038/sc.2013.139.
- [79] N. Šarabon, N. Vreček, C. Hofer, S. Löfler, Ž. Kozinc, and H. Kern, "Physical abilities in low back pain patients: a cross-sectional study with exploratory comparison of patient subgroups," *Life*, vol. 11, no. 3, p. 226, 2021.
- [80] I. C. Aranda-Valera *et al.*, "Measuring spinal mobility using an inertial measurement unit system: a validation study in axial spondyloarthritis," *Diagnostics*, vol. 10, no. 6, p. 426, 2020.
- [81] W. S. Marras and P. E. Wongsam, "Flexibility and velocity of the normal and impaired lumbar spine," *Arch Phys Med Rehabil*, vol. 67, no. 4, pp. 213-7, Apr 1986. [Online]. Available: <https://www.ncbi.nlm.nih.gov/pubmed/2938557>.
- [82] S. S. Hlaing, R. Puntumetakul, S. Wanpen, and R. Boucaut, "Balance control in patients with subacute non-specific low back pain, with and without lumbar instability: A cross-sectional study," *Journal of pain research*, pp. 795-803, 2020.
- [83] Y. Barzilay *et al.*, "Patients with chronic non-specific low back pain who reported reduction in pain and improvement in function also demonstrated an improvement in gait pattern," *European Spine Journal*, vol. 25, pp. 2761-2766, 2016.
- [84] A. P. Monie, R. I. Price, C. R. P. Lind, and K. P. Singer, "Structure-Specific Movement Patterns in Patients With Chronic Low Back Dysfunction Using Lumbar Combined Movement Examination," *J Manipulative Physiol Ther*, vol. 40, no. 5, pp. 340-349, Jun 2017, doi: 10.1016/j.jmpt.2017.02.011.
- [85] M. M. Panjabi, "Clinical spinal instability and low back pain," *Journal of electromyography and kinesiology*, vol. 13, no. 4, pp. 371-379, 2003.
- [86] S. J. Dreyer and P. H. Dreyfuss, "Low back pain and the zygapophysial (facet) joints," *Archives of physical medicine and rehabilitation*, vol. 77, no. 3, pp. 290-300, 1996.
- [87] L. Hestbaek, A. Kongsted, T. S. Jensen, and C. Leboeuf-Yde, "The clinical aspects of the acute facet syndrome: results from a structured discussion among European chiropractors," *Chiropractic & Osteopathy*, vol. 17, no. 1, pp. 1-10, 2009.
- [88] A. J. Fennell, A. P. Jones, and D. W. Hukins, "Migration of the nucleus pulposus within the intervertebral disc during flexion and extension of the spine," *Spine*, vol. 21, no. 23, pp. 2753-2757, 1996.

- [89] A. P. Monie, R. I. Price, C. R. Lind, and K. P. Singer, "Structure-Specific Movement Patterns in Patients With Chronic Low Back Dysfunction Using Lumbar Combined Movement Examination," *Journal of manipulative and physiological therapeutics*, vol. 40, no. 5, pp. 340-349, 2017.
- [90] J. Nazari, M. H. Pope, and R. A. Graveling, "Reality about migration of the nucleus pulposus within the intervertebral disc with changing postures," *Clinical Biomechanics*, vol. 27, no. 3, pp. 213-217, 2012.
- [91] J. N. Katz and M. B. Harris, "Lumbar spinal stenosis," *New England Journal of Medicine*, vol. 358, no. 8, pp. 818-825, 2008.
- [92] T. Petersen, M. Laslett, and C. Juhl, "Clinical classification in low back pain: best-evidence diagnostic rules based on systematic reviews," *BMC musculoskeletal disorders*, vol. 18, no. 1, pp. 1-23, 2017.
- [93] G. Christe, L. Redhead, T. Legrand, B. M. Jolles, and J. Favre, "Multi-segment analysis of spinal kinematics during sit-to-stand in patients with chronic low back pain," *Journal of Biomechanics*, vol. 49, no. 10, pp. 2060-2067, 2016/07/05/ 2016, doi: <https://doi.org/10.1016/j.jbiomech.2016.05.015>.
- [94] S. D. Tagliaferri *et al.*, "Towards data-driven biopsychosocial classification of non-specific chronic low back pain: a pilot study," *Scientific Reports*, vol. 13, no. 1, p. 13112, 2023.
- [95] K. Sievers and T. Klaukka, "Back pain and arthrosis in Finland," *Acta Orthopaedica Scandinavica*, vol. 62, no. sup241, pp. 3-5, 1991/01/01 1991, doi: 10.3109/17453679109155095.
- [96] S. D. Tagliaferri, U. H. Mitchell, T. Saueressig, P. J. Owen, C. T. Miller, and D. L. Belavy, "Classification Approaches for Treating Low Back Pain Have Small Effects That Are Not Clinically Meaningful: A Systematic Review With Meta-analysis," *Journal of Orthopaedic & Sports Physical Therapy*, vol. 52, no. 2, pp. 67-84, 2022.
- [97] D. Cella *et al.*, "The Patient-Reported Outcomes Measurement Information System (PROMIS) developed and tested its first wave of adult self-reported health outcome item banks: 2005–2008," *Journal of Clinical Epidemiology*, vol. 63, no. 11, pp. 1179-1194, 2010/11/01/ 2010, doi: <https://doi.org/10.1016/j.jclinepi.2010.04.011>.
- [98] J. C. T. Fairbank and P. B. Pynsent, "The Oswestry Disability Index," *Spine*, vol. 25, no. 22, pp. 2940-2953, 2000. [Online]. Available: https://journals.lww.com/spinejournal/Fulltext/2000/11150/The_Oswestry_Disability_Index.17.aspx.
- [99] M. Hagströmer, P. Oja, and M. Sjöström, "The International Physical Activity Questionnaire (IPAQ): a study of concurrent and construct validity," *Public Health Nutrition*, vol. 9, no. 6, pp. 755-762, 2006, doi: 10.1079/PHN2005898.
- [100] P. H. Lee, D. J. Macfarlane, T. H. Lam, and S. M. Stewart, "Validity of the international physical activity questionnaire short form (IPAQ-SF): A systematic review," *International Journal of Behavioral Nutrition and Physical Activity*, vol. 8, no. 1, p. 115, 2011/10/21 2011, doi: 10.1186/1479-5868-8-115.
- [101] "What is PROMIS?" <https://www.promishealth.org> (accessed 6/24/2023, 2023).
- [102] N. E. Rothrock, D. Amtmann, and K. F. Cook, "Development and validation of an interpretive guide for PROMIS scores," *Journal of Patient-Reported Outcomes*, vol. 4, pp. 1-7, 2020.
- [103] A. C. Carle, K. B. Bevans, C. A. Tucker, and C. B. Forrest, "Using nationally representative percentiles to interpret PROMIS pediatric measures," *Quality of Life Research*, vol. 30, no. 4, pp. 997-1004, 2021/04/01 2021, doi: 10.1007/s11136-020-02700-5.
- [104] A. Ramasamy *et al.*, "Assessment of Patient-Reported Outcome Instruments to Assess Chronic Low Back Pain," *Pain Medicine*, vol. 18, no. 6, pp. 1098-1110, 2017, doi: 10.1093/pm/pnw357.
- [105] G. Hassett, "Performance of the Patient-Reported Outcomes Measurement Information System 29 (PROMIS-29) Item Profile in a Cohort of Australians with RA, OA and Other Inflammatory Arthritic Conditions," *American College of Rheumatology Meeting Abstracts*, 2019.
- [106] J. H. Hong, H. D. Kim, H. H. Shin, and B. Huh, "Assessment of depression, anxiety, sleep disturbance, and quality of life in patients with chronic low back pain in Korea," *Keja*, vol. 66, no. 6, pp. 444-450, 06 2014, doi: 10.4097/kjae.2014.66.6.444.
- [107] N. Schilaty, N. Bates, B. Holmes, and T. Nagai, "Group differences and associations between patient-reported outcomes and physical characteristics in chronic low back pain patients and healthy controls," *Clinical Biomechanics*, vol. 106, p. 106009, 2023/06/01/ 2023, doi: <https://doi.org/10.1016/j.clinbiomech.2023.106009>.

- [108] K. Khutok, P. Janwantanakul, M. P. Jensen, and R. Kanlayanaphotporn, "Responsiveness of the PROMIS-29 scales in individuals with chronic low back pain," *Spine*, vol. 46, no. 2, pp. 107-113, 2021.
- [109] B. Lapin, S. Davin, M. Stilphen, E. Benzel, and I. L. Katzan, "Validation of PROMIS CATs and PROMIS global health in an interdisciplinary pain program for patients with chronic low back pain," *Spine*, vol. 45, no. 4, pp. E227-E235, 2020.
- [110] A. F. Mannion, J. I. Brox, and J. C. T. Fairbank, "Comparison of spinal fusion and nonoperative treatment in patients with chronic low back pain: long-term follow-up of three randomized controlled trials," *The Spine Journal*, vol. 13, no. 11, pp. 1438-1448, 2013/11/01/ 2013, doi: <https://doi.org/10.1016/j.spinee.2013.06.101>.
- [111] J. D. Markman *et al.*, "Association Between Opioid Use and Patient-Reported Outcomes in a Randomized Trial Evaluating Basivertebral Nerve Ablation for the Relief of Chronic Low Back Pain," *Neurosurgery*, vol. 86, no. 3, pp. 343-347, 2020, doi: 10.1093/neuros/nyz093.
- [112] B. S. Boody, S. Bhatt, A. S. Mazmudar, W. K. Hsu, N. E. Rothrock, and A. A. Patel, "Validation of Patient-Reported Outcomes Measurement Information System (PROMIS) computerized adaptive tests in cervical spine surgery," (in English), *Journal of Neurosurgery: Spine SPI*, vol. 28, no. 3, pp. 268-279, 01 Mar. 2018 2018, doi: <https://doi.org/10.3171/2017.7.SPINE17661>.
- [113] M. Hung *et al.*, "Responsiveness of the Patient-Reported Outcomes Measurement Information System (PROMIS), Neck Disability Index (NDI) and Oswestry Disability Index (ODI) instruments in patients with spinal disorders," *The Spine Journal*, vol. 19, no. 1, pp. 34-40, 2019/01/01/ 2019, doi: <https://doi.org/10.1016/j.spinee.2018.06.355>.
- [114] A.-M. Orbai, "Validation of the PROMIS-29 Profile in Patients with Active Psoriatic Arthritis Using Data from a Phase 3, Randomized, Placebo-Controlled Study Evaluating Guselkumab," *American College of Rheumatology Meeting Abstracts*, 2021.
- [115] S. Sadiqi *et al.*, "Reliability, validity and responsiveness of the Dutch version of the AOSpine PROST (Patient Reported Outcome Spine Trauma)," *European Spine Journal*, vol. 30, no. 9, pp. 2631-2644, 2021/09/01 2021, doi: 10.1007/s00586-020-06554-w.
- [116] D. Niederer *et al.*, "Which Functional Outcomes Can be Measured in Low Back Pain Trials and Therapies?: A Prospective 2-Year Factor-, Cluster-, and Reliability-Multicenter Analysis on 42 Variables in 1049 Individuals," *Spine*, vol. 46, no. 21, 2021. [Online]. Available: https://journals.lww.com/spinejournal/Fulltext/2021/11010/Which_Functional_Outcomes_Can_b_e_Measured_in_Low.15.aspx.
- [117] A. L. Gruber-Baldini, C. Velozo, S. Romero, and L. M. Shulman, "Validation of the PROMIS® measures of self-efficacy for managing chronic conditions," *Quality of Life Research*, vol. 26, no. 7, pp. 1915-1924, 2017.
- [118] P. G. Passias *et al.*, "ODI cannot account for all variation in PROMIS scores in patients with thoracolumbar disorders," *Global Spine Journal*, vol. 10, no. 4, pp. 399-405, 2020.
- [119] M. S. Fidai *et al.*, "Patient-reported outcomes measurement information system and legacy patient-reported outcome measures in the field of orthopaedics: a systematic review," *Arthroscopy: The Journal of Arthroscopic & Related Surgery*, vol. 34, no. 2, pp. 605-614, 2018.
- [120] D. S. Brodke, V. Goz, M. W. Voss, B. D. Lawrence, W. R. Spiker, and M. Hung, "PROMIS® PF CAT outperforms the ODI and SF-36 physical function domain in spine patients," *Spine*, vol. 42, no. 12, p. 921, 2017.
- [121] E. C. Makhni *et al.*, "Correlation of PROMIS Physical Function, Pain Interference, and Depression in Pediatric and Adolescent Patients in the Ambulatory Sports Medicine Clinic," *Orthopaedic Journal of Sports Medicine*, vol. 7, no. 6, p. 2325967119851100, 2019/06/01 2019, doi: 10.1177/2325967119851100.
- [122] B. E. Haws *et al.*, "The patient-reported outcomes measurement information system in spine surgery: a systematic review," *Journal of Neurosurgery: Spine*, vol. 30, no. 3, pp. 405-413, 2019.
- [123] J. C. Tishelman *et al.*, "Patient-Reported Outcomes Measurement Information System instruments: outperforming traditional quality of life measures in patients with back and neck pain," *Journal of Neurosurgery: Spine*, vol. 30, no. 4, pp. 545-550, 2019.

- [124] A. F. Mannion, A. Junge, S. Taimela, M. Müntener, K. Lorenzo, and J. Dvorak, "Active therapy for chronic low back pain: part 3. Factors influencing self-rated disability and its change following therapy," *Spine*, vol. 26, no. 8, pp. 920-929, 2001.
- [125] M. Amjadi, K.-U. Kyung, I. Park, and M. Sitti, "Stretchable, Skin-Mountable, and Wearable Strain Sensors and Their Potential Applications: A Review," *Advanced Functional Materials*, vol. 26, no. 11, pp. 1678-1698, 2016, doi: <https://doi.org/10.1002/adfm.201504755>.
- [126] M. Amjadi, Y. J. Yoon, and I. Park, "Ultra-stretchable and skin-mountable strain sensors using carbon nanotubes–Ecoflex nanocomposites," *Nanotechnology*, vol. 26, no. 37, p. 375501, 2015.
- [127] O. K. Johnson, G. C. Kaschner, T. A. Mason, D. T. Fullwood, and G. Hansen, "Optimization of nickel nanocomposite for large strain sensing applications," *Sensors and Actuators A: Physical*, vol. 166, no. 1, pp. 40-47, 2011/03/01/ 2011, doi: <https://doi.org/10.1016/j.sna.2010.12.022>.
- [128] S. Yong and K. Aw, "Modeling Electrical Resistance Behavior of Soft and Flexible Piezoresistive Sensors Based on Carbon-Black/Silicone Elastomer Composites," *Sensing and Imaging*, vol. 23, no. 1, p. 22, 2022.
- [129] T. D. Remington, "Biomechanical Applications and Modeling of Quantum Nano-Composite Strain Gauges," M.Sc., Brigham Young University, Ann Arbor, 28105896, 2014. [Online]. Available: <http://erl.lib.byu.edu/login/?url=https://www.proquest.com/dissertations-theses/biomechanical-applications-modeling-quantum-nano/docview/2490992132/se-2?accountid=4488>
http://www.lib.byu.edu/jfinder.pl?url_ver=Z39.88-2004&ft_val_fmt=info:ofi/fmt:kev:mtx:dissertation&genre=dissertations+%26+theses&sid=ProQ:ProQuest+Dissertations+%26+Theses+Global&atitle=&title=Biomechanical+Applications+and+Modeling+of+Quantum+Nano-Composite+Strain+Gauges&issn=&date=2014-01-01&volume=&issue=&spage=&au=Remington%2C+Taylor+D.&isbn=9798662520394&jtitle=&bt
- [130] G. D. Airey, B. Rahimzadeh, and A. C. Collop, "Viscoelastic linearity limits for bituminous materials," *Materials and Structures*, vol. 36, no. 10, pp. 643-647, 2003/12/01 2003, doi: 10.1007/BF02479495.
- [131] D. S. Wood *et al.*, "Accurate Prediction of Knee Angles during Open-Chain Rehabilitation Exercises Using a Wearable Array of Nanocomposite Stretch Sensors," *Sensors*, vol. 22, no. 7, p. 2499, 2022. [Online]. Available: <https://www.mdpi.com/1424-8220/22/7/2499>.
- [132] R. M. Guedes, A. Singh, and V. Pinto, "Viscoelastic modelling of creep and stress relaxation behaviour in PLA-PCL fibres," *Fibers and Polymers*, vol. 18, no. 12, pp. 2443-2453, 2017.
- [133] M. F. Clayton, R. A. Bilodeau, A. E. Bowden, and D. T. Fullwood, "Nanoparticle orientation distribution analysis and design for polymeric piezoresistive sensors," *Sensors and Actuators A: Physical*, vol. 303, p. 111851, 2020.
- [134] L. Wang, T. Ding, and P. Wang, "Research on stress and electrical resistance of skin-sensing silicone rubber/carbon black nanocomposite during decompressive stress relaxation," *Smart Materials and Structures*, vol. 18, no. 6, p. 065002, 2009.
- [135] A. Can-Ortiz, J. L. Abot, and F. Avilés, "Electrical characterization of carbon-based fibers and their application for sensing relaxation-induced piezoresistivity in polymer composites," *Carbon*, vol. 145, pp. 119-130, 2019/04/01/ 2019, doi: <https://doi.org/10.1016/j.carbon.2018.12.108>.
- [136] Y. H. Song, Q. Zheng, and J. F. Zhou, "Time-dependent uniaxial piezoresistive behavior of high-density polyethylene/short carbon fiber conductive composites," *Journal of Materials Research*, vol. 19, no. 9, pp. 2625-2634, 2004, doi: 10.1557/JMR.2004.0355.
- [137] Y. R. Jeong, H. Park, S. W. Jin, S. Y. Hong, S.-S. Lee, and J. S. Ha, "Highly Stretchable and Sensitive Strain Sensors Using Fragmentized Graphene Foam," *Advanced Functional Materials*, vol. 25, no. 27, pp. 4228-4236, 2015, doi: <https://doi.org/10.1002/adfm.201501000>.
- [138] A. D. Martineau, "Estimation of Knee Kinematics Using Non-Monotonic Nanocomposite High-Deflection Strain Gauges," M.Sc., Brigham Young University, Ann Arbor, 28103751, 2018. [Online]. Available: <http://erl.lib.byu.edu/login/?url=https://www.proquest.com/dissertations->

[theses/estimation-knee-kinematics-using-non-monotonic/docview/2432850839/se-2?accountid=4488](https://theses.lib.byu.edu/jfinder.pl?url_ver=Z39.88-2004&rft_val_fmt=info:ofi/fmt:kev:mtx:dissertation&genre=dissertations+%26+theses&sid=ProQ:ProQuest+Dissertations+%26+Theses+Global&atitle=&title=Estimation+of+Knee+Kinematics+Using+Non-Monotonic+Nanocomposite+High-Deflection+Strain+Gauges&issn=&date=2018-01-01&volume=&issue=&spage=&au=Martineau%2C+Adin+Douglas&isbn=9798662497665&jtitle=&bttitle=&rft_id=info:eric/&rft_id=info:doi/)

http://www.lib.byu.edu/jfinder.pl?url_ver=Z39.88-

[2004&rft_val_fmt=info:ofi/fmt:kev:mtx:dissertation&genre=dissertations+%26+theses&sid=ProQ:ProQuest+Dissertations+%26+Theses+Global&atitle=&title=Estimation+of+Knee+Kinematics+Using+Non-Monotonic+Nanocomposite+High-Deflection+Strain+Gauges&issn=&date=2018-01-01&volume=&issue=&spage=&au=Martineau%2C+Adin+Douglas&isbn=9798662497665&jtitle=&bttitle=&rft_id=info:eric/&rft_id=info:doi/](https://theses.lib.byu.edu/jfinder.pl?url_ver=Z39.88-2004&rft_val_fmt=info:ofi/fmt:kev:mtx:dissertation&genre=dissertations+%26+theses&sid=ProQ:ProQuest+Dissertations+%26+Theses+Global&atitle=&title=Estimation+of+Knee+Kinematics+Using+Non-Monotonic+Nanocomposite+High-Deflection+Strain+Gauges&issn=&date=2018-01-01&volume=&issue=&spage=&au=Martineau%2C+Adin+Douglas&isbn=9798662497665&jtitle=&bttitle=&rft_id=info:eric/&rft_id=info:doi/)

- [139] T. D. Remington, "Biomechanical Applications and Modeling of Quantum Nano-Composite Strain Gauges," 2014.
- [140] T. Hyatt, D. Fullwood, R. Bradshaw, A. Bowden, and O. Johnson, "Nano-composite sensors for wide range measurement of ligament strain," in *Experimental and Applied Mechanics, Volume 6*, T. Proulx, Ed. New York, NY: Springer, 2011, pp. 359-364.
- [141] Z. Sang, K. Ke, and I. Manas-Zloczower, "Effect of carbon nanotube morphology on properties in thermoplastic elastomer composites for strain sensors," *Composites Part A: Applied Science and Manufacturing*, vol. 121, pp. 207-212, 2019/06/01/ 2019, doi: <https://doi.org/10.1016/j.compositesa.2019.03.007>.
- [142] S. Gong *et al.*, "Highly stretchy black gold e-skin nanopatches as highly sensitive wearable biomedical sensors," *Advanced Electronic Materials*, vol. 1, no. 4, p. 1400063, 2015.
- [143] D. A. Baradoy, "Composition Based Modaling of Silicone Nano-Composite Strain Gauges," M.Sc., Brigham Young University, Ann Arbor, 28105748, 2015. [Online]. Available: <http://erl.lib.byu.edu/login/?url=https://www.proquest.com/dissertations-theses/composition-based-modaling-silicone-nano/docview/2445589613/se-2?accountid=4488>

http://www.lib.byu.edu/jfinder.pl?url_ver=Z39.88-

[2004&rft_val_fmt=info:ofi/fmt:kev:mtx:dissertation&genre=dissertations+%26+theses&sid=ProQ:ProQuest+Dissertations+%26+Theses+Global&atitle=&title=Composition+Based+Modaling+of+Silicone+Nano-Composite+Strain+Gauges&issn=&date=2015-01-01&volume=&issue=&spage=&au=Baradoy%2C+Daniel+Alexander&isbn=9798662516854&jtitle=&bttitle=&rft_id=info:eric/&rft_id=info:doi/](https://theses.lib.byu.edu/jfinder.pl?url_ver=Z39.88-2004&rft_val_fmt=info:ofi/fmt:kev:mtx:dissertation&genre=dissertations+%26+theses&sid=ProQ:ProQuest+Dissertations+%26+Theses+Global&atitle=&title=Composition+Based+Modaling+of+Silicone+Nano-Composite+Strain+Gauges&issn=&date=2015-01-01&volume=&issue=&spage=&au=Baradoy%2C+Daniel+Alexander&isbn=9798662516854&jtitle=&bttitle=&rft_id=info:eric/&rft_id=info:doi/)

- [144] S. A. Baker, M. D. McFadden, E. E. Bowden, A. E. Bowden, U. H. Mitchell, and D. T. Fullwood, "Accounting for Viscoelasticity When Interpreting Nano-Composite High-Deflection Strain Gauges," *Sensors*, vol. 22, no. 14, p. 5239, 2022. [Online]. Available: <https://www.mdpi.com/1424-8220/22/14/5239>.
- [145] S. A. Baker *et al.*, "Wearable nanocomposite sensor system for motion phenotyping chronic low back pain: a BACPAC Technology Research Site," *Pain Medicine*, p. pna017, 2023, doi: 10.1093/pm/pnad017.
- [146] D. S. Wood, D. T. Fullwood, and A. E. Bowden, "Multi-objective Bayesian optimization for the design of a piezoresistive composite," *Society for the Advancement of Material and Process Engineering*, 2021.
- [147] R. Shamsi, G. H. Asghari, G. Mir Mohamad Sadeghi, and H. Nazarpour-Fard, "The effect of multiwalled carbon nanotube and crosslinking degree on creep–recovery behavior of PET waste originated-polyurethanes and their nanocomposites," *Polymer Composites*, vol. 39, no. S2, pp. E1013-E1024, 2018.
- [148] Z. Yao, D. Wu, C. Chen, and M. Zhang, "Creep behavior of polyurethane nanocomposites with carbon nanotubes," *Composites Part A: Applied Science and Manufacturing*, vol. 50, pp. 65-72, 2013/07/01/ 2013, doi: <https://doi.org/10.1016/j.compositesa.2013.03.015>.
- [149] "Low Back Pain Fact Sheet." National Institute of Neurological Disorders and Stroke. https://www.ninds.nih.gov/sites/default/files/low_back_pain_20-ns-5161_march_2020_508c.pdf (accessed 10/28/2021, 2021).
- [150] W. S. Marras *et al.*, "The quantification of low back disorder using motion measures: Methodology and validation," *Spine*, vol. 24, no. 20, p. 2091, 1999.

- [151] J. Diani, B. Fayolle, and P. Gilormini, "A review on the Mullins effect," *European Polymer Journal*, vol. 45, no. 3, pp. 601-612, 2009/03/01/ 2009, doi: <https://doi.org/10.1016/j.eurpolymj.2008.11.017>.
- [152] A. V. Marich, C.-T. Hwang, G. B. Salsich, C. E. Lang, and L. R. Van Dillen, "Consistency of a lumbar movement pattern across functional activities in people with low back pain," *Clinical Biomechanics*, vol. 44, pp. 45-51, 2017/05/01/ 2017, doi: <https://doi.org/10.1016/j.clinbiomech.2017.03.004>.
- [153] J. K. Freburger *et al.*, "The rising prevalence of chronic low back pain," *Arch Intern Med*, vol. 169, no. 3, pp. 251-8, Feb 9 2009, doi: 10.1001/archinternmed.2008.543.
- [154] Y.-g. Zhang, T.-m. Guo, X. Guo, and S.-x. Wu, "Clinical diagnosis for discogenic low back pain," *International journal of biological sciences*, vol. 5, no. 7, p. 647, 2009.
- [155] S. M. Meints and R. R. Edwards, "Evaluating psychosocial contributions to chronic pain outcomes," *Progress in Neuro-Psychopharmacology and Biological Psychiatry*, vol. 87, pp. 168-182, 2018/12/20/ 2018, doi: <https://doi.org/10.1016/j.pnpbp.2018.01.017>.
- [156] L. J. Crofford, "Chronic pain: where the body meets the brain," *Transactions of the American Clinical and Climatological Association*, vol. 126, p. 167, 2015.
- [157] M. C. Bushnell, M. Čeko, and L. A. Low, "Cognitive and emotional control of pain and its disruption in chronic pain," *Nature Reviews Neuroscience*, vol. 14, no. 7, pp. 502-511, 2013/07/01 2013, doi: 10.1038/nrn3516.
- [158] L. Solberg Nes, C. R. Carlson, L. J. Crofford, R. d. Leeuw, and S. C. Segerstrom, "Self-regulatory deficits in fibromyalgia and temporomandibular disorders," *PAIN®*, vol. 151, no. 1, pp. 37-44, 2010/10/01/ 2010, doi: <https://doi.org/10.1016/j.pain.2010.05.009>.
- [159] A. Batorsky *et al.*, "The BACPAC Research Program Data Harmonization: Rationale for Data Elements and Standards," *Pain Medicine*, p. pna008, 2023, doi: 10.1093/pm/pna008.
- [160] M. O. Papuga, A. Mesfin, R. Molinari, and P. T. Rubery, "Correlation of PROMIS physical function and pain CAT instruments with Oswestry Disability Index and Neck Disability Index in spine patients," *Spine*, vol. 41, no. 14, p. 1153, 2016.
- [161] P. Tyrer and D. Baldwin, "Generalised anxiety disorder," *The Lancet*, vol. 368, no. 9553, pp. 2156-2166, 2006.
- [162] F. Plummer, L. Manea, D. Trepel, and D. McMillan, "Screening for anxiety disorders with the GAD-7 and GAD-2: a systematic review and diagnostic metaanalysis," *General Hospital Psychiatry*, vol. 39, pp. 24-31, 2016/03/01/ 2016, doi: <https://doi.org/10.1016/j.genhosppsy.2015.11.005>.
- [163] M. J. Sullivan, S. R. Bishop, and J. Pivik, "The pain catastrophizing scale: development and validation," *Psychological assessment*, vol. 7, no. 4, p. 524, 1995.
- [164] F. A.-O. Franchignoni, A. A.-O. Giordano, G. A.-O. Ferriero, and M. A.-O. X. Monticone, "Measurement precision of the Pain Catastrophizing Scale and its short forms in chronic low back pain," (in eng), no. 2045-2322 (Electronic).
- [165] E. Cerin *et al.*, "Correlates of agreement between accelerometry and self-reported physical activity," *Medicine and science in sports and exercise*, vol. 48, no. 6, p. 1075, 2016.
- [166] J. H. Sullivan, M. Warkentin, and L. Wallace, "So many ways for assessing outliers: What really works and does it matter?," *Journal of Business Research*, vol. 132, pp. 530-543, 2021/08/01/ 2021, doi: <https://doi.org/10.1016/j.jbusres.2021.03.066>.
- [167] D. R. Grimes and J. Heathers, "The new normal? Redaction bias in biomedical science," *Royal Society open science*, vol. 8, no. 12, p. 211308, 2021.
- [168] B. G. Tabachnick, L. S. Fidell, and J. B. Ullman, *Using multivariate statistics*. pearson Boston, MA, 2013.
- [169] J. Cohen, *Statistical power analysis for the behavioral sciences*. Academic press, 2013.
- [170] R. D. Hays, J. B. Bjorner, D. A. Revicki, K. L. Spritzer, and D. Cella, "Development of physical and mental health summary scores from the patient-reported outcomes measurement information system (PROMIS) global items," *Quality of life Research*, vol. 18, pp. 873-880, 2009.
- [171] A. Ezeukwu, G. Ebisike, D. John, O. Okezue, and J. John, "Predictors of self-reported physical activity level in patients with non-specific chronic low back pain," *Int Phys Med Rehab J*, vol. 4, no. 1, pp. 25-35, 2019.

- [172] M. van Weering, M. M. R. Vollenbroek-Hutten, E. Kotte, and H. J. Hermens, "Daily physical activities of patients with chronic pain or fatigue versus asymptomatic controls. A systematic review," *Clinical Rehabilitation*, vol. 21, no. 11, pp. 1007-1023, 2007.
- [173] R. A. Laird, J. L. Keating, and P. Kent, "Subgroups of lumbo-pelvic flexion kinematics are present in people with and without persistent low back pain," *BMC Musculoskeletal Disorders*, vol. 19, no. 1, p. 309, 2018/08/28 2018, doi: 10.1186/s12891-018-2233-1.
- [174] J. H. B. Stuart and A. Mavis, "Physical activity and mental health in children and adolescents: a review of reviews," *British Journal of Sports Medicine*, vol. 45, no. 11, p. 886, 2011, doi: 10.1136/bjsports-2011-090185.
- [175] M. A. M. Peluso and L. H. S. G. d. Andrade, "PHYSICAL ACTIVITY AND MENTAL HEALTH: THE ASSOCIATION BETWEEN EXERCISE AND MOOD," *Clinics*, vol. 60, no. 1, pp. 61-70, 2005/02/01/ 2005, doi: <https://doi.org/10.1590/S1807-59322005000100012>.
- [176] S. A. Paluska and T. L. Schwenk, "Physical Activity and Mental Health," *Sports Medicine*, vol. 29, no. 3, pp. 167-180, 2000/03/01 2000, doi: 10.2165/00007256-200029030-00003.
- [177] S. Biddle, "Physical activity and mental health: evidence is growing," *World Psychiatry*, vol. 15, no. 2, p. 176, 2016.
- [178] J. S. Labus, F. J. Keefe, and M. P. Jensen, "Self-reports of pain intensity and direct observations of pain behavior: when are they correlated?," *Pain*, vol. 102, no. 1, pp. 109-124, 2003/03/01/ 2003, doi: [https://doi.org/10.1016/s0304-3959\(02\)00354-8](https://doi.org/10.1016/s0304-3959(02)00354-8).
- [179] H.-R. Guo *et al.*, "Back pain among workers in the United States: National estimates and workers at high risk," *American Journal of Industrial Medicine*, vol. 28, no. 5, pp. 591-602, 1995, doi: <https://doi.org/10.1002/ajim.4700280504>.
- [180] J. A. Verbunt, K. R. Westerterp, G. J. van der Heijden, H. A. Seelen, J. W. Vlaeyen, and J. A. Knottnerus, "Physical activity in daily life in patients with chronic low back pain," *Archives of Physical Medicine and Rehabilitation*, vol. 82, no. 6, pp. 726-730, 2001/06/01/ 2001, doi: <https://doi.org/10.1053/apmr.2001.23182>.
- [181] M. C. Jensen, M. N. Brant-Zawadzki, N. Obuchowski, M. T. Modic, D. Malkasian, and J. S. Ross, "Magnetic resonance imaging of the lumbar spine in people without back pain," *New England Journal of Medicine*, vol. 331, no. 2, pp. 69-73, 1994.
- [182] J. N. Katz, "Lumbar disc disorders and low-back pain: socioeconomic factors and consequences," *JBJS*, vol. 88, no. suppl_2, pp. 21-24, 2006.
- [183] W. R. VanWye, "Nonspecific low back pain: evaluation and treatment tips," *Journal of Family Practice*, vol. 59, no. 8, p. 445, 2010.
- [184] W. S. Marras, K. G. Davis, S. A. Ferguson, B. R. Lucas, and P. Gupta, "Spine loading characteristics of patients with low back pain compared with asymptomatic individuals," *Spine (Phila Pa 1976)*, vol. 26, no. 23, pp. 2566-74, Dec 1 2001, doi: 10.1097/00007632-200112010-00009.
- [185] D. Lindsay and J. Horton, "Comparison of spine motion in elite golfers with and without low back pain," *Journal of sports sciences*, vol. 20, no. 8, pp. 599-605, 2002.
- [186] I. Shojaei, E. G. Salt, Q. Hooker, L. R. Van Dillen, and B. Bazrgari, "Comparison of lumbo-pelvic kinematics during trunk forward bending and backward return between patients with acute low back pain and asymptomatic controls," *Clinical Biomechanics*, vol. 41, pp. 66-71, 2017.
- [187] R. A. Laird, J. Gilbert, P. Kent, and J. L. Keating, "Comparing lumbo-pelvic kinematics in people with and without back pain: a systematic review and meta-analysis," *BMC Musculoskeletal Disord*, vol. 15, p. 229, Jul 10 2014, doi: 10.1186/1471-2474-15-229.
- [188] W. S. Marras *et al.*, "The classification of anatomic- and symptom-based low back disorders using motion measure models," *Spine*, vol. 20, no. 23, pp. 2531-46, Dec 1 1995, doi: 10.1097/00007632-199512000-00013.
- [189] S. Schmid, C. Bangerter, P. Schweinhardt, and M. L. Meier, "Identifying Motor Control Strategies and Their Role in Low Back Pain: A Cross-Disciplinary Approach Bridging Neurosciences With Movement Biomechanics," *Front Pain Res (Lausanne)*, vol. 2, p. 715219, 2021, doi: 10.3389/fpain.2021.715219.

- [190] R. Haskins, D. A. Rivett, and P. G. Osmotherly, "Clinical prediction rules in the physiotherapy management of low back pain: a systematic review," *Manual Therapy*, vol. 17, no. 1, pp. 9-21, 2012.
- [191] K. V. Fersum, P. O'Sullivan, A. Kvåle, and J. Skouen, "Inter-examiner reliability of a classification system for patients with non-specific low back pain," *Manual Therapy*, vol. 14, no. 5, pp. 555-561, 2009.
- [192] M. Alrwaily *et al.*, "Treatment-Based Classification System for Low Back Pain: Revision and Update," *Physical Therapy*, vol. 96, no. 7, pp. 1057-1066, 2016, doi: 10.2522/ptj.20150345.
- [193] S. Mahallati, H. Rouhani, R. Preuss, K. Masani, and M. R. Popovic, "Multisegment Kinematics of the Spinal Column: Soft Tissue Artifacts Assessment," *Journal of Biomechanical Engineering*, vol. 138, no. 7, p. 8, 2016, doi: 10.1115/1.4033545.
- [194] A. M. Gibbons, Paul; Peterson, Joseph; Baker, Spencer; Clingo, Kelly; Mitchell, Ulrike H.; Fullwood, David T.; and Bowden, Anton E., "Correlation of Segmental Lumbar Kinematics with a Wearable Skin Strain Sensor Array," presented at the Biomedical Engineering Society Conference, Orlando, FL, 2021.
- [195] T. Giorgino, P. Tormene, F. Lorussi, D. De Rossi, and S. Quaglini, "Sensor evaluation for wearable strain gauges in neurological rehabilitation," *IEEE Transactions on Neural Systems and Rehabilitation Engineering*, vol. 17, no. 4, pp. 409-415, 2009.
- [196] D. Billmire *et al.*, "Clinician and Patient Evaluation of a Wearable Strain-Gauge Based Vertebral Motion Tracking System," presented at the Biomedical Engineering Society, Orlando, Florida, 2021.
- [197] A. Gibbons, J. Peterson, J. Carter, U. H. Mitchell, D. T. Fullwood, and A. E. Bowden, "A study on the properties of wearable nanocomposite sensors in diagnosing LBP," presented at the SAMPE University Research Symposium, Dallas, Texas, 2021.
- [198] K. Clingo *et al.*, "Application and Validation of Nano-composite Wearable Technology for Studying Lower Back Pain," presented at the SAMPE University Research Symposium, Sep 22, 2021, 2021.
- [199] B. A. MacWilliams *et al.*, "Three-Dimensional Lumbar Spine Vertebral Motion During Running Using Indwelling Bone Pins," *Spine*, vol. 39, no. 26, pp. E1560-E1565, 2014, doi: 10.1097/brs.0000000000000646.
- [200] S. McGill, J. Seguin, and G. Bennett, "Passive Stiffness of the Lumbar Torso in Flexion, Extension, Lateral Bending, and Axial Rotation: Effect of Belt Wearing and Breath Holding," *Spine*, vol. 19, no. 6, pp. 696-704, 1994. [Online]. Available: https://journals.lww.com/spinejournal/Fulltext/1994/03001/Passive_Stiffness_of_the_Lumbar_Torso_in_Flexion,9.aspx.
- [201] X. Meng, A. G. Bruno, B. Cheng, W. Wang, M. L. Boussein, and D. E. Anderson, "Incorporating Six Degree-of-Freedom Intervertebral Joint Stiffness in a Lumbar Spine Musculoskeletal Model—Method and Performance in Flexed Postures," *Journal of Biomechanical Engineering*, vol. 137, no. 10, 2015, doi: 10.1115/1.4031417.
- [202] D. S. Wood, "Optimization of a Smart Sensor Wearable Knee Sleeve for Measuring Skin Strain to Determine Joint Biomechanics," PhD, Mechanical Engineering, Brigham Young University, BYU ScholarsAchieve Citation, 2022.
- [203] K. A. Clark, U. Mitchell, A. Bowden, and P. McMullin, "Segmental Kinematic Analysis Of The Lumbar Spine Using Skin-mounted Markers: Preliminary Results.: 524," *Medicine & Science in Sports & Exercise*, vol. 53, no. 8S, pp. 173-174, 2021.
- [204] A. Gibbons, D. Emmett, U. H. Mitchell, D. T. Fullwood, and A. E. Bowden, "Shear Stresses on Skin Adhered Wearables due to Lumbar Skin Strain during Flexion," presented at the Biomedical Engineering Society Conference, San Antonio Texas, 2022.
- [205] J. Brooke, *Usability evaluation in industry, chap. SUS: a "quick and dirty" usability scale*. London: Taylor and Francis, 1996.
- [206] J. Sauro, "Measuring usability with the system usability scale," URL: <http://www.measuringusability.com/sus.php> and *procedure (9.4. 2012.)*, 2011.
- [207] Z. Qian *et al.*, "Inverse piezoresistive nanocomposite sensors for identifying human sitting posture," *Sensors*, vol. 18, no. 6, p. 1745, 2018.

- [208] P. G. Rosquist, *Modeling Three Dimensional Ground Reaction Force Using Nanocomposite Piezoresponsive Foam Sensors*. Brigham Young University, 2017.
- [209] P. G. Rosquist *et al.*, "Estimation of 3D ground reaction force using nanocomposite piezo-responsive foam sensors during walking," *Annals of biomedical engineering*, vol. 45, no. 9, pp. 2122-2134, 2017.
- [210] W. S. Marras and P. Wongsam, "Flexibility and velocity of the normal and impaired lumbar spine," *Archives of Physical Medicine and Rehabilitation*, vol. 67, no. 4, pp. 213-217, 1986.
- [211] J. Slaboda, "Application of Jerk Analysis to a Repetitive Lifting Task in Patients with Chronic Lower Back Pain," University of Pittsburgh, 2004.
- [212] R. A. da Silva *et al.*, "Back muscle fatigue of younger and older adults with and without chronic low back pain using two protocols: a case-control study," *Journal of Electromyography and Kinesiology*, vol. 25, no. 6, pp. 928-936, 2015.
- [213] S. Schmid, C. Bangerter, P. Schweinhardt, and M. L. Meier, "Identifying Motor Control Strategies and Their Role in Low Back Pain: A Cross-Disciplinary Approach Bridging Neurosciences With Movement Biomechanics," *Frontiers in Pain Research*, p. 42, 2021.
- [214] N. Campbell, A. B. Rosenkrantz, and I. Pedrosa, "MRI phenotype in renal cancer: is it clinically relevant?," *Topics in magnetic resonance imaging: TMRI*, vol. 23, no. 2, p. 95, 2014.
- [215] J. H. Määtä, J. I. Karppinen, K. D. K. Luk, K. M. C. Cheung, and D. Samartzis, "Phenotype profiling of Modic changes of the lumbar spine and its association with other MRI phenotypes: a large-scale population-based study," *The Spine Journal*, vol. 15, no. 9, pp. 1933-1942, 2015/09/01/2015, doi: <https://doi.org/10.1016/j.spinee.2015.06.056>.
- [216] M. Keith, *Machine Learning in Python*, 2022. [Online]. Available: <https://app.myeducator.com/reader/web/1702c/cluster/lb3nj/>. Accessed on: February 11, 2022.
- [217] "2.3. Clustering." scikit-learn developers. <https://scikit-learn.org/stable/modules/clustering.html> (accessed February 1, 2022, 2022).
- [218] Pedregosa *et al.*, "Scikit-learn: Machine Learning in Python," *scikit learn*, vol. 12, pp. 2825-2830, 2011. [Online]. Available: https://scikit-learn.org/stable/auto_examples/cluster/plot_linkage_comparison.html#sphx-glr-auto-examples-cluster-plot-linkage-comparison-py.
- [219] DataNovia, "Cluster Dendrogram," in R, C. Dendrogram, Ed., ed. <https://www.datanovia.com/en/lessons/examples-of-dendrograms-visualization/>: DataNovia, 2018.
- [220] W. S. Marras, B. A. Walter, D. Purmessur, P. Mageswaran, and M. G. Wiet, "The contribution of biomechanical-biological interactions of the spine to low back pain," *Human factors*, vol. 58, no. 7, pp. 965-975, 2016.
- [221] Andrew Gibbons *et al.*, "Correlation of Segmental Lumbar Kinematics with a Wearable Skin Strain Sensor Array," presented at the Biomedical Engineering Society, Orlando, Florida, 2021.